NETWORK THERMODYNAMICS: THE ANALYSIS OF BIOLOGICAL SYSTEMS

Oster, George F.

1972-02-01

Submitted to Quarterly Reviews
of Biophysics

LBL-588 c.1
Preprint

NETWORK THERMODYNAMICS: THE ANALYSIS OF BIOLOGICAL SYSTEMS

George F. Oster, Alan S. Perelson, and
Aharon Katchalsky
DONNER LABORATORY

February 1972

AEC Contract No. W-7405-eng-48

DISCLAIMER

NETWORK THERMODYNAMICS: THE ANALYSIS OF BIOLOGICAL SYSTEMS

Contents

I. INTRODUCTION 1

1.1 Classical thermodynamic approach 1

1.2 The network approach 3

1.3 Thermodynamics and multiports 8

1.4 State variables 15

1.5 Constitutive relations 19

II. TOPOLOGICAL GRAPH REPRESENTATION FOR SIMPLE SYSTEMS 25

2.1 Representation of a mechanical model 25

2.2 Nonelectrolyte diffusion through a homogeneous membrane 35

2.3 The relaxation time of a single permeation flow 42

III. THE BOND GRAPH REPRESENTATION 47

3.1 Bond graph fundamentals 47

3.2 Causality 54

3.3 Transition to continuum equations 57

3.4 Tellegen's theorem for bond graphs 62

IV. NETWORK REPRESENTATIONS OF COUPLED FLOWS 67

4.1 Stationary flow of nonelectrolytes across a membrane 67

4.2 Nonstationary flows of nonelectrolytes and their relaxation times 77

4.3 Continuum equations 82

4.4 Transport in ideal electrolyte solutions 89
4.5 The treatment of real electrolyte solutions 90
4.6 Membrane permeability to electrolytes 90

V. CHEMICAL PROCESSES 93
5.1 Bond graph representation of chemical flows 93
5.2 Chemical kinetics close to equilibrium 98
5.3 Two-port representation of chemical dissipative processes 106
5.4 Analysis of chemical systems 109

VI. THE COUPLING OF CHEMICAL AND DIFFUSIONAL PROCESSES 115
6.1 Bond graph representation of coupled chemical and diffusional processes 115
6.2 Port constitutive relations 117
6.3 Relaxation times for chemico-diffusional processes 119
6.4 Continuum equations 124
6.5 Facilitated transport 129

VII. SIGNAL FLOWS AND CONTROL PROCESSES 135
7.1 Unilateral energy transmission and activated bonds 135
7.2 Signal flow bonds 136
7.3 Unilateral energy transmission and reciprocity 137
7.4 Unilateral energy flow and dissipation 137
7.5 Nonlinear oscillations 139

VIII. THEORETICAL CONSIDERATIONS 143
8.1 Introduction 143
8.2 Duality 143
8.3 Reciprocity 147

8.4 Potential functions for reciprocal n-ports 155
8.5 Interconnection of n-ports 156
8.6 Canonical form for the equations of motion 160
8.7 Stability of the steady state 163
8.8 Extremal principles 170

IX. REFERENCES 173

X. APPENDIX A 241

NETWORK THERMODYNAMICS: THE ANALYSIS OF BIOLOGICAL SYSTEMS

George F. Oster, Alan S. Perelson, and
Aharon Katchalsky

Donner Laboratory and Lawrence Berkeley Laboratory
University of California, Berkeley, California 94720

I. INTRODUCTION

1.1. Classical thermodynamic approach

The success of equilibrium thermodynamics in describing static phenomena has inspired many attempts to develop a rigorous thermodynamics of rate processes.

Onsager (1931) proposed a formalism for dealing with coupled irreversible processes. His theory was extended by Prigogine (1947), Degroot (1951), Meixner (1941, 1942, 1943) and other workers, who developed it into an important tool for the treatment of coupled physical chemical processes. Onsager's formalism relates thermodynamic flows to their conjugate forces by linear algebraic equations. Sufficiently close to equilibrium the constitutive relations between flows and forces become linear and, as shown by Onsager, the matrix of the coefficients is frequently symmetric (Truesdell, 1970). The major advantage of the Onsager theory for the analysis of experimental data derives from this symmetry condition, which plays the same role in the study of rate processes as that of the Maxwell relations in equilibrium phenomena: it permits the evaluation of flows or forces which are difficult to obtain by direct measurement.

Another approach, more compatible with modern continuum mechanics, has been formulated by Truesdell and his co-workers (Truesdell, 1970). This formalism is a true nonlinear field theory, developed with great attention to mathematical rigor; however, it seems more suited to the mechanics of continua than to the complex and heterogeneous structures encountered in the living cell.

More recently, Meixner (1963) has proposed a nonequilibrium thermodynamic theory based on the general theory of linear passive systems. The Meixner theory, like the approach developed by the present authors, leans heavily on concepts first developed in electrical network theory. Meixner, however, has limited himself to linear processes, and like the Truesdell school, his work deals primarily with the thermodynamics of materials, and not with the highly reticulated structures of biological interest.

In this paper, we propose a formalism which, we feel, is more appropriate for the phenomenological description of biological systems. The thrust of modern biology is toward the investigation of increasingly complex structures. It has become almost a cliché to acknowledge that living entities are extremely complicated, heterogeneous, nonlinear systems. They are based on a subtle interplay between the energetic rate processes of transport, reaction and conformational change, on the one hand, and cybernetic flows of information, whose regulatory effects are not proportional to their energetic level, on the other. The theory outlined in this paper is designed specifically for the treatment of coupled, nonlinear, time-dependent thermodynamic processes in heterogeneous media and is also capable of incorporating nonenergetic, informational flows. The general formalism employs a simple and intuitive graphical notation which emphasizes the topological relations of the system under consideration.

1.2. The network approach

The prime function of physical theories is to organize our knowledge into a formal structure for ease in deduction and manipulation. Classical mechanics was the earliest prototype for the class of physical models now called "state determined systems". In recent years, the underlying mathematical unity of most dynamical theories of physics has been clarified (Sudarshan, 1962; Hermann, 1971). The notion of dynamical systems has been formalized, and includes as special cases not only classical mechanics but also quantum mechanics, electromagnetism, hydrodynamics, elasticity, control theory and electrical circuit theory (Desoer, 1970). The principal purpose of this paper is to propose an extension of the thermodynamic model with a mathematical structure in conformity with the existing dynamical theories of physics. We will not enter too deeply into the mathematical justification here; this would take us too far afield into the realm of algebraic topology and differential geometry. We will limit ourselves to a detailed account of how network thermodynamics may be applied to systems of interest in the biological sciences.

There are several reasons for approaching irreversible thermodynamics from the point of view of network theory. The problem of analyzing biological systems using the classical field equations is analogous to attempting to describe a television set by integrating Maxwell's equations. It is certainly possible "in principle"; but in practice, too much irrelevant information is required to integrate over such a heterogeneous object. Clearly, network theory is the correct analytical tool for the study of such a system. The complexity of, say, a mitochondrion is more on the order of a television set than of an anisotropic continuum!

An electrical network may certainly be considered an irreversible thermodynamic system. However, the mathematical techniques developed by electrical engineers for dealing with circuits appear at first glance to be quite foreign to the classical methods of thermodynamics. Nevertheless, we will show that the two disciplines are not, in fact, so incompatible, and that, by making suitable modifications, we can draw upon the engineering literature in modern network and control theory to deal with problems of biological complexity.

A graphical representation for thermodynamic systems similar to the circuit diagram in electrical network theory will be introduced. Aside from being a pictorial representation of the system with obvious intuitive advantages, this graphical notation will reveal the role of system topology in dynamic behavior. It is clear that the organizational structure of biological systems is one of their characteristic features. How a television set or a biological system is "hooked up" is as vital an ingredient to its proper functioning as the energetics of the thermodynamic processes. This aspect of thermodynamic systems has only recently been considered explicitly.* We will see that many characteristics of thermodynamic systems previously ascribed to energetic restrictions are more properly classified as "topological constraints", and, as such, are consequences of the system structure rather than the laws of thermodynamics.

We will present an algorithm for obtaining the dynamical equations directly from the graph, and consequently one may look upon the network graph as another notation for the differential equations themselves. However, since the graph reveals the system's topology, it contains more information than the

---

*Newman and Rice (1971) discuss topological constraints in biochemical networks in relation to self-regulatory behavior, while Morowitz et al. (1964) discuss the role of such constraints in determining the stability of metabolic networks. Othmer and Sriven (1971) have also recently considered the network aspects of biological organization.

dynamical equations alone, i.e., many systems with different topology are governed by the same dynamical equations (Desoer, 1970; Oster and Desoer, 1971).

A word of caution would be proper: one should not equate the methods presented here with the usual notion of "equivalent circuits". Although our vocabulary will be heavily laced with terminology drawn from electrical engineering, the concepts apply equally well to a wide class of dynamical systems described by ordinary differential equations (MacFarlane, 1970; Koenig et al. 1969).

It should be noted that, in the network representation of thermodynamic systems, one introduces a schematic separation of various reversible and irreversible processes which actually may proceed simultaneously at each point in the system. This reticulation of distributed processes is merely a conceptual device which does not affect the resulting mathematical description. Previously, this purely mathematical device has been employed mainly with reference to those systems where such a separation assumes concrete form, as in electrical networks, hydraulic pipe systems, etc.* (MacFarlane, 1970; Koenig et al. 1969; Shearer et al. 1967).

"Network analogs" for continuous systems have been a long-standing tool in engineering and neurophysiology (Cole, 1968).

---

*However, Penfield and Haus (1967) have also employed this construction for continuum electrodynamics.

Kron (1943, 1944, 1945, 1946, 1948), in fact, devised network analogs for practically all the field theories of physics, including the equations of Schroedinger, Maxwell, and Navier-Stokes. The success of these analogs in emulating the dynamical behavior of continuum systems to any desired degree of accuracy seemed remarkable. However, it was soon realized that this success was no accident, but rather a natural consequence of the underlying unity of the mathematical structures of network and field theory. Roth (1955), and later, Branin (1962, 1966), demonstrated that the operational structures of linear graph theory and the vector calculus were identical (a fact long known to algebraic topologists). Trent (1955) first demonstrated how an isomorphism between a distributed physical system and a linear graph (network) could be constructed. Later authors further developed this technique; and presently, network methods for treating dynamical systems are becoming standard tools in engineering curricula (MacFarlane, 1970; Koenig et al. 1969; Shearer et al. 1967). In each instance, there are well defined criteria for determining the validity of the network approximation to the field equations; these conditions turn out to be equivalent to the "local equilibrium" postulate of nonequilibrium thermodynamics. We will see, however, that not all network representations arise from a reticulation of the continuum. The most important example for our purpose will be chemical reaction networks, which are a priori "naturally discrete".

A major difficulty in extending the network technique to general thermodynamic systems, aside from the mathermatical questions, is one of notation. While the network approach offers obvious advantages in treating complicated systems, the linear graph notation usually employed in engineering becomes cumbersome and devoid of intuitive content. Moreover, thermodynamics is concerned principally with transduction of energy from one form to another, e.g. mechanochemical, electrochemical, thermoelectric processes, etc. Linear graphs are not a suitable tool for such situations; but fortunately there exists an alternative notation for energetic systems: "bond graphs".* These will prove admirably suited to the purposes of irreversible thermodynamics. The elucidation of the bond graph representation is one of the main objectives of this work.

1.3. Thermodynamics and multiports

1.3.1.

The network approach developed herein requires that we view thermodynamics from a slightly different set of premises. Attention is focussed on measurable quantities such as temperature and pressure; and the thermodynamic potential functions

---

*So-called because of their formal resemblance to chemical bond structures.

lose their primacy, emerging as derived quantities for certain systems. This approach was originally taken by Brönsted more than thirty years ago, but because of the great convenience of the thermodynamic potential functions for computing equilibrium conditions, it did not come into common use.* However, Brönsted's approach is implicitly followed by modern axiomatic developments of circuit theory. To emphasize the difference in conceptual structure, we will briefly reexamine equilibrium thermodynamics from the "multiport" viewpoint. In Section VIII, we will return to these matters for a more rigorous inspection.

1.3.2.

Both network theory and thermodynamics can be regarded, as pointed out by Shottky, as the science of "black boxes". That is, we regard a thermodynamic system as a black box whose entire internal constitution is characterized only by a set of <u>external</u> measurements ("constitutive relations"). For example, consider the familiar piston-cylinder arrangement shown in Fig. 1.1a.

This is a system capable of interacting with its environment via two energetic modes, thermal and mechanical. In

---

*A review of Brönsted's approach to thermodynamics, with references to the original literature, may be found in the article of LeMer et al. (1949).

general, we will refer to each such interaction mode as an energy "port". The piston-cylinder is a thermomechanical two-port. Later, we will see that an energy port need not refer to any physically distinct location but is simply a picturesque nomenclature for the interaction mode itself. (Indeed, an n-port may not be a physically distinct entity at all; shortly, we will give a precise definition of an n-port as a mathematical object.)

Associated with each port of a thermodynamic system are a pair of variables, the measurement of which determines the constitutive behavior of the system. For example, the two-port in Fig. 1.1a has two constitutive planes, (p, V) and (T, S), where the mechanical and thermal response of the system to external manipulations is plotted. In general, the response curves at any one port will depend on the boundary conditions imposed at all of the other ports.

To facilitate the graphical notation for interconnecting n-ports to be introduced later, we will represent each port by an ideal energy bond, Fig. 1.1b. These bonds, a generalization of perfectly conducting wires or infinitely stiff rods, are assumed to transmit energy instantaneously and without delay or loss between one system and another. In the case of electrical devices, the ports are the terminal pairs, Fig. 1.1c. For other thermodynamic systems, these are only schematic reticulations of system interfaces.

The port variables come in pairs, for reasons to be discussed in Section VIII. However, of the 2n-port variables (e.g. p, V, T, S) not all are independent. A selection of some subset serves to fix the values of the remaining ones. For an ideal gas, (p, V) suffice to determine the state. If the cylinder in Fig. 1.1a contains a condensing fluid, (V, T) may be chosen as independent variables. (In the usual case, specifying one variable from each port suffices to determine the state).

The function mapping the independent port variables into the dependent port variables is called the constitutive relation, or equation of state, of the n-port. Formally, we will define an n-port via its constitutive relation.

> DEFINITION:* An n-port is a map $\mathbb{F}$ which assigns to a set of n independent port variables the set of n conjugate variables:

$$\mathbb{F}: \mathbb{R}^n \to \mathbb{R}^n, \qquad \underset{\sim}{x} \to \underset{\sim}{y}(\underset{\sim}{x}), \tag{1.1}$$

where $\underset{\sim}{x}$ and $\underset{\sim}{y}$ are the vectors of port variables,** e.g.

$$(S, V, n_i) \to (T, -p, \mu_i).$$

For simplicity, we shall assume that $\mathbb{F}$ is sufficiently differentiable. For example, the simple electrical capacitor shown in Fig. 1.1c is a one-port whose constitutive relation is simply: $q \to \mathscr{V}(q)$, where q is the charge stored by the capacitor and $\mathscr{V}$ is the

---

*This definition will be made more precise in Section VIII.

**$\mathbb{R}^n$ is simply Euclidean n-space equipped with the usual vector space structure.

voltage across the capacitor plates.

1.3.3.

There is an important difference in viewpoint between classical thermodynamics and circuit theory regarding the role of the port variables and constitutive relations. This difference is reflected most strongly in the different methods used to compute equilibrium or stationary states.

The classical approach to equilibrium thermodynamics may be summarized succinctly in the following way (Callen, 1960): A "state space" is constructed, the coordinates of which are the relevant thermodynamic "displacements" for the system under consideration. The displacements are, according to Gibbs, the "extensive" properties–entropy (S), volume (V), number of moles of the ith component (n_i), etc. Representing all the displacements by a vector $\underset{\sim}{x} = (S, V, n_1, n_2 \dots)^T$, we may define a real-valued function on this state space, $U: \mathbb{R}^n \to \mathbb{R}$:

$$U = U(S, V, n_1, \cdots, n_k). \qquad (1.2)$$

It is now postulated that the equilibrium properties of the system are completely specified by the function U. For example, we may define the potentials, conjugate to the displacements, as the components of $\underset{\sim}{DU}$, the gradient of U.*

---

*We denote by D the differential operator (Jacobian), as in Fleming (1965).

$$\begin{aligned}\underset{\sim}{y}(\underset{\sim}{x}) &\triangleq \underset{\sim}{DU}(\underset{\sim}{x}) = \left(\frac{\partial U}{\partial S}, \frac{\partial U}{\partial V}, \frac{\partial U}{\partial n_1}, \cdots, \frac{\partial U}{\partial n_k}\right) \\ &\triangleq (T, -p, \mu_1, \cdots, \mu_k).\end{aligned} \tag{1.3}$$

The matrix of second partial derivatives of U, i.e., the Hessian, is then trivially symmetric by the equality of mixed parital derivatives.

$$\underset{\sim}{D^2}U(\underset{\sim}{x}) = \underset{\sim}{D^2}U(\underset{\sim}{x})^T, \tag{1.4}$$

yielding the familiar reciprocal relations of Maxwell* (Callen, 1960).

In addition, the equilibrium configuration of a thermodynamic n-port is computed by minimizing U (or the appropriate Legendre transform) subject to the appropriate boundary constraints (e.g. T = constant; V = constant) (Callen, 1960).

Brönsted's approach, however, takes as primitive quantities the experimentally measurable port variables $\underset{\sim}{x}$ and $\underset{\sim}{y}$, rather than the internal energy U. Without employing a potential function, the equilibrium state cannot be characterized by an extremum principle, but must be computed explicitly from the constitutive relation and the boundary constraints. Maxwell reciprocity is <u>not</u> an automatic consequence of a differentiable potential function, but must now be viewed as an experimental

---

*Roughly speaking, reciprocity implies that the input and output ports of a system may be interchanged without affecting the system's "small signal" response to a given excitation.

property which places an additional restriction on the constitutive relation $\underset{\sim}{\mathbb{F}}(\cdot)$. In Section VIII, we will investigate the nature of this restriction further. This shift in viewpoint is necessary; for although reciprocity is usually assumed to be valid for all uniform equilibrium systems, we will frequently encounter non-equilibrium processes that are not reciprocal (e.g. transistors and chemical reactions) and whose constitutive relation therefore cannot be characterized by a potential function.

The description of an n-port is, of course, considerably simplified when reciprocity holds. For when the Jacobian of $\underset{\sim}{\mathbb{F}}$ is symmetric, $\mathbb{F}$ may be expressed as a gradient vector field on $\mathbb{R}^n$. That is, all port constitutive relations are summarized by a single potential function and may be regained explicitly from the components of DU[*] (c.f., equation 1.3).

---

[*] For uniform fluid systems, another constitutive relation is usually postulated in addition to reciprocity: homogeneity. That is, given a reciprocal constitutive relation, one supposes that the fluid mass may be augmented by any desired amount without altering the values of the intensive variables (T, p, etc.) Hence, the constitutive assumption takes the form $U(\lambda \underset{\sim}{x}) = \lambda U(\underset{\sim}{x})$, i.e., U has the form of a generalized cone over $\mathbb{R}^n$.

We will have occasion to use this constitutive assumption frequently for processes occurring in uniform solutions. It is not a generally valid thermodynamic relation, but merely characteristic of a certain class of systems. For such systems, the Gibbs-Duhem relation allows us to eliminate one of the extensive variables.

1.4. State variables.

1.4.1.

The only dynamical "processes" permitted by classical thermodynamics are the reversible or "quasi-static" processes, which are merely a parametrized sequence of equilibrium states. We cannot obtain a true dynamical theory by "dividing an equilibrium equation by dt". Consequently, we will start with a dynamical theory and require that it reduce to the correct equilibrium theory. The basic procedure of network thermodynamics is as follows.

If the overall system is continuous, it is first subdivided mentally into homogeneous subsystems; and, as previously mentioned, each subsystem is further separated conceptually into reversible and irreversible parts. The reversible subsystems are assumed to store energy without loss, while the irreversible subsystems are assumed to dissipate energy without storage.*
Each of these subsystems will be identified with an n-port.

The fundamental thermodynamic quantity in this treatment is energy rate, or "power", instead of energy. Systems amenable to a network representation frequently share one common property: the energy rate processes may be expressed as a

---

*In electrical networks, this conceptual separation assumes concrete form: an ideal capacitor stores without dissipation, an ideal resistor dissipates without storage, and they may be approximated as separate physical devices.

product of an <u>effort</u> or force variable e and a <u>flow</u> variable f such that the power P = ef. (In electrical networks these are, of course, voltage and current.) Most thermodynamic processes can be so characterized. Note that we are <u>defining</u> effort and flow as the primitive state variables, rather than constructing them from the Gibbs equation, as is the usual practice; consequently, it is not necessary that their product have the units of power.

The variables e and f represent two types of "measurements" which may be carried out conceptually on each ideal subsystem. Since much of our terminology and notation is borrowed from circuit and system theory, we will not hesitate to introduce a somewhat colloquial but descriptive vocabulary into our discussion. Indeed, the engineering terminology employed to describe the conjugate variables e and f is that of <u>across</u> and <u>through</u> variables, suggesting that the potential variable or effort is a "two-point" measurement performed "across" the network element (or between a point and some implied reference state, e.g, voltage difference). The flow is imagined measured "through" an appropriate instrument, e.g. an ammeter, and is a "one-point" measurement.

These terms will be clarified subsequently, but here they serve to introduce, in an intuitive manner, some important topological notions.* They will be illustrated by a simple example from mechanics in Section II, which will also serve to introduce the topological graph notation.

We have taken e (effort) and f (flow) as our basic dynamical variables. In electrical network theory, one associates a current and a voltage with each branch of the network. The current is required to obey a local conservation law in the form of Kirchhoff's Current Laws (KCL), and the potential is required to be unique at each point of the network. This latter condition is just Kirchhoff's Voltage Law (KVL).

Kirchhoff's laws are restatements of conservation and continuity restrictions and are therefore independent of the nature of the elements comprising a network. They constitute a set of linear constraints on the instantaneous values that the through and across variables can attain. Since the form of these constraints depends only upon the way in which the network elements are connected, Kirchhoff's laws are called topological constraints. Viewing a network as another notation for the differential equations describing a system, Kirchhoff's laws are

---

*The classification of "extensive" and "intensive" variables makes little sense for nonequilibrium systems, since all "extension variables" must be reduced to local, or specific quantities, i.e., per unit mass or volume. Moreover, for the systems theory to be developed here, a quantity may or may not be additive, depending on the system topology, e.g. the additivity of voltages on capacitors depends on whether they are connected in series or in parallel (Redlich, 1970).

seen to be nothing more than the boundary conditions each subsystem imposes on its neighbors.

We will impose a similar requirement on our effort and flow variables: the through variables are *defined* by the requirement of conservation through subsystem boundaries while the across variables, by definition, are unique and continuous functions of position across the boundaries. We will refer to conserved, or through, variables generically as *KCL variables*, and potential, or across, variables as *KVL variables*.

1.4.2.

Since, in the network representation, the $\underset{\sim}{e}$ and $\underset{\sim}{f}$ variables are primary concepts, the displacements of classical thermodynamics appear in our theory as new state variables defined by integration. Thus, the generalized "displacement" $\underset{\sim}{q}$ is related to the flow $\underset{\sim}{f}$ by the definition:

$$\underset{\sim}{q}(t) \triangleq \underset{\sim}{q}(0) + \int_0^t \underset{\sim}{f}(t)\,dt. \tag{1.5}$$

Similarly, a generalized "momentum" (or "impulse") $\underset{\sim}{\wp}$ may be defined by integration of the effort $\underset{\sim}{e}$:

$$\underset{\sim}{\wp}(t) \triangleq \underset{\sim}{\wp}(0) + \int_0^t \underset{\sim}{e}(t)\,dt. \tag{1.6}$$

Thus, for example, the advancement of a chemical reaction ξ is a generalized displacement variable defined by:

$$\xi(t) \triangleq \xi(0) + \int_0^t J_r \, dt,$$

where J_r, the rate of the chemical reaction, is the flow variable. In electrical networks, the equivalent to the generalized momentum $\wp$ is the magnetic flux ϕ, which is related to the voltage v by an equation identical with 1.6.* Note that, since f and e are through and across variables, respectively, the derived quantities q and $\wp'$ are also, respectively, through and across variables.

Table 1 lists the most common choices of through and across variables encountered in practice.**

1.5. Constitutive relations

1.5.1

Before the state functions (e, f, $\wp$, q) can be used to describe the behavior of a real system, we must introduce the physical properties of the system. This is done by defining functional relationships between the state variables, called

---

*In mechanics, Newton's original definition of momentum was in the integral form, $\wp = \wp_0 + \int F dt$, i.e., a mass stores energy by accumulating the net effect of an applied force.

**Note that mechanical force is a KCL variable since it obeys a "conservation" rule, i.e., d'Alembert's Principle: $\Sigma F - F_I = 0$, where F_I is the "inertial force" $m\dot{v}$. This apparent reversal of role between effort and flow quantities arises from the use of Lagrangian (moving) coordinate frames in mechanics and Eulerian (stationary) frames in continuum theory (Trent, 1955).

<u>constitutive relations</u> (equations of state, characteristic equations, etc.). These functions must be determined either experimentally or from a "lower order" theory such as statistical mechanics.

Each constitutive relation relates a KCL variable (f or q) with a KVL variable (e or $\wp$). There are four possible binary relations between the four state variables.

In paragraph 1.3.2, we defined a multiport by its constitutive relation, $\underset{\sim}{\mathbb{F}}: \mathbb{R}^n \to \mathbb{R}^n$. Since there are four dynamical variables available to us now, we define four basic multiport elements by the following constitutive relations. The four possible constitutive relations are:

$$\begin{aligned}
&\text{(a)}\quad \underset{\sim}{\phi}_C(\underset{\sim}{e}, \underset{\sim}{q}) = \underset{\sim}{0} &&\text{capacitance;}\\
&\text{(b)}\quad \underset{\sim}{\phi}_L(\underset{\sim}{\wp}, \underset{\sim}{f}) = \underset{\sim}{0} &&\text{inductance;}\\
&\text{(c)}\quad \underset{\sim}{\phi}_R(\underset{\sim}{e}, \underset{\sim}{f}) = \underset{\sim}{0} &&\text{resistance;}\\
&\text{(d)}\quad \underset{\sim}{\phi}_M(\underset{\sim}{\wp}, \underset{\sim}{q}) = \underset{\sim}{0} &&\text{memristance.}
\end{aligned} \tag{1.7}$$

Now there are three ways to integrate the basic energy rate equation, $P = e \cdot f$:

$$\text{(a)}\quad E_C(t) = E_C(0) + \int_0^t \underset{\sim}{e} \cdot \underset{\sim}{f}\, dt = E_C(0) + \int_{\underset{\sim}{q}(0)}^{\underset{\sim}{q}(t)} \underset{\sim}{e}(\underset{\sim}{q})\, d\underset{\sim}{q}$$

$$\text{(b)}\quad E_L(t) = E_L(0) + \int_0^t \underset{\sim}{e} \cdot \underset{\sim}{f}\, dt = E_L(0) + \int_{\underset{\sim}{\wp}(0)}^{\underset{\sim}{\wp}(t)} \underset{\sim}{f}(\underset{\sim}{\wp})\, d\underset{\sim}{\wp}$$

$$\text{(c)}\quad E_D(0,t) \triangleq \int_0^t \underset{\sim}{e} \cdot \underset{\sim}{f}\, dt.^{*}$$

---

[*] Note that $E_D(-\infty, t) > 0$ is the passivity condition (Desoer and Kuh, 1969).

The first integral (1.8a) represents "displacement" or capacitive energy storage; in order to perform the integration, we require the constitutive function (1.7a) in the form $\underset{\sim}{e}(\underset{\sim}{q})$. For a linear electrical capacitor, this is just $e = q/C$. In an ideal mixture, the chemical potential of species i, μ_i, is the effort variable and the mole number n_i is the displacement variable. The constitutive relation is $n_i = V \exp(\frac{\mu_i - \mu_i^0}{RT})$, where V is the volume of the element and μ_i^0 is the reference potential. The <u>incremental capacitance</u> is defined as:

$$\underset{\sim}{C} \triangleq \frac{\partial \underset{\sim}{q}}{\partial \underset{\sim}{e}} = \left(\frac{\partial n_i}{\partial \mu_j}\right)_{V,T,n_j}, \qquad (1.9)$$

which, for an ideal mixture, gives $C_i = \frac{n_i}{RT}$.

The existence and uniqueness of the incremental capacitance C(e) is equivalent to the condition of "local equilibrium", which is the basic postulate underlying both network and conventional irreversible thermodynamics.

Energy may also be stored as a result of relative motion of mass or charge (i.e., kinetic or electromagnetic energy). If we are given the constitutive relation (1.7b) between $\wp$ and f, the second integration (1.8b) may be carried out. This type of energy storage is called inductive, or kinetic energy, and the <u>incremental inductance</u> is defined by:

$$\underset{\sim}{L} = \frac{\partial \underset{\sim}{\wp}}{\partial \underset{\sim}{f}}. \qquad (1.10)$$

The third integral (1.8c) represents energy dissipation. Time cannot be parametrized out of the integral, and the "resistive" constitutive relation (1.7c) between e and f must be supplied. For example, the effort conjugate to a diffusional flow J is a chemical potential difference $\Delta\mu$, and the <u>incremental resistance</u> is defined by:

$$\underset{\sim}{R} \triangleq \frac{\partial \underset{\sim}{e}}{\partial \underset{\sim}{f}} = \frac{\partial(\Delta \mu)}{\partial J}.$$

The fourth constitutive relation (1.7d) between integrated flow and integrated effort has not been employed in thermodynamics heretofore. Chua (1971) has given the name "memristance" to this relation, since it behaves dynamically like a displacement controlled resistance:

$$\underset{\sim}{\mathscr{p}} = \underset{\sim}{\psi}(\underset{\sim}{q}); \quad \dot{\underset{\sim}{\mathscr{p}}} = \underset{\sim}{D\psi}(\underset{\sim}{q})\,\dot{\underset{\sim}{q}}; \qquad \text{or} \quad \underset{\sim}{e} = \underset{\sim}{M}(\underset{\sim}{q})\,\underset{\sim}{f},$$

where $\underset{\sim}{M}(\underset{\sim}{q})$ is the "incremental memristance". For the present, we merely note that, from an axiomatic viewpoint, this constitutive relation is as fundamental as the other three and is encountered in engineering practice. Figure 1.2 is the "state diagram" illustrating these relationships. This diagram summarizes the entire logical structure of the dynamical systems dealt with here.

Each method of integration or energy processing requires a constitutive relation: $\underset{\sim}{e}(\underset{\sim}{q})$ for the first; $\underset{\sim}{f}(\underset{\sim}{\mathscr{p}})$ for the second;

and $\underset{\sim}{e}(\underset{\sim}{f})$ or $\underset{\sim}{f}(\underset{\sim}{e})$ for the third. We now introduce a symbolic shorthand for each process by defining ideal "elements", denoted by C, L, R, M, respectively. The process of energy storage and dissipation proceeds at each point in the system, but the elements C, L, R, M are to be regarded as conceptually separate subsystems, which communicate energetically only via ideal energy bonds. This separation, which is purely conceptual, will always regain in the appropriate limiting process the correct continuum behavior. We emphasize that the symbols (R, L, C, M) are merely a symbolic shorthand for the constitutive relations determining the method of energy processing.* The manner in which these elements, or subsystems, are to be connected is determined by the system topology and will be the subject of Section II.

The fact that each element may be characterized by a pair of conjugate variables with a unique constitutive relation between them is a fundamental postulate for our formalism. Physically,

---

* For convenience, we will also use separate symbols, E and F, to denote effort and flow sources, respectively. Sources are not new elements but may be viewed as nonlinear resistors. An effort source is a one-port resistor whose constitutive relation is $e(f) = E =$ constant for all f, while a flow source is a one-port resistor whose constitutive relation is $f(e) = F =$ constant for all e. Alternatively, an effort source may be viewed as a capacitor, with infinite capacitance, since for a capacitor $\frac{de}{dt} = \frac{f}{C}$, and, if $C \rightarrow \infty$, $e \rightarrow E =$ constant. Similarly, a flow source may be viewed as an inductor with infinite inductance.

it says that it is possible to choose a volume element small enough that its internal relaxation times are much shorter than those of the whole system, yet large enough to make fluctuations in the state parameters negligible.

The ideal elements R, L, C, M, E, F, plus one additional device to deal with energy coupling and transduction (introduced in Section II), are sufficient to represent, by ordinary differential state equations, most thermodynamic systems.

II. TOPOLOGICAL GRAPH REPRESENTATION FOR SIMPLE SYSTEMS

2.1. Representation of a mechanical model

2.1.1

In order to introduce the topological methods of representing physical systems, we shall consider a simple mechanical example consisting of masses, springs and dashpots. Such a system is inherently discrete and will serve as a convenient illustration to introduce the topological notions needed for the analysis of more complex biological systems. We shall not deal to any great extent with linear graph theory since it is adequately treated in the technical literature (Berge, 1962; Berge and Ghouila-Houri, 1965; Harary, 1969; Seshu and Reed, 1961).

The example consists of two masses, two springs and a dashpot connected as shown in Fig. 2. 1a.

According to Newton's second law, the sum of the forces acting on any element in this system must be equal to $m\dot{v}$; or

$$\sum F_i - m\dot{v} = 0, \qquad (2.1)$$

which is d'Alembert's principle. Considering $m\dot{v}$ as an inertial force, equation (2.1) has the same form as Kirchhoff's current law at a node. Therefore, mechanical forces may be treated as "through" variables, i.e., as a conserved quantity "flowing" through the element. The state variables of our system corresponding to the generalized variables e, f, q, $\wp$ are v', F, x' and $\wp$, where v' is the relative velocity, F is the force, x' the relative displacement, and $\wp$ the momentum. The relative velocity at any location in the system is a unique function of position, and therefore sums to zero around a closed loop. Hence relative velocity is a KVL variable. In mechanical systems, power is expressed as $P = Fv'$, and is therefore a product of a through and an across variable.

In mechanical systems force is a KCL variable; in electrical or thermodynamic systems it is a KVL variable. This peculiar difference is due to a change in the choice of coordinate system. Electrical or thermodynamic systems are generally described in a fixed or Eulerian coodinate system, while for mechanical systems it is more convenient to choose a Lagrangian coordinate system which moves with the particular element of the system. It is this difference in viewpoint which makes the mechanical forces KCL variables, while the electrical or thermodynamic potentials are KVL variables (Trent, 1955). [If, however, we generate the dual linear graph of a mechanical system, the forces become across variables and d'Alembert's principle may be interpreted as Kirchhoff's loop law. This leads to the usual "mass-inductance analogy"* and demonstrates the

---

*The mass-inductance correspondence, however, fails for nonplanar graphs (Shearer et al., 1967).

flexibility of the choice of KCL and KVL variables.]

Now let us examine in some detail the characteristics of the elements composing the mechanical system. We wish to demonstrate that the masses, the springs and the dashpot can each be identified with the appropriate branch of a linear graph, or network, and so may be regarded as a *one-port*, or *two-terminal*, element. A two-terminal element has two distinguishable ends or terminals, as is the case with an electrical resistor or mechanical spring. In a more abstract sense, a one-port element may be considered any element which can be described by a constitutive relation between a single through and a single across variable. This notion, as we have seen, can be generalized: an n-port element is describable by a constitutive relation between n-through and n-across variables represented geometrically as an n-dimensional constitutive surface in a 2n-dimensional space.

a). *The ideal spring* has no mass and the forces acting at each point of the spring must balance; thus force is transmitted "through" the spring. The force developed by the spring depends on x', the instantaneous displacement of its ends or terminals from the equilibrium position $\bar{x}$, i.e., $x' \equiv x - \bar{x}$. Evidently x' is an across variable.

The spring is characterized by a relation between one through and one across variable and is accordingly a two-terminal or one-port element. In a linear graph, the spring is represented by a branch whose terminals correspond to those of the spring itself.

The spring may be considered as a generalized inductor since its constitutive relation

$$x' = g_L(F) \tag{2.2}$$

can be differentiated to yield

$$v' \equiv \frac{dx'}{dt} = \frac{dg_L}{dF}\frac{dF}{dt}. \tag{2.3}$$

If we denote dg_L/dF by L, and identify the force F with the KCL variable f, and the across variable v' with e, equation (2.3) becomes

$$e = L\frac{df}{dt},$$

which is isomorphic to the inductor equation. The energy stored by the spring at any instant of time is given by

$$E = \int F dx' \tag{2.4}$$

which, for a linear constitutive relation, $F = g_L^{-1}(x') = Kx'$, gives the quadratic form

$$E = \frac{1}{2} K(x')^2.$$

b). <u>The ideal dashpot</u> is a purely dissipative element, analogous to a generalized resistor, and is characterized by a constitutive relation between the force F and the velocity v'. The velocity v' is the relative velocity of the dashpot ends $v' = v_1 - v_2$, where v_1 and v_2 are the velocity of the terminals of the dashpot with respect to an arbitrarily chosen ground. The dashpot is clearly a two-terminal element and is represented in the linear graph by a branch. The constitutive relation of the dashpot generates a state function, "the content" $G \equiv \int_0^F v'dF$. For linear constitutive relations,

$$v' = g_R(F) = RF \tag{2.5}$$

$$G = \int_0^F v'dF = \frac{1}{2} RF^2. \tag{2.6}$$

c). <u>The mass</u> is an element whose momentum obeys a "universal" constitutive relation

$$\not{p} = m_0 v(1 - \frac{v^2}{c^2})^{-1/2}. \tag{2.7}$$

In most applications, the velocity v of the mass is so small, as compared to the velocity of light, that $\not{p} = mv$ is a valid approximation. It is not obvious that the mass is a two-terminal object until one considers how its velocity is measured. The mass stores energy due to its motion relative to an inertial reference frame, i.e., v is actually $v' = v - v_g$, where v_g is the velocity of the "ground" (or inertial frame). To establish the mass as a two-terminal element, we place one terminal on the mass itself and the other on the ground with respect to which v' is measured. The constitutive relation for the mass is Newton's law, $m(dv/dt) = F$. If we note that F is a through variable (f) and v an across variable (e), and identify m with the capacitance C, we see that a mass is isomorphic to a generalized capacitor:

$$C\frac{de}{dt} = f.$$

Let us now come back to the system of 2 masses, 2 springs and a dashpot represented in Fig. 2.1a. The "wiring" diagram of the hypothetical instruments ("across meters") required to continuously monitor the state of each element is shown in Fig. 2.1b. Since the nodes (b, c, e, 1) and (f, d, 2) have the same velocity, they may be identified and the system represented schematically as in Fig. 2.1c. Finally, by suppressing the element symbols, we arrive at the structure shown in Fig. 2.1d, which is called a linear graph, or topological graph. In this form, only the system connections, i.e., the topological relationships between elements, are displayed.

If we append a set of arbitrary sign conventions to the graph, as shown in the figure, we obtain a <u>directed graph</u>. Associated with each branch of the graph are two dynamical quantities, one obeying KCL and the other KVL: in this example they are the force and the velocity difference.

2.1.2

Let us now write Kirchhoff's laws explicitly using the numbering and sign conventions on the graph. For the node laws (KCL), a branch will be considered positive if it is directed out of a node and negative if it is directed into a node. For the loop laws (KVL), we number the m loops or "meshes" and define clockwise as the positive mesh direction, so that a branch bounding a mesh is positive if it agrees with the mesh direction and negative otherwise. Hence, in Fig. 2.1d,

$$\begin{array}{lll} \text{KCL:} & \text{Node A;} & F_1 + F_2 + F_4 + F_5 = 0 \\ & \text{Node B:} & F_3 - F_4 - F_5 = 0 \\ & \text{Node g:} & -F_1 - F_2 - F_3 = 0. \end{array} \tag{2.8}$$

$$\begin{array}{lll} \text{KVL:} & \text{Mesh a:} & -v_1 + v_2 = 0 \\ & \text{Mesh b:} & -v_2 + v_3 + v_4 = 0 \\ & \text{Mesh c:} & -v_4 + v_5 = 0. \end{array} \tag{2.9}$$

Note that only two of the three node equations are linearly independent; so, by convention, we may omit the ground node from our considerations.

Equations (2.8) and (2.9) may be written in matrix form by introducing the state vectors $\underset{\sim}{F} = (F_1, F_2, F_3, F_4, F_5)$, $\underset{\sim}{v} = (v_1, v_2, v_3, v_4, v_5)$.

$$\text{n nodes}\left\{\underbrace{\begin{bmatrix}1&1&0&1&1\\0&0&1&-1&-1\end{bmatrix}}_{\text{b-branches}}\right. \begin{bmatrix}F_1\\F_2\\F_3\\F_4\\F_5\end{bmatrix} = 0 \quad \text{or } \underset{\sim}{A} \cdot \underset{\sim}{F} = \underset{\sim}{0}\,; \tag{2.10}$$

$$\text{m meshes}\left\{\underbrace{\begin{bmatrix}-1&1&0&0&0\\0&-1&1&1&0\\0&0&0&-1&1\end{bmatrix}}_{\text{b-branches}}\right\} \begin{bmatrix}v_1\\v_2\\v_3\\v_4\\v_5\end{bmatrix} = 0 \quad \text{or } \underset{\sim}{M} \cdot \underset{\sim}{v} = \underset{\sim}{0}. \tag{2.11}$$

These matrices could have been obtained directly from the graph by the following algorithm:

$$a_{ij} = \begin{cases} +1 & \text{if branch } j \text{ is directed out of node } i \\ -1 & \text{if branch } j \text{ is directed into node } i \\ 0 & \text{otherwise} \end{cases}$$

$$m_{kj} = \begin{cases} +1 & \text{if branch } j \text{ bounds mesh } k \text{ in the positive direction} \\ -1 & \text{if branch } j \text{ bounds mesh } k \text{ in the negative direction} \\ 0 & \text{if branch } j \text{ is not in mesh } k \end{cases}$$

The matrices A and M are called the connection matrices for the linear graph since they summarize how the system is "hooked up," i.e., its topology. It may be shown that, for continuum systems, A and M are related to the vector field operators divergence and curl (Branin, 1962, 1966).

The equations of motion for an arbitrarily complicated system can be written down simply and algorithmically by constructing the linear graph for the system, writing the connection matrices and substituting in the constitutive relations for the elements (Desoer & Kuh, 1969). The mathematical role of the conservation and continuity conditions as embodied in KCL and KVL is to impose certain linear restrictions on the possible behavior of each element in the system, i.e., the complete 2b-dimensional space of states is restricted to a set of linear subspaces (the Kirchhoff subspace). In this fashion, the elements act as boundary conditions on one another, giving the entire assembly a dynamical character which is quite different from the subunit behavior. The connection matrices provide a simple and important method of coding the system topology in a three word code: (+1, -1, 0). Of course, the present system was conveniently <u>discrete</u> to begin with; however, the same technique can be applied to general thermodynamic systems by constructing the appropriate graphical representations.

The fact that $\underset{\sim}{F}$ acts as a conserved quantity and $\underset{\sim}{v}$ is a unique function of position can be summarized in two alternate expressions of Kirchhoff's laws. We define two new state vectors as follows (Desoer & Kuh, 1969):

(i) Since the velocity is a unique function of position, we may determine the velocity difference v' across each branch by measurements with respect to the common ground node g, (the inertial frame), e.g. $v_5' = v_B - v_A = (v_A - v_g) - (v_B - v_g)$. Therefore, if we define a new state vector $\hat{v}$, whose components are the node to ground velocity differences $(v_k - v_g)$, KVL may be written in the alternative form:

$$\underset{\sim}{v} = \underset{\sim}{A}^{T} \hat{\underset{\sim}{v}} . \tag{2.12}$$

(ii) By assigning a flow to each mesh of the linear graph, another state vector may be defined, $\hat{\underset{\sim}{F}} \equiv (F_a, F_b, F_c)$. We may regard each branch flow to be a linear combination of mesh flows, e.g., $F_4 = F_b - F_c$. Then KCL may be written in the equivalent form:

$$\underset{\sim}{F} = \underset{\sim}{M}^T \, \hat{\underset{\sim}{F}} \, . \tag{2.13}$$

The reader may easily verify by direct multiplication the following crucial fact concerning the connection matrices $\underset{\sim}{A}$ and $\underset{\sim}{M}$:

$$\begin{aligned} \underset{\sim}{A}\underset{\sim}{M}^T &= 0, \\ \underset{\sim}{M}\underset{\sim}{A}^T &= 0. \end{aligned} \tag{2.14}$$

These relations may be summarized as follows (Branin, 1962, 1966):

$$\begin{tikzcd}
\hat{\underset{\sim}{F}} \arrow[r, "\underset{\sim}{M}^T"] & \underset{\sim}{F} \arrow[r, "\underset{\sim}{A}"] & \underset{\sim}{0} & \text{(KCL)} \\
\underset{\sim}{0} & \underset{\sim}{v} \arrow[l, "\underset{\sim}{M}"'] & \hat{\underset{\sim}{v}} \arrow[l, "\underset{\sim}{A}^T"'] & \text{(KCL)} \\
\text{mesh} & \text{branch} & \text{node} &
\end{tikzcd}$$

Let us now examine the total power flowing in the system:

$$\underset{\sim}{F}^T \underset{\sim}{v} = \sum_{i=1}^{b} F_i v_i \, . \tag{2.15}$$

From equations (2.10) and (2.12),

$$\underset{\sim}{F}^T \underset{\sim}{v} = \underset{\sim}{F}^T \underset{\sim}{A}^T \hat{\underset{\sim}{v}} = (\underset{\sim}{A}\underset{\sim}{F})^T \hat{\underset{\sim}{v}} = 0. \tag{2.16}$$

The statement $\underset{\sim}{F}^T \underset{\sim}{v} = 0$, or in general for any set of KCL and KVL variables

$$\underset{\sim}{e}^T \underset{\sim}{f} = 0, \tag{2.17}$$

is known as <u>Tellegen's Theorem</u>, and may be interpreted as an orthogonality condition between the state vectors $\underset{\sim}{F}$ and $\underset{\sim}{v}$ in $\mathbb{R}^{2b}$ (Tellegen, 1952; Brayton & Moser, 1964; Penfield et al., 1970). In paragraph 8.7 we will derive several important thermodynamic results from this theorem. It is important to realize that only

KCL and KVL were employed in the derivation of Tellegen's Theorem; it is thus seen to depend only on the system topology and is completely independent of the nature of the elements represented by the branches (nonlinear, time dependent, etc.).

2.2 Nonelectrolyte diffusion through a homogeneous membrane

The extension of the linear graph concept to a continuous system such as membrane transport is a straightforward operation. The system we will consider consists of a homogeneous membrane and two bounding reservoirs, Fig. 2.2a. The transport of a chemical species across the membrane is accompanied by the loss of free energy stored in the chemical potential difference between the two reservoirs. In addition to transport, before a steady state is reached, the membrane acts as a reversible capacitor, able to store some of the chemical species being transported. We will conceptually separate these processes and assume that the membrane consists of three regions. The central layer represents the membrane capacitance in which storage, but no dissipation, occurs, while the outer layers represent transition regions across which dissipation, but no storage, of free energy occurs. Our model may be made more accurate by partitioning the membrane into infinitesimal volume elements and then conceptually separating each of these volume elements into two subsystems, one of which represents the capacitance, and one the resistance, of the volume element (Fig. 2.2b). In paragraph 3.3 we will show that in the limit this process leads to the usual continuum equations. It is important to realize that we are not assuming that the membrane is actually composed of layers, but rather we are merely assigning individual elements to separate processes.

The primary step in constructing an isomorphism between the physical system and the topological graph is the assignment of a branch to each element. We then associate with each branch a thermodynamic flow variable, f, and a force or effort variable, e, in such a way that an exact correspondence is established between the network equations and the thermodynamic relations.

Consider first the transition regions of the membrane, as in Fig. 2.2, which represent the dissipative processes associated with the transport of a nonelectrolyte through the membrane. We may represent each of these dissipative "elements" by a branch, as shown in Fig. 2.3a. For the left transition region, we associate its branch with the effort $\Delta\mu = \mu_1 - \mu_m$ and the flow J_m^1 across this region. Similarly for the right transition region, we associate the effort $(\mu_m - \mu_2)$ and the flow J_m^2. Note that a reference direction has been chosen and that the product of the effort and flow variables is the power (free energy) dissipated in each element.

Next, consider the central layer of the membrane and the two bounding reservoirs, which are all compartments in which storage, but no dissipation, of free energy occurs. The representation of these reversible elements requires additional consideration since apparently no force of the nature of $\Delta\mu$ can be assigned to the reservoirs. In reality, however, the chemical potentials characterizing the reservoirs and the membrane compartment are not uniquely determined unless they are referred to a standard reference potential, $\bar{\mu}$. The theory of potential measurement implies the explicit consideration of $\bar{\mu}$, which has the same value for the permeant in the reservoirs and the membrane. Thus the branch representing reservoir 1, for example, can be drawn as shown in Fig. 2.3b. Associated with this directed branch is the effort $\mu_1 - \bar{\mu}$ and the flow J_1. One usually does not consider reservoir flows, but such a flow can be <u>defined</u> as dn_i/dt, where n_i is the number of moles of the permeant in the reservoirs. The product of the effort and flow variable, $J_1(\mu_1 - \bar{\mu})$, is the power delivered by the reservoir to the membrane.

The fact that it is usually permissible to assume that $\bar{\mu} = 0$ does not diminish the importance of the reference potential and its implied definition in the reversible forces of thermodynamic systems. (We draw the part of the branch representing the capacitive elements as a broken line, to remind us that there is no actual flow into the reference nodes.) The analogous situation was encountered in the previous section, in representing the mass as a two-terminal element. (Note that the branches of the linear graph have no "geometrical" significance here; e.g. the reversible flows are in no sense "perpendicular" to the plane of the membrane.) With these remarks, and noting that reservoirs 1 and 2 and the central membrane layer are treated similarly, the total membrane system assumes the form shown in Fig. 2.3c.

It may be immediately noted that the reference nodes in each compartment have the same value of $\overline{\mu}$, i.e., they are characterized by the same magnitude of the local parameters of state. This observation is of importance to the network formulation, for each node of a network is characterized by a unique value of a state function, and hence the three reference terminals may be combined into a single node. Similarly, we may connect the other terminals of equal chemical potential into single nodes as shown in Fig. 2.4.

We see that the topological graph structure comprises two meshes, (1) and (2), to which we have assigned, arbitrarily, a clockwise sign direction. Let us now sum the forces operating along the branches enclosing each of the meshes. The forces are regarded as positive when directed in the same direction as the mesh circulation and negative if directed in the opposite sense. For mesh (1), the sum of the forces is: $(\mu_1-\bar{\mu}) - (\mu_m-\bar{\mu}) - (\mu_1-\mu_m) = 0$; and similarly for mesh (2): $(\mu_m-\bar{\mu}) - (\mu_2-\bar{\mu}) - (\mu_m-\mu_2) = 0$. These are simple examples of Kirchhoff's Voltage Law for a thermodynamic system. The law, in its most general form, states that if thermodynamic potentials can be assigned uniquely to the nodes of a graph, the sum of the forces (taken with appropriate sign) around any mesh of the graph equals zero.

The other restriction imposed on every node is Kirchhoff's Current Law (KCL), which is an expression of the assumption that the flows passing a node are conservative; there is, by definition, no accumulation or depletion at the nodes.* The static character of the nodes does not imply that the process is stationary, but only that the nodes are abstract entities which have no capacity to store matter or charge, and hence are maintained at a steady state. Since the majority of thermodynamic flows are conservative, or can be chosen to be conservative,

---

*If we write the continuity equation for a volume element surrounding a node, it takes the form

$$\frac{\partial \rho}{\partial t} = \nabla \cdot J.$$

If we further assume that matter is neither accumulated nor depleted at the node, then $\partial \rho/\partial t = 0$ and $\nabla J_i = 0$. In the discrete representation this implies that the sum of the flows of a given species at a node is zero, which is, of course, Kirchhoff's Current Law.

and since the thermodynamic state functions are defined uniquely, the thermodynamics of flow processes can be readily fitted into a topological graph representation.

In order to write the KCL equations, a sign convention for the flows must be adopted. Although we can choose the directions of flow arbitrarily, we will retain the convention that a flow entering a node is negative and a flow leaving a node is positive.

Having chosen a sign convention, we may now apply KCL to the four nodes of Fig. 2.4; doing so, we obtain the equations

$$\begin{aligned}
&J_1 + J_m^1 = 0\\
&-J_m^1 + J_m + J_m^2 = 0\\
&-J_m^2 + J_2 = 0\\
&-J_1 - J_2 - J_m = 0
\end{aligned} \tag{2.18}$$

These equations are not linearly independent, and by convention we will exclude the equation for the reference node, leaving a set of three linearly independent constraint equations on the branch currents. These equations reduce the number of independent flows from five to two. Generally, J_m^1, the influx into the membrane, and J_m^2, the outflux from the membrane, are considered as the independent flows. The set of all thermodynamic flows and thermodynamic forces constitutes a vector space. KCL and KVL are a set of linear constraints and, as mentioned above, restrict the flows and forces to a set of hyperplanes in this space.

At this point it is advantageous to pause and consider the energetic aspects of the permeation process described above. According to the treatment of nonequilibrium thermodynamics, the dissipation function ϕ of the membrane system under isothermal conditions is given by the sum of the products of the dissipative flows J_m^1 and J_m^2 and the forces across the resistive elements $\mu_1 - \mu_m$ and $\mu_m - \mu_2$, i.e.,

$$\phi = J_m^1(\mu_1 - \mu_m) + J_m^2(\mu_m - \mu_2) . \tag{2.19}$$

On the other hand, the free energy change accompanying the charging or discharging of the reservoirs, dG/dt, may also be expressed as a sum of terms having the dimension of power:

$$\frac{dG}{dt} = (\mu_1 - \bar{\mu})J_1 + (\mu_m - \bar{\mu})J_m + (\mu_2 - \bar{\mu})J_2 . \tag{2.20}$$

Adding equations (2.19) and (2.20) and inserting the KCL requirements (2.18), we find that

$$\frac{dG}{dt} + \phi = 0 . \tag{2.21}$$

This is a well known result of nonequilibrium thermodynamics: the dissipation is measured reversibly by the drop in the free energy of the adjacent reservoirs, $\phi = -(dG/dt)$.

In the present theory, however, equation (2.21) represents a special case of Tellegen's theorem. Inserting (2.19) and (2.20) explicitly into (2.21), we find that

$$J_m^1(\mu_1 - \mu_m) + J_m^2(\mu_m - \mu_2) + J_1(\mu_1 - \bar{\mu}) + J_m(\mu_m - \bar{\mu}) + J_2(\mu_2 - \bar{\mu}) = 0 \tag{2.22}$$

Equation (2.22) may be regarded as a scalar product of a general flow vector $\underset{\sim}{J}$ and a general force vector $\underset{\sim}{X}$, the components of which are

$$\underset{\sim}{J} = \begin{pmatrix} J_m^1 \\ J_m^2 \\ J_1 \\ J_m \\ J_2 \end{pmatrix} \qquad \text{and} \qquad \underset{\sim}{X} = \begin{pmatrix} \mu_1 - \mu_m \\ \mu_m - \mu_2 \\ \mu_1 - \bar{\mu} \\ \mu_m - \bar{\mu} \\ \mu_2 - \bar{\mu} \end{pmatrix} \qquad (2.23)$$

or

$$\underset{\sim}{X} \cdot \underset{\sim}{J} = 0. \qquad 2.24$$

Equation (2.24) has the same interpretation as equation (2.17): the full 2b-dimensional thermodynamic space of states is partioned into two fixed <u>orthogonal</u> subspaces -- the subspace of the flows and the subspace of the forces.

2.3 The relaxation time of a single permeation flow

To consolidate our ideas about the network representation for membrane processes we shall consider a relaxation experiment in which the flow across the membrane develops towards a steady state. It is assumed that the membrane is initially free of permeant, and that at a given moment (t=0) it is put into contact with two reservoirs with chemical potential μ_1 and μ_2, respectively. The problem is to find the relaxation time for the "charging" of the membrane capacitance with the permeant.

As we did above for the reservoir flows, we define the membrane flow $J_m = dn_m/dt$. From Fig. 2.4 and equation (2.18) it is clear that the rate of permeant accumulation in a membrane of unit area is

$$\frac{dn_m}{dt} = J_m \cdot 1\ \mathrm{cm}^2 = (J^1_m - J^2_m)\ 1\ \mathrm{cm}^2. \qquad (2.25)$$

To make use of equation (2.25) we substitute for dn_m/dt its equivalent in terms of chemical potential and capacitance, and relate J^i_m to its driving force by a suitable constitutive relation. It is clear that

$$dn_m/dt = (dn_m/d\mu_m)(d\mu_m/dt)$$

or, with equation (1.9),

$$J_m = dn_m/dt = C_m(d\mu_m/dt). \qquad (2.26)$$

The simplest dissipative relation between flow and force is the linear phenomenological relation of nonequilibrium thermodynamics

$$J^i_m = L_i \Delta\mu_i = \frac{\Delta\mu_i}{R_i}, \qquad (2.27)$$

which in the present case assumes the form

$$J^1_m - J^2_m = \left(\frac{\mu_1 - \mu_m}{R_1} - \frac{\mu_m - \mu_2}{R_2}\right) = \left(\frac{\mu_1}{R_1} + \frac{\mu_2}{R_2}\right) - \mu_m\left(\frac{1}{R_1} + \frac{1}{R_2}\right). \qquad (2.28)$$

If we let R_m denote the total membrane resistance,* then we can associate half of this resistance with each of the membrane transition layers, i.e., $R_1=R_2=R_m/2$; equation (2.25) then takes the simple form

$$\frac{d\mu_m}{dt} = 2\left(\frac{\mu_1+\mu_2}{R_m C_m}\right) - \left(\frac{4}{R_m C_m}\right)\mu_m \;. \tag{2.29}$$

By examining the homogeneous part of equation (2.29), it is clear that the relaxation time of the process is of the same form as in electrical networks:

$$\tau_m = \frac{R_m C_m}{4} \;. \tag{2.30}$$

Equation (2.29) may now be written in the form

$$\tau_m \frac{d\mu_m}{dt} = \frac{\mu_1+\mu_2}{2} - \mu_m = \langle \mu \rangle - \mu_m, \tag{2.31}$$

where $\langle \mu \rangle = \dfrac{\mu_1+\mu_2}{2}$.

---

* In nonequilibrium thermodynamics we write a linear constitutive relation for the local flows and local forces $J = L\,(-d\mu/dx)$, where for an ideal solution $L = cD/RT$ and D is the diffusion constant. Assuming L to be constant, the integration over a membrane of thickness Δx gives, for a constant flow

$$J\int_0^{\Delta x} dx = L\int_0^{\Delta\mu} (-d\mu) \qquad \text{or} \qquad J\,\Delta x = L\,\Delta\mu \;.$$

Therefore,

$$J = \frac{\Delta\mu}{RT\Delta x/cD} \quad \text{and } R_m = \frac{RT\Delta x}{c_m D_m} \;.$$

The solution of equation (2.31) for constant τ_m is straightforward and need not be considered here. To get a feeling for the meaning of τ_m it is worth noting that for the simple membrane transport process we are discussing,

$$R_m = RT\Delta x/c_m D_m, \qquad (2.32)$$

where Δx is the thickness of the membrane and D_m the diffusion coefficient in the membrane. The capacitance of the membrane is given by

$$C_m = \partial n_m/\partial \mu_m = c_m V/RT, \qquad (2.33)$$

where for simplicity we have assumed that the constitutive relation between μ and n is that of an ideal solution. Since the membrane is being charged symmetrically from both sides, we must consider only the time for diffusion across half the membrane volume. Noting that the membrane volume per unit area is $V = \Delta x \cdot 1\text{cm}^2$ and taking into consideration the symmetrical filling, we find,

$$C_m = c_m \Delta x/2RT. \qquad (2.34)$$

Inserting equations (2.32) and (2.34) into equation (2.31), we obtain

$$\tau_m = \frac{R_m C_m}{4} = \frac{RT\Delta x}{4c_m D_m} \; \frac{c_m \Delta x}{2RT} = \frac{(\Delta x/2)^2}{2D_m}, \qquad (2.35)$$

which is identical with the well known equation of Einstein

$$2D_m \tau_m = (\frac{\Delta x}{2})^2 \; .$$

III. THE BOND GRAPH REPRESENTATION

3.1 Bond graph fundamentals

3.1.1

The next step in the network analysis of thermodynamic systems is the discussion of coupled flows. However, linear graph notation becomes cumbersome when applied to systems involving energy transductions: a separate graph is required for each energy domain and the energetic relationships are obscured. During the last few years, another method of representation, called bond graphs, has been developed which is more suitable than topological graphs for the description of physical systems (Paynter, 1961; Karnopp & Rosenberg, 1968). To introduce the method, we shall start again with a single permeation process across a homogeneous membrane and then proceed to more complex systems.

The basic element of the bond graph is the "ideal energy bond." As pointed out in paragraph 1.3.2, a bond is regarded as a perfect conductor which transmits power instantaneously and without energy loss. In this respect it is an idealization similar to perfect electrical conductors or infinitely stiff rods. As in the case of topological graphs, we must assume some sign convention in order to apply Kirchhoff's laws. This choice is for the most part arbitrary. We shall indicate bond orientations by appending to them a half-arrow ($\rightharpoondown$).

The network elements that we shall use in bond graphs are resistors, capacitors, inductors and effort sources (transduction will be discussed in Section IV), which we represent by the generic symbols denoting their constitutive relations: R, C, L and E. To each letter we adjoin a single line segment which represents an ideal energy bond. This bond replaces the *pair* of wires used in circuit representation, i.e., the branches of the linear graph. With each bond we associate an effort and flow variable, e.g. $\underset{f}{\overset{e}{-\!\!-\!\!-}}$ R.

3.1.2

In circuit theory, one can in principle choose independent reference directions for current and voltage. However, it is both customary and convenient to choose *associated reference directions*; that is, one assumes the current flow is positive if it flows from the positively marked terminal to the negatively marked terminal. Both associated and nonassociated reference directions are illustrated in Fig. 3.1. In bond graphs, we shall adopt the convention that on bonds oriented into elements the effort and flow have associated reference directions, e.g.

$\rightharpoondown$ R denotes associated reference directions and

$\leftharpoondown$ R denotes nonassociated reference directions.

Notice from Fig. 3.1 that for a linear resistor $v = iR$ when associated reference directions are chosen, but that $v = -iR$ with nonassociated reference directions. Similarly in bond graphs

$$\xrightharpoonup[f]{e} R \text{ implies } e = Rf, \text{ while}$$

$$\xleftharpoondown[f]{e} R \text{ implies } e = -Rf.$$

The reader with a background in circuit theory is forewarned that in the following sections we shall have occasion to use nonassociated reference directions.

When the product of the effort and flow variables has the dimensions of power, as will be the case in all that follows, then the power delivered to any element will obey the following equation:

$$P_{\text{delivered}} = \begin{cases} e \cdot f & \text{for associated reference directions} \\ -e \cdot f & \text{for nonassociated reference directions} \end{cases}$$

Thus we see that the half-arrow on an oriented bond indicates the reference direction for positive power flow. Power does not necessarily flow in the direction indicated by the half-arrow, but when power is flowing in this direction it is taken to be positive. Thus if power flows out of an effort source, we shall use the convention $E \rightharpoondown$, while $E \leftharpoonup$ denotes an effort sink.

The useful innovations introduced by the bond graph method are two ideal junctions: a parallel or "zero-junction" denoted as 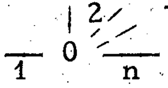

and a series or "one-junction" denoted as 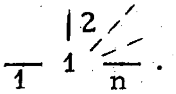

. Each bond in the graph is numbered; and associated with the i'th bond is an effort e_i and a flow f_i. Occasionally, and especially for simple bond graphs, the e's and f's will be written directly on the graph, e.g.

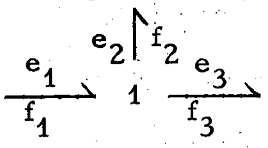

Note that a sign convention has been chosen for this one-junction.

Since power is neither stored nor dissipated at an ideal junction, the total power entering any junction must equal the power leaving the junction:

$$\sum_{i=1}^{n} \sigma_i e_i f_i = 0, \tag{3.1}$$

where σ_i equals +1 if bond i is directed out of the junction and $\sigma_i = -1$ if it is directed toward the junction. In a parallel array of elements, the forces on each element are equal. Thus we shall define the zero-junction by the constraint condition

$$e_1 = e_2 = \cdot \cdot \cdot \; e_n \equiv e \tag{3.2}$$

and by equation (3.1):

$$\sum_{i=1}^{n} \sigma_i f_i = 0 \tag{3.3}$$

Hence a zero-junction obeys Kirchhoff's Current Law and consequently corresponds to a node of the topological graph.* All of the efforts on the zero-junction are assumed to be equal and thus necessarily have the same sign. The flows f then determine the direction of power flow, and their reference directions must agree with the sign convention assigned to the bonds incident on the zero-junction.

On the other hand, a series arrangement of elements has a single flow, since f is conserved, and hence a one-junction will be defined by

$$f_1 = f_2 = \cdot \cdot \cdot f_n \equiv f, \qquad (3.4)$$

which upon insertion into equation (3.1) gives

$$\sum \sigma_i e_i = 0, \qquad (3.5)$$

i.e, KVL. This junction is a useful device for the grouping of all bonds having the same flow.

Let us now redraw Fig. 2.4 and denote each branch of the topological graph by the symbols for the elements (Fig. 3.2a). We can immediately translate Fig. 3.2a into a bond graph by assigning to every node of the figure a zero-junction, and to each resistor or capacitor a one-junction with three bonds

---

* Alternatively, if the product e · f did not have the dimensions of power, we could simply define the zero-junction by equations (3.2) and (3.3).

which connect the two adjacent zero-junctions to the element itself. By following this procedure and then assigning reference directions to the bonds, we arrive at Fig. 3.2b. It will be observed that every node of the topological graph is now a zero-junction. The one-junctions have replaced the branches of the linear graph through which a unique current flowed. However, only the bond on the one-junction that connects to an element (i.e., the energy "port") represents a branch of the topological graph; the other bonds that connect the one-junction to the zero-junction have no counterpart in topological graphs and may be used to represent geometrical quantities (dimensions) in the physical system.

Thus the meaning of, say, the combination of elements

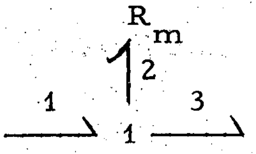

is that at this junction $-\mu_1+\mu_2+\mu_3 = 0$ and the same flow J^1_m which enters the system passes the resistor R^1_m; or that a flow J^1_m, driven by a force $(\mu_1-\mu_3) = \mu_2$, is regulated by a resistance R^1_m.

Alternatively, if we had chosen the sign convention

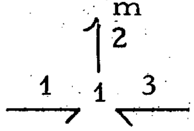

for the one-junction, the driving force for the flow J^1_m would have been $\mu_1 + \mu_3$. Since physically the driving force is always a "drop" in potential, we shall adopt the former sign convention for one-junctions.

The graph 3.2b is rather cumbersome and difficult to handle. It may, however, be simplified appreciably in the following way. First, we may assume that the reference potential $\overline{\mu} \equiv 0$. When $\overline{\mu} = 0$, the power transmission along all bonds incident on the ground node is zero, so they may be eliminated. The bond graph may now be drawn as in Fig. 3.2c, in which all bonds leading to the zero-junction of $\overline{\mu}$ are deleted.

Both zero-junctions and one-junctions which have only two bonds incident in the same direction merely transfer power and may also be eliminated. For example, consider a zero-junction

$$\xrightharpoondown[f_1]{e_1} 0 \xrightharpoondown[f_2]{e_2} .$$

By definition, $e_1 = e_2$; and by KCL, $-f_1+f_2 = 0$ or $f_1=f_2$. Hence the junction serves no purpose and may be removed from the graph. Similarly, for a one-junction there is, by definition, a common flow through the junction and $f_1=f_2$. Applying KVL, we see that $-e_1+e_2 = 0$ or $e_1=e_2$; and thus, the one-junction with only two bonds connected to it, both pointing in the same direction, may also be deleted from the bond graph.

When we apply these simplifications to Fig. 3.2c, the bond graph assumes its final form, as shown in Fig. 3.2d. It is readily apparent that Fig. 3.2d is very close to the physical representation (Fig. 2.2a).

3.2 Causality

The bond graph representation may be amplified by the introduction of another piece of information, called "experimental causality." Consider, for example, the filling of the membrane compartment by the permeant. The process is represented by equation (2.26) as $C_m(d\mu_m/dt) = J_m$. It is evident that μ_m cannot change instantaneously (i. e., $d\mu_m/dt < \infty$) unless the flow J_m becomes infinite. Similarly, an electrical capacitor which obeys the equation $C(dV/dt) = i$, or any capacitive element — for which we may write $C(de/dt) = f$ — may change its effort e only according to the dictum of the flow variable f. The flow is therefore the "natural" input (i. e., independent) variable for a capacitive element. The converse is true for inductive elements, such as a mechanical or electrical inductor, for which the basic relation is $L(df/dt) = e$; i. e., inductors have the effort e as their natural input, since an arbitrary flow (velocity) may not be imposed on the element (mass) as an initial condition. In the case of a resistor, there is no independent variable of choice, since the relation between flow and effort contains no time derivatives. It should be clear that the recognition of the independent variable, i. e., the causal relation, is nontrivial, as may be seen in the example of an R constitutive relation such as is encountered in a tunnel diode or nerve membrane (Fig. 3.3).

Evidently, to any value of e there corresponds a single value of f, while for a single value of f we may have three values of e. Thus it is important to know which is the independent variable, and the introduction of a suitable symbol for this notion is useful. Paynter (1961) has suggested appending to a bond a vertical bar, called a "causal stroke," with the following meaning: an element adjacent to the vertical bar is governed by the effort variable. Therefore inductive elements are written as L ├── ; on the other hand, when the causal stroke is placed at the opposite end of the bond, the element has the flow f as an independent variable, so that capacitive elements should be written as C ──┤ . Resistors may be of either type: R ├──, effort-controlled, or R ──┤, flow-controlled. (An easy way to remember the causality convention is to think of R ├── as a plunger exerting an effort on the resistor, and R ──┤ as an arrow ◁──□ directing flow into the resistor.) The choice of the independent variable is not related to the sign conventions discussed above. Hence we may have C ↼──| or C ──⇀| , where the half-arrow indicates the sign convention for positive power flow. With this definition of the causality symbol, we may immediately predict the organization of the symbols around the zero- or one-junction. It will be recalled that by KVL, all bonds incident upon a zero-junction have the same effort value, $e_1 = e_2 \cdots = e_n$. This means that upon choosing one of the e's as the independent variable, all the rest become dependent on the first. This is represented in symbolic form in Fig. 3.4a.

Similarly, for the one-junction it is the equality of the flows (KCL) which characterize the behavior $f_1 = f_2 \cdots = f_n$, hence the choice of a single independent flow makes the rest dependent. This is shown in Fig. 3.4b. Conversely, n-1 independent flows incident on a zero-junction determine the n'th flow, while for a one-junction, due to KVL, there are only n-1 independent efforts. On the basis of these considerations we may now redraw Fig. 3.2d in a more information-rich form (Fig. 3.4c). Note that for convenience the sign conventions have been chosen according to the assumed direction of power flow in the system. The assignment of causality to a bond graph ensures that the dynamic elements, L and C, cannot be given initial conditions which violate Kirchhoff's laws. That is, the initial state, and hence the entire dynamic trajectory, is confined to the Kirchhoff subspace as discussed in Section II.

In concluding this section it is worth noting that the assigning of correct causality symbols to a bond graph is a rather sensitive criterion for the completeness of the physical model underlying the representation.

Table 2 summarizes the basic "dictionary" of bond graphs elements.

3.3 Transition to continuum equations

Before beginning the analysis of more complex coupled permeation flows, it is useful to reconsider the bond graph representation from a more general point of view. As shown by Branin (1962, 1966), the operational structure of network theory is identical with vector calculus; hence networks can represent finite dimensional approximations to field equations. We shall illustrate this important statement in the case of membrane transport. Our analysis will be devoted to describing a limiting process which will convert the discontinuous network representation into the differential equations for the continuous membrane system. For simplicity, we will consider only linear constitutive relations.

We will now introduce the transmission matrix $\underset{\sim}{T}$, which relates the output of a multiport element (or group of elements) to the input. For elements that are sequentially arranged, their transmission matrices multiply to give a matrix which relates the output of the sequence to its input. The concept is thus very useful for analyzing long chains of elements, as in a transmission line, from which its name derives. As an example, we will consider the transmission matrix of a series resistance R:

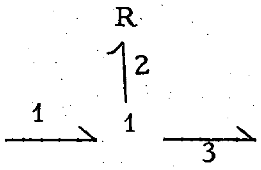

Since we assume that the resistor is linear, $e_2 = Rf_2$. For a one-junction all the flows are equal ($f_1=f_2=f_3$), and hence we may write $e_2=Rf_3$. Applying KVL and replacing e_2 by the expression just derived, we find that $e_1=e_2+e_3 = Rf_3+e_3$. The equations characterizing the series resistance may be combined into:

$$\begin{bmatrix} e_1 \\ f_1 \end{bmatrix} = \begin{bmatrix} 1 & R \\ 0 & 1 \end{bmatrix} \begin{bmatrix} e_3 \\ f_3 \end{bmatrix} \equiv \underset{\sim}{T}_R \begin{bmatrix} e_3 \\ f_3 \end{bmatrix} . \qquad (3.6)$$

In a similar manner, we may determine the transmission matrix for a parallel capacitance C:

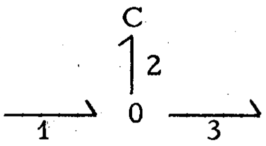

By definition $e_1=e_2=e_3$ and

$f_1=f_2+f_3$.

The constitutive relation of an ideal capacitive element is $C\,\frac{de_2}{dt} = f_2$, and hence

$$\begin{aligned} e_1 &= e_3 \\ f_1 &= C(de_3/dt) + f_3 \end{aligned} \quad \text{or} \quad \begin{bmatrix} e_1 \\ f_1 \end{bmatrix} = \begin{bmatrix} 1 & 0 \\ CD_t & 1 \end{bmatrix} \begin{bmatrix} e_3 \\ f_3 \end{bmatrix} \equiv \underset{\sim}{T}_C \begin{bmatrix} e_3 \\ f_3 \end{bmatrix} , \qquad (3.7)$$

where D_t is the operator d/dt.

Finally, we consider the combination of a series resistor and parallel capacitor:

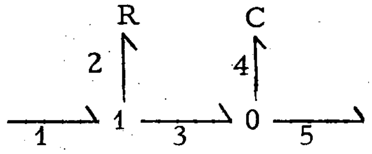

Using the transmission matrix $\underset{\sim}{T}_R$ for the resistor, we arrive at the input as a function of the intermediate variables (e_3, f_3) while the transmission matrix $\underset{\sim}{T}_C$, for the capacitor, gives the dependence of the output on these intermediate variables. Thus we see that the transmission matrix $\underset{\sim}{T}$ for the combination of elements is the product of the transmission matrices of the individual elements, i.e., $\underset{\sim}{T} = \underset{\sim}{T}_R \cdot \underset{\sim}{T}_C$. This expression is easily generalized, and hence the transmission matrix of any sequential chain of elements is the product of the transmission matrices of the single units.

Let us now consider a membrane of unit area broken up into volume elements of thickness dx. Within each volume element diffusion occurs; this can be described by an RC bond graph, as depicted above, with a resistance given by the specific resistance $\tilde{R}$ multiplied by the volume $1 \cdot cm^2 \cdot dx$, and a capacitance equal to the specific capacitance $\tilde{C}$ multiplied by the volume $1 \cdot cm^2 \cdot dx$.* The bond graph representing diffusion through a

---

* Note: from equations (2.32) and (2.33) we obtain for the ideal case $\tilde{R} = RT/cD$, while $\tilde{C} = c/RT$.

membrane would thus be as shown in Fig. 3.5.

The number of volume elements that one chooses in a membrane model depends upon how accurate a model is required and on the number of data points one would like in a concentration or chemical potential profile of the membrane. In a model with n volume elements there are n capacitors; and thus n values for the chemical potential can be obtained at n intervals within the membrane. In the limit, as the number of volume elements tends to infinity, or as the thickness dx of each element approaches zero, the bond graph equations approach the partial differential equations describing diffusion in a homogeneous membrane.

Since the transmission matrix characterizes the properties of an RC chain, let us examine the transmission matrix for a given volume element as dx becomes very small. The input flow and effort that we consider here are f and e, while the output is $f + \nabla f \cdot dx$ and $e + \nabla e \cdot dx$, where $\nabla = \frac{d}{dx}$.

It is clear that the total transmission matrix $\underset{\sim}{T}$ is the product of $\underset{\sim}{T}_R$ and $\underset{\sim}{T}_C$ as stated above, or

$$\begin{bmatrix} e \\ f \end{bmatrix} = \begin{bmatrix} 1 & \tilde{R} \cdot dx \\ 0 & 1 \end{bmatrix} \begin{bmatrix} 1 & 0 \\ \tilde{C} \cdot dx \cdot D_t & 1 \end{bmatrix} \begin{bmatrix} e + \nabla e \cdot dx \\ f + \nabla f \cdot dx \end{bmatrix} . \qquad (3.8)$$

Carrying out the matrix multiplication and neglecting terms of order $(dx)^2$, we find

$$\underset{\sim}{T} = \begin{bmatrix} 1 & \tilde{R} \cdot dx \\ \tilde{C} dx \cdot D_t & 1 \end{bmatrix} , \qquad (3.9)$$

which upon insertion into equation (3.8), and multiplication, gives

$$\nabla e + \tilde{R} \cdot f = 0 \qquad (3.10)$$

and

$$\tilde{C}(de/dt) + \nabla f = 0, \qquad (3.11)$$

in which second-order terms have again been neglected. Equation (3.11) may be readily transformed into the equation of continuity for the permeant in the membrane. Since by equation (2.26)

$$\frac{1}{V}\ \frac{dn_m}{dt} = \frac{C_m}{V}\ \frac{d\mu_m}{dt} = \tilde{C}\ \frac{de}{dt}$$

and by definition $f = J_m$, equation (3.11) can be rewritten as

$$\frac{\partial\ c_m}{dt} = -\ \nabla\ J_m,$$

where $c_m = n_m/V$, which is the equation of continuity. If we identify e with μ_m, equation (3.10) is seen to be the usual phenomenological equation $\nabla(-\mu_m) = RJ$.

The interesting expressions (3.10) and (3.11) may be transformed into two other equations. Upon differentiating equation (3.10),

$$\nabla^2 e + f \nabla \tilde{R} + \tilde{R} \nabla f = 0. \qquad (3.12)$$

Inserting equations (3.10) and (3.11), we obtain

$$\nabla^2 e - \frac{\nabla \tilde{R}}{\tilde{R}}\ \nabla e - \tilde{R}\tilde{C}\ \frac{de}{dt} = 0. \qquad (3.13)$$

Upon assuming ideality, we find

$$\tilde{R}\tilde{C} = \left(\frac{RT}{c_m D}\right)\left(\frac{c_m}{RT}\right) = \frac{1}{D} \quad \text{and} \quad \frac{\nabla \tilde{R}}{\tilde{R}} = \frac{\nabla c_m}{c_m}. \qquad (3.14)$$

Further identifying e with μ_m gives

$$\frac{dC_m}{dt} = D\nabla^2 C_m, \tag{3.15}$$

which is the conventional form of Fick's second law.

This example demonstrates that, in the limit, the network treatment indeed reduces to the classical field equations of physical chemistry (Kron, 1943).

3.4 Tellegen's theorem for bond graphs

In paragraph 2.1.2 we derived Tellegen's theorem from the linear graph representation. However, since the graphical representation that we shall use for the remainder of this paper is bond graphs, it is important to demonstrate that Tellegen's theorem is valid for bond graphs. We shall assume that a sign convention has been chosen consistent with associated reference directions, i.e., that bonds are directed into elements.

Theorem 3.1. For a bond graph G composed of one-port elements and junctions,

$$\sum_{\text{elements}} e_i f_i = 0.$$

Proof. Since all one-port elements are connected to either a zero-junction or a one-junction, one can count all the elements in a bond graph by counting the elements connected to each junction and then counting all the junctions. Making use of equations (3.2) and (3.4), we may then write:

$$\sum_{\text{elements}} e_i f_i = \sum_{j=1}^{N_0} e_j \sum_{i=1}^{\alpha_j} f_{ji} + \sum_{j=1}^{N_1} f_j \sum_{i=1}^{\beta_j} e_{ji}, \tag{3.16}$$

where N_0 and N_1 denote the total number of zero-junctions and one-junction in G, respectively; and where α_j and β_j denote the number of elements connected to the j^{th} zero-junction and j^{th} one-junction of G, respectively. Introducing the Kirchhoff constraints, equations (3.3) and (3.5), and utilizing the assumption that all bonds are directed into elements (associated reference directions), we have

$$\sum_{\text{elements}} e_i f_i = -\sum_{j=1}^{N_0} e_j \sum_{b=1}^{N_0^j - \alpha_j} \sigma_{jb} f_{jb} - \sum_{j=1}^{N_1} f_j \sum_{b=1}^{N_1^j - \beta_j} \sigma_{jb} e_{jb}, \qquad (3.17)$$

where N_0^j and N_1^j are the total number of bonds incident on the j^{th} zero-junction and j^{th} one-junction of G, respectively. The only bonds that are counted in the summations of equation (3.17) are bonds that connect two junctions together. Each one of these bonds is counted twice — once on the junction it leaves and once on the junction it enters. The two terms in the summations that correspond to any bond connecting two zero-junctions or two one-junctions cancel, since their efforts and flows will be equal but σ will be +1 for one term and -1 for the other. The remaining terms in the summation correspond to bonds connecting a zero-junction with a one-junction. Defining an "adjacency operator"

$$\delta_{st} = \begin{cases} +1 & \text{if junction s and t are bonded together} \\ 0 & \text{otherwise} \end{cases} \qquad (3.18)$$

we may rewrite equation (3.17) in the form

$$\sum_{\text{elements}} e_i f_i = -\sum_{s=1}^{N_0} \sum_{t=1}^{N_1} e_s f_{st} \sigma_{st} \delta_{st} - \sum_{t=1}^{N_1} \sum_{s=1}^{N_0} f_t e_{ts} \sigma_{ts} \delta_{ts}. \qquad (3.19)$$

Noting that by their definitions, equations (3.1) and (3.18),

$\sigma_{ts} = -\sigma_{st}$ and $\delta_{ts} = \delta_{st}$, we have

$$\sum_{\text{elements}} e_i f_i = -\sum_{s=1}^{N_0} \sum_{t=1}^{N_1} \delta_{st}\, \sigma_{st} (e_s f_{st} - e_{ts} f_t). \tag{3.20}$$

However, since the definitions of the junctions, equations (3.2) and (3.4), imply that

$$\begin{aligned} e_s &= e_{ts} && \text{for all } t \text{ such that } \delta_{st} = 1 \text{ and} \\ f_t &= f_{st} && \text{for all } s \text{ such that } \delta_{st} = 1, \end{aligned} \tag{3.21}$$

then

$$\sum_{\text{elements}} e_i f_i = 0.$$

Q. E. D.

As emphasized in Section II, this theorem is a purely topological result depending only upon KCL and KVL, not on the nature of the bond graph elements.

<u>Corollary 3.1.1.</u> For a bond graph G composed of multiport elements and junctions,

$$\sum_{\text{elements}} e_i f_i = 0.$$

<u>Proof</u>. The assumption of associated reference directions implies that all port bonds of multiport elements are connected to a junction. For if two multiports were bonded together, it would be impossible to orient the bond so that it simultaneously pointed into both multiports. Hence we have equation (3.16), and the remainder of the proof follows from above.

Q. E. D.

As mentioned previously, we shall have occasion to use nonassociated reference directions. In many cases this simplifies the bond graph by eliminating junctions separating multiport elements and simplifies many computations. However, when utilizing theoretical results from network theory, such as Tellegen's theorem, it is necessary to choose associated reference directions. This will be the case in Section VIII.

IV. NETWORK REPRESENTATIONS OF COUPLED FLOWS

4.1. Stationary flow of nonelectrolytes across a membrane

4.1.1.

In Sections II and III, we derived the bond graph representation for the flow of a single nonelectrolyte across a membrane. It is clear that if many noninteracting nonelectrolytes are simultaneously permeating a membrane, the flow of each chemical species may be represented by a separate RC chain of the type discussed above. However, if the permeants interact, a new feature must be considered: the coupling between the flows. Provisionally, we can lump all the coupling effects into a new element which we shall call a coupling n-port, denoted as CPL.

In paragraph 4.1.3, we will show how this new element is connected to a bond graph representing the permeation flows of components A and B through a membrane. Then we will reticulate CPL into elementary bond graph structures. In order to accomplish this task, however, we must first introduce another ideal bond graph element, the transducer, which will permit the representation of thermodynamic coupling and energy conversion.

4.1.2.

The transducer is a two-port which converts energy without loss from one form to another. In bond graphs we use the notation $\xrightarrow{1}\overset{(r)}{\mathrm{TD}}\xrightarrow{2}$ to denote an ideal transducer, where r is the transducer modulus, or transfer ratio. Being a two-port, the transducer requires two defining equations*:

$$\begin{aligned} e_1 &= \frac{1}{r}\ e_2 \\ f_1 &= r\ f_2 \end{aligned} \quad \text{or} \quad \begin{pmatrix} e_1 \\ f_1 \end{pmatrix} = \begin{pmatrix} \frac{1}{r} & 0 \\ 0 & r \end{pmatrix} \begin{pmatrix} e_2 \\ f_2 \end{pmatrix} . \qquad (4.1)$$

Notice that the transducer behaves very much like an ideal junction—its constitutive relation imposes a set of linear constraints on its port variables, and it conserves power by scaling the port efforts and flows according to the modulus r. Also note that

$$P_{in} = e_1 f_1 = (\frac{1}{r}\ e_2)(r\ f_2) = e_2 f_2 = P_{out} .$$

The TD may be thought of as a graphical representation for the area-preserving (i.e., power preserving) coordinate map (equation 4.1).

The transducer also preserves causality and must have the form:

$$\text{———}\!\dashv\ \mathrm{TD}\ \text{———}\!\dashv \quad \text{or} \quad \vdash\!\text{———}\ \mathrm{TD}\ \vdash\!\text{———} .$$

---

*Using associated reference directions $\xrightarrow{1}\overset{(r)}{\mathrm{TD}}\xleftarrow{2}$ the defining equations are:

$$\begin{pmatrix} e_1 \\ f_1 \end{pmatrix} = \begin{pmatrix} \frac{1}{r} & 0 \\ 0 & -r \end{pmatrix} \begin{pmatrix} e_2 \\ f_2 \end{pmatrix} .$$

4.1.3.

The transducer modulus need not be a constant. A mechanical analog might be a simple lever rolling on a semicircle; r is then a function of θ (see Fig. 4.1). Frequently, the modulus r will be a function of the state of another element in the system. We will return to this point in Section VII where signal flows will be introduced into our formalism.

4.1.4.

We are now in a position to describe the coupling between nonelectrolyte flows. First, we notice that the coupling exists only as long as flow continues. Moreover, we realize that the existence of coupling manifests itself by the diversion of a portion of the driving force for one species to affect another component. These two considerations imply that the bond graph coupling element CPL must be attached to one-junctions. This is illustrated for the case of a two-component system in Fig. 4.2. Note that by KVL some effort is diverted into the coupling structure; but, by KCL, no flow is diverted by introducing the coupling element. The assignment of causality, as shown in Fig. 4.2, is consistent with the definition of the one-junction, and means physically that the flow of A transmits an effort via the coupling two-port to the flow of B, and vice versa.

Having established the general structure for coupled flows, we now proceed to reticulate CPL into elementary bond graph structures. For illustrative purposes only, we will consider the two-component case. It is well established that the coupling is dissipative, so that CPL must be a resistive two-port. Since the dissipation depends on the flow of A relative to B, a dissipative element R_C must be attached to a zero-junction within CPL. Furthermore, it is clear that it is not the flow of A itself, (J_A), nor of B, (J_B), which is involved in the coupling dissipation, but only the interaction of the flows. We may say that a transduction process is involved, scaling the efforts and flows by the correct magnitudes, which are then applied to R_C.

The complete bond graph representing all of the above information concerning coupled flows is illustrated in Fig. 4.3.

4.1.5.

For the sake of simplicity, it is convenient to begin the analysis of coupled permeation flows with a consideration of steady state transport. In this case, there is no flow on the membrane capacitors C_A^m and C_B^m, so that their connection to the bond graph becomes superfluous, The two-sided structure of Fig. 4.3 then condenses to the single structure shown in Fig. 4.4, with resistances R_A, R_B, and R_C, for which we assume $R_A^1 = R_A^2 = \frac{R_A}{2}$, $R_B^1 = R_B^2 = \frac{R_B}{2}$ and $R_C^1 = R_C^2 = \frac{R_C}{2}$.

Let us start our analysis at the middle zero-junction of the coupling element. A coupling force X_C may be assigned to this zero-junction; X_C is then related to the coupling flow J_C by the constitutive relation of the coupling resistance R_C. In the linear case,

$$X_C = R_C J_C \tag{4.2}$$

while, in general,

$$X_C = R_C(J_C) \tag{4.3}$$

is an unspecified function of J_C. Since all the forces on a zero-junction are equal, and since the transducer moduli are r_A for the A and r_B for the B component, the forces entering the transducers are, by equation (4.1), equal to $\frac{X_C}{r_A}$ on the A-side and to $\frac{X_C}{r_B}$ on the B-side.

We now turn our attention to the one-junctions. By KVL, the sum of the forces on each junction vanishes; thus, for the one-junction of the A-flow, we have

$$-\mu_A^1 + X_A + \mu_A^2 + \frac{X_C}{r_A} = 0$$

or

$$\mu_A^1 - \mu_A^2 = \Delta\mu_A = X_A + \frac{X_C}{r_A}, \tag{4.4}$$

where X_A is the driving force across the resistance R_A, and $\Delta\mu_A$ is an externally measurable force. The constitutive relation for the diffusional resistance is $X_A = R_A \cdot J_A$ in the linear case, while in general

$$X_A = R_A(J_A). \tag{4.5}$$

In an identical manner we may write

$$\Delta\mu_B = X_B + \frac{X_C}{r_B} \tag{4.6}$$

and

$$X_B = R_B(J_B). \tag{4.7}$$

The flows of A and B after passing their respective transducers are, as required by equation (4.1), $\frac{J_A}{r_A}$ and $\frac{J_B}{r_B}$. Since the flows on the zero-junction of the coupling element are additive, we find that

$$J_C = \frac{J_A}{r_A} + \frac{J_B}{r_B}. \tag{4.8}$$

It is now a simple matter to write the relation between the external flows and external forces. Inserting into equations (4.4) and 4.6 the force-flow relations (4.3), (4.5) and (4.7), we find

$$\Delta\mu_A = R_A(J_A) + \frac{1}{r_A} R_C(J_C),$$

$$\Delta\mu_B = \frac{1}{r_B} R_C(J_C) + R_B(J_B). \tag{4.9}$$

Equations (4.9) are a generalization of the phenomenological equation of Onsager and reduce to the conventional form used in non-equilibrium thermodynamics if linear constitutive relations are assumed. In the linear case, we obtain on the basis of equations (4.8) and (4.9):

$$\Delta\mu_A = \left(R_A + \frac{R_C}{r_A^{\,2}}\right) J_A + \frac{R_C}{r_A r_B} J_B$$

$$= \mathcal{R}_A J_A + \mathcal{R}_{AB} J_B, \qquad (4.10)$$

and

$$\Delta\mu_B = \frac{R_C}{r_A r_B} J_A + \left(R_B + \frac{R_C}{r_B^{\,2}}\right) J_B$$

$$= \mathcal{R}_{BA} J_A + \mathcal{R}_B J_B,$$

where the script $\mathcal{R}$'s denote Onsager coefficients. As expected, the matrix of the phenomenological coefficient is symmetric for the coupling term $\mathcal{R}_{AB} = \mathcal{R}_{BA} = R_C/r_A r_B$.

4.1.6.

It is, however, remarkable that in the nonlinear case the system of equations is also symmetric. The condition for the reciprocity of a nonlinear function is the equality of the Jacobian and its transpose. In our case, this would impose the requirement that $(\partial\Delta\mu_A/\partial J_B)_{J_A}$ should equal $(\partial\Delta\mu_B/\partial J_A)_{J_B}$.

To prove this important statement, we examine equations (4.8) and (4.9), we note that the derivative of $R_A(J_A)$ with respect to J_B at constant J_A is zero, and that the transduction factors r_A and r_B are independent of flows and forces, so that $(\partial J_C/\partial J_A)_{J_B} = 1/r_A$ and $(\partial J_C/\partial J_B)_{J_A} = 1/r_B$. Upon differentiating equation (4.9), we now find that

$$\left(\frac{\partial \Delta\mu_A}{\partial J_B}\right)_{J_A} = -\frac{1}{r_A}\left(\frac{\partial R_C(J_C)}{\partial J_B}\right)_{J_A} = -\frac{1}{r_A}\frac{dR_C(J_C)}{dJ_C}\left(\frac{\partial J_C}{\partial J_B}\right)_{J_A}$$

$$= -\frac{1}{r_A r_B}\frac{d}{dJ_C}R_C(J_C)$$

and (4.11)

$$\left(\frac{\partial \Delta\mu_B}{\partial J_A}\right)_{J_B} = -\frac{1}{r_B}\left(\frac{\partial R_C(J_C)}{\partial J_A}\right)_{J_B} = -\frac{1}{r_B}\frac{dR_C(J_C)}{dJ_C}\left(\frac{\partial J_C}{\partial J_A}\right)_{J_B}$$

$$= -\frac{1}{r_A r_B}\frac{d}{dJ_C}R_C(J_C),$$

so that

$$\left(\frac{\partial \Delta\mu_A}{\partial J_B}\right)_{J_A} = \left(\frac{\partial \Delta\mu_B}{\partial J_A}\right)_{J_B}. \tag{4.12}$$

Equation (4.12) is similar to Onsager's theorem but was derived directly from network reasoning and applies in the nonlinear region. This result is based on the topology of the bond graph and the intrinsic reciprocity of the one-port network elements. This point will be discussed in more detail in Section VIII.

4.1.7.

Equation (4.10), for the linear case, leads to an interesting conclusion about the relation between phenomenological coefficients determined in the presence and absence of coupling. Let us denote the coefficients in the absence of coupling as $\mathcal{R}_A'$ and $\mathcal{R}_B'$. These straight coefficients are simply the bond graph resistances R_A and R_B, respectively. From equation (4.10) we see that

$$\mathcal{R}_A - \mathcal{R}_A' = R_C / r_A^2$$

and

$$\mathcal{R}_B - \mathcal{R}_B' = R_C / r_B^2 .$$

Hence the coefficients are related by the equation

$$(\mathcal{R}_A - \mathcal{R}_A')(\mathcal{R}_B - \mathcal{R}_B') = \frac{R_C^2}{r_A^2 r_B^2} = (\mathcal{R}_{AB})^2; \qquad (4.13)$$

and the phenomenological coupling coefficient can be determined up to sign by the measurement of straight coefficients.

4.1.8.

To conclude this section, it is worth comparing the conclusions of the bond graph with the predictions that arise from considerations of the frictional parameters (Bearman and Kirkwood, 1958), following the treatment developed by Spiegler (1958), Kedem and Katchalsky (1961), and others. It is known that the frictions may be written as follows:

$$\Delta\mu_A = \frac{1}{c_A}\left[c_B\zeta_{AB} + c_m\zeta_{Am}\right] J_A - \zeta_{AB} J_B,$$

$$\Delta\mu_B = -\zeta_{AB} J_A + \frac{1}{c_B}\left[c_A\zeta_{AB} + c_m\zeta_{Bm}\right] J_B, \qquad (4.14)$$

where ζ_{ij} is the partial binary frictional coefficient between species i and j. When $c_B = 0$ and $J_B = 0$,

$$\Delta\mu_A = \frac{1}{c_A}[c_m \zeta_{Am}] J_A \equiv \frac{f_{Am}}{c_A} J_A$$

so that $R_A = f_{Am}/c_A$ where f_{Am} is a constant. Similarly, $R_B = f_{Bm}/c_B$ where f_{Bm} is constant. The comparison of equation (4.14) with equation (4.10) now leads to the following:

$$\frac{R_C}{r_A^2} = \frac{c_B}{c_A}\zeta_{AB}; \frac{R_C}{r_B^2} = \frac{c_A}{c_B}\zeta_{AB}; \frac{R_C}{r_A r_B} = -\zeta_{AB}. \quad (4.15)$$

Equations (4.15) do not permit a unique solution for R_C, r_A and r_B since they imply only $r_A/r_B = -c_A/c_B$. A consistent solution is, however,

$$r_A = c_A, \quad r_B = -c_B; \quad (4.16)$$

and hence

$$R_C = c_A c_B \zeta_{AB}. \quad (4.17)$$

This solution is reasonable and could have been assumed a priori from physical reasoning. As was stated earlier, the dissipation due to coupling is proportional to the relative velocities of the permeants; since $J_A = c_A v_A$ while $J_B = c_B v_B$, it is clear that

$$J_C = \frac{J_A}{r_A} + \frac{J_B}{r_B} = \frac{J_A}{c_A} - \frac{J_B}{c_B} = v_A - v_B. \quad (4.18)$$

Since the coupling resistance is dependent upon the hydrodynamic interaction of substances A and B, it is plausible that R_C be proportional to the product of c_A and c_B.

4.2. Nonstationary flows of nonelectrolytes and their relaxation times

4.2.1.

For the evaluation of nonstationary behavior with the aid of bond graphs, it is convenient to invert the stationary equations (4.9) and represent the flows as functions of the forces. In the linear case, we may write

$$J_A^{st} = \mathcal{L}_A \, \Delta\mu_A + \mathcal{L}_{AB} \, \Delta\mu_B$$

and (4.19)

$$J_B^{st} = \mathcal{L}_{BA} \, \Delta\mu_A + \mathcal{L}_B \, \Delta\mu_B ,$$

where the superscript st denotes a stationary flow and where the conductance $\mathcal{L}$ is related to the resistance by the expressions

$$\mathcal{L}_A = \frac{\mathcal{R}_A}{|\mathcal{R}|}, \quad \mathcal{L}_B = \frac{\mathcal{R}_B}{|\mathcal{R}|} \quad \text{and} \quad \mathcal{L}_{AB} = \mathcal{L}_{BA} = - \frac{\mathcal{R}_{AB}}{|\mathcal{R}|} .$$

$|\mathcal{R}|$ is the determinant of the matrix of the phenomenological resistances:

$$\begin{pmatrix} R_A + \dfrac{R_C}{r_A^2} & \dfrac{R_C}{r_A r_B} \\[2ex] \dfrac{R_C}{r_A r_B} & R_B + \dfrac{R_C}{r_B^2} \end{pmatrix} = \begin{pmatrix} \mathcal{R}_A & \mathcal{R}_{AB} \\[2ex] \mathcal{R}_{BA} & \mathcal{R}_B \end{pmatrix}$$

The explicit values of the thermodynamic conductances are

$$\mathcal{L}_A = \frac{r_A^2 (r_B^2 R_B + R_C)}{\Delta}, \quad \mathcal{L}_B = \frac{r_B^2 (r_A^2 R_A + R_C)}{\Delta}$$

and

$$\mathcal{L}_{AB} = -\frac{r_A r_B R_C}{\Delta}, \tag{4.20}$$

where $\Delta = r_A^2 r_B^2 R_A R_B + r_A^2 R_A R_C + r_B^2 R_B R_C$.

The complete bond graph for the case of nonsteady flow across a membrane is repeated in Fig. 4.5. It is readily recognized that the graph is composed of two parallel linear parts connected by the capacitors C_A^m and C_B^m. The parallel parts have a structure identical to that considered for the case of stationary flows. Indeed, it is the existence of the intramembrane capacitors which allows for a nonsteady variation of the flows. On a priori grounds, R_A^1, R_C^1 and R_B^1 may differ from R_A^2, R_C^2 and R_B^2. For simplicity, however, we will assume that $R_A^1 = R_A^2 = R_A/2$, etc. It is now possible to use equation (4.19) for each flank of the bond graph and write

$$\frac{J_A^1}{2} = \mathcal{L}_A(\mu_A^1 - \mu_A^m) + \mathcal{L}_{AB}(\mu_B^1 - \mu_B^m)$$

and

$$\frac{J_A^2}{2} = \mathcal{L}_A(\mu_A^m - \mu_A^2) + \mathcal{L}_{AB}(\mu_B^m - \mu_B^2), \tag{4.21}$$

as well as

$$\frac{J_B^{1}}{2} = \mathcal{L}_{AB}(\mu_A^{2} - \mu_A^{m}) + \mathcal{L}_B(\mu_B^{1} - \mu_B^{m})$$

and

$$J_B^{2} = \mathcal{L}_{AB}(\mu_A^{m} - \mu_A^{2}) + \mathcal{L}_B(\mu_B^{m} - \mu_B^{2}).$$

From the diagram, we recognize readily that J_A^1 is the influx of A into the membrane, while J_A^2 is the outflow, and similarly, $J_B^1 = J_B^{in}$ and $J_B^2 = J_B^{out}$. Combining equations (4.21) in pairs, we find

$$\begin{aligned} \frac{J_A^{in} + J_A^{out}}{2} &= \mathcal{L}_A(\mu_A^{1} - \mu_A^{2}) + \mathcal{L}_{AB}(\mu_B^{1} - \mu_B^{2}) \\ &= \mathcal{L}_A \, \Delta\mu_A + \mathcal{L}_{AB} \, \Delta\mu_B . \end{aligned}$$

But, this is the expression for J_A^{st} in equation (4.19); hence

$$\frac{J_A^{in} + J_A^{out}}{2} = J_A^{st} \text{ and, similarly, } \frac{J_B^{in} + J_B^{out}}{2} = J_B^{st}. \quad (4.22)$$

Thus the average of the nonstationary influx and outflux flows is independent of time and equal to the stationary flow. It is evident that equations (4.22) are very useful experimentally and are closely related to the relaxation phenomena discussed below.

4.2.2.

Since we have assumed that the reservoirs bounding the membrane are "infinite", i.e., are sources of constant chemical potential, all relaxation process takes place in the intramembrane capacitors. An inspection of Fig. 4.5 shows that the transient flow of material into the membrane capacitor C_A^m is given by $J_A^m = J_A^1 - J_A^2 = J_A^{in} - J_A^{out}$; or inserting the values from equation (4.21) and letting

$$\frac{\mu_A^1 + \mu_A^2}{2} = \langle \mu_A \rangle \quad \text{and} \quad \frac{\mu_B^1 + \mu_B^2}{2} = \langle \mu_B \rangle,$$

$$\frac{J_A^m}{4} = \mathcal{L}_A(\langle \mu_A \rangle - \mu_A^m) + \mathcal{L}_{AB}(\langle \mu_B \rangle - \mu_B^m) \tag{4.23}$$

and

$$\frac{J_B^m}{4} = \mathcal{L}_{AB}(\langle \mu_A \rangle - \mu_A^m) + \mathcal{L}_B(\langle \mu_B \rangle - \mu_B^m).$$

Upon reaching a steady state, both J_A^m and J_B^m vanish, which in this case implies $(\mu_A^m)^{st} = \langle \mu_A \rangle$ and $(\mu_B^m)^{st} = \langle \mu_B \rangle$.

Since the capacitive flows are related to the membrane chemical potentials by the expressions

$$C_A^m \frac{d\mu_A^m}{dt} = J_A^m \quad \text{and} \quad C_B^m \frac{d\mu_B^m}{dt} = J_B^m,$$

we may write the relaxation equations

$$\begin{aligned} \frac{d\mu_A^m}{dt} &= \frac{4\mathcal{L}_A}{C_A^m}(\langle \mu_A \rangle - \mu_A^m) + \frac{4\mathcal{L}_{AB}}{C_A^m}(\langle \mu_B \rangle - \mu_B^m), \\ \frac{d\mu_B^m}{dt} &= \frac{4\mathcal{L}_{AB}}{C_B^m}(\langle \mu_A \rangle - \mu_A^m) + \frac{4\mathcal{L}_B}{C_B^m}(\langle \mu_B \rangle - \mu_B^m). \end{aligned} \tag{4.24}$$

Since $\langle \mu_A \rangle$ and $\langle \mu_B \rangle$ are constants, it is advantageous to introduce new variables

$$X = \mu_A{}^m - \langle \mu_A \rangle \quad \text{and} \quad Y = \mu_B{}^m - \langle \mu_B \rangle,$$

which transform equations (4.24) into

$$\begin{pmatrix} \dot{X} \\ \dot{Y} \end{pmatrix} = -4 \begin{pmatrix} \dfrac{\mathcal{L}_A}{C_A{}^m} & \dfrac{\mathcal{L}_{AB}}{C_A{}^m} \\ \dfrac{\mathcal{L}_{AB}}{C_B{}^m} & \dfrac{\mathcal{L}_B}{C_B{}^m} \end{pmatrix} \begin{pmatrix} X \\ Y \end{pmatrix}. \qquad (4.25)$$

The relaxation times of the process are given by $\tau = \lambda/4$, where the eigenvalues λ of the coefficient matrix are

$$\lambda = \frac{1}{2}\Bigg[\left(\frac{\mathcal{L}_A}{C_A{}^m} + \frac{\mathcal{L}_B}{C_B{}^m}\right) \pm \sqrt{\left(\frac{\mathcal{L}_A}{C_A{}^m} + \frac{\mathcal{L}_B}{C_B{}^m}\right)^2 - 4\left(\frac{\mathcal{L}_A\mathcal{L}_B - \mathcal{L}_{AB}^2}{C_A{}^m C_B{}^m}\right)}\,. \qquad (4.26)$$

We shall not pursue this topic further here. However, it is important to realize that the relaxation times are completely determined by equilibrium and steady state measurements only, since the conductance coefficients $\mathcal{L}_A$, $\mathcal{L}_B$ and $\mathcal{L}_{AB}$ are determined when the system is at steady state, and the capacitances $C_A{}^m$ and $C_B{}^m$ when the system is at equilibrium. Furthermore, it is worth noting that in the uncoupled case where $\mathcal{L}_{AB} = 0$,

$$\lambda_1 = \mathcal{L}_A/C_A^m = 1/R_A C_A^m, \quad \lambda_2 = \mathcal{L}_B/C_B^m = 1/R_B C_B^m$$

and

$$\tau_A = \frac{R_A C_A^m}{4}, \quad \tau_B = \frac{R_B C_A^m}{4},$$

where τ_A and τ_B are the relaxation times of the independent flows of A and B. In the case of full coupling, which occurs when $R_C \rightarrow \infty$ and $\mathcal{L}_{AB}^2 = \mathcal{L}_A \mathcal{L}_B$,

$$\lambda_1 = \frac{\mathcal{L}_A}{C_A^m} + \frac{\mathcal{L}_B}{C_B^m} = \frac{1}{4\tau}; \; \lambda_2 = 0.$$

In this case, only one relaxation time exists, which is to be expected since the flows of A and B are no longer independent.

4.3. Continuum equations

In paragraph 3.3 we demonstrated how the differential equations describing the transport of a single nonelectrolyte through a continuum membrane could be generated from a bond graph. In this section we will illustrate a similar procedure for coupled flows.

Let us consider a membrane of unit area divided into volume elements of thickness dx. Within each volume element coupled diffusion occurs. Figure 4.6 shows the bond graph for such a volume element, where $\tilde{R}$ and $\tilde{C}$ denote the specific resistance and capacitance.

Calculating the transmission matrix as we did in paragraph 3.3 will be somewhat tedious since in the present case it is a

4×4 matrix. Moreover, the transmission matrix method is restricted to systems in which the constitutive relations are linear. Therefore we shall follow an alternate procedure that is valid in the nonlinear regime.

Reading directly from the bond graph, or from equations (4.4), (4.3), (4.5) and (4.8), we find that

$$\mu_A = \tilde{R}_A(J_A)\,dx + \frac{1}{r_A}\tilde{R}_C\left(\frac{J_A}{r_A} + \frac{J_B}{r_B}\right)dx$$
$$+ \mu_A + \nabla\mu_A \cdot dx$$

or

$$\nabla(-\mu_A) = \tilde{R}_A(J_A) + \frac{1}{r_A}\tilde{R}_C\left(\frac{J_A}{r_A} + \frac{J_B}{r_B}\right). \qquad (4.27)$$

Applying KCL on the zero-junctions at the capacitors yields:

$$J_A = \tilde{C}_A dx \frac{d}{dt}(\mu_A + \nabla\mu_A \cdot dx) + J_A + \nabla J_A\,dx,$$

or to first order in dx:

$$-\nabla J_A = \tilde{C}_A \frac{d\mu_A}{dt}. \qquad (4.28)$$

In an identical manner we may write

$$\nabla(-\mu_B) = \tilde{R}_B(J_B) + \frac{1}{r_B}\tilde{R}_C\left(\frac{J_A}{r_A} + \frac{J_B}{r_B}\right) \qquad (4.29)$$

and

$$-\nabla J_B = \tilde{C}_B \frac{d\mu_B}{dt}. \qquad (4.30)$$

Utilizing the definition of specific capacitance,

$$\tilde{C} = \frac{C}{V} = \frac{1}{V} \frac{\partial n}{\partial \mu} ,$$

we see that equations (4.28) and (4.30) are the familiar equations of continuity

$$\nabla \cdot J_i = \frac{\partial c_i}{\partial t} .$$

The nonlinear field equations (4.27) and (4.29) for the chemical potential distribution reduce, in the case of linear constitutive relations, to

$$\begin{aligned} \nabla(-\mu_A) &= \left(\tilde{R}_A + \frac{\tilde{R}_C}{r_A^{\,2}}\right) J_A + \frac{\tilde{R}_C}{r_A r_B} J_B \\ &= \tilde{\mathcal{R}}_A J_A + \tilde{\mathcal{R}}_{AB} J_B \end{aligned}$$

and

$$\begin{aligned} \nabla(-\mu_B) &= \frac{\tilde{R}_C}{r_A r_B} J_A + \left(\tilde{R}_B + \frac{\tilde{R}_C}{r_B^{\,2}}\right) J_B \\ &= \tilde{\mathcal{R}}_{BA} J_A + \tilde{\mathcal{R}}_B J_B, \end{aligned}$$

which are the local phenomenological equations of nonequilibrium thermodynamics.

4.4. <u>Transport in ideal electrolyte solutions</u>

4.4.1.

While coupling in nonelectrolyte flows is based on hydrodynamic interaction, the flow of electrolytes provides another coupling possibility— through electrostatic interaction. Electrolyte processes encountered in biophysics are maintained very close to electroneutral; thus the cationic and anionic flows are dominated by strong electrostatic coupling. In general, ionic flows may interact both hydrodynamically and electrically; in ideal solutions, however, the hydrodynamic interference may be neglected, and it is possible to consider only the dictum of electroneutrality.

Although the ideal case will not provide any new information about electrolyte solutions, it will serve as a convenient introduction to the bond graph representation of electrolyte transport. In the next section we shall treat the more complex case of electrostatic and hydrodynamic interaction; and the last section of this chapter will be devoted to the permeation of charged permselective membranes. As an initial example, we shall represent the behavior of a fully dissociated mono-monovalent salt in aqueous solution. Although we deal with a system of cations, anions, and water, the Gibbs-Duhem relation reduces the number of independent flows to two, so that only the ionic flows will be considered.

Each ion is capable of diffusing under the influence of a concentration difference; hence the bond graph must include a separate RC diffusion chain for both the anion and cation. Local electrical interactions between the ions couple these independent diffusion chains.

In order to deduce the coupling structure, note that the electrochemical potential of the ith ion with valence z_i is $\tilde{\mu}_i = \mu_i^0 + RT \ell n\, c_i + z_i \mathcal{F} \psi$, where ψ is the local electrical potential and $\mathcal{F}$ is Faraday's constant. For the present purpose, we distinguish between the concentration dependent part $\mu_i^c = \mu_i^0 + RT \ell n\, c_i$, which is represented by a chemical capacitor in the RC diffusion chain, and the electrical part $z_i \mathcal{F} \psi$. Since there is a unique electrical potential at each point in the solution, we assign a local electrical capacitor to each lump of the bond graph; then we connect this capacitor to transducers with moduli $z_i \mathcal{F}$ so that the contribution to the driving force of ion i due to electrical effects is $z_i \mathcal{F} \Delta\psi$. It should be noted that the electrical capacitors, which represent the variable potential ψ, carry an extremely small amount of free charge since deviations from electroneutrality are usually extremely small. Figure 4.7 illustrates the arrangement of the concentration and electrical capacitors at points x and x + Δx of an electrolyte solution, while Fig. 4.8 includes the transducers needed to represent cation flow. By KCL on the one-junction,

$$-\mu_+^1 - \mathcal{F}\psi_1 + \mu_+^2 + \mathcal{F}\psi_2 + X_+ = 0$$

or

$$X_+ = (\mu_+^1 + \mathcal{F}\psi_1) - (\mu_+^2 + \mathcal{F}\psi_2) = \mu_+^1 - \mu_+^2 = \Delta\tilde{\mu}_+ . \quad (4.31)$$

The driving force for the transport of a cation has the correct form, and consequently the bond graph in Fig. 4.8 adequately represents the forces on a cation in solution.

In the linear case, the constitutive relation between the force X_+ and the flow J_+ is

$$X_+ = \Delta\tilde{\mu}_+ = R_+ J_+ . \tag{4.32}$$

The complete bond graph representing the flow of both the cation and the anion is shown in Fig. 4.9. From the bond graph we obtain the equation

$$X_- = (\mu_-^1 - \mathcal{F}\psi_1) - (\mu_-^2 - \mathcal{F}\psi_2) = \Delta\tilde{\mu}_- ; \tag{4.33}$$

and the assumption of a linear constitutive relation for R_- implies

$$X_- = \Delta\tilde{\mu}_- = R_- J_- . \tag{4.34}$$

4.4.2.

There is no difficulty in reconstructing all the classical expressions for ionic conductance, transference and diffusion from the bond graph. As an example, we shall derive only the liquid junction potential, which in the present case is simply the difference in ψ between points x and $x + \Delta x$. In the determination of liquid junction potentials, the flow of electrical current is assumed to be zero, i.e., $J_+ = J_-$, or $\frac{\Delta\tilde{\mu}_+}{R_+} = \frac{\Delta\tilde{\mu}_-}{R_-}$. (4.35)

Inserting the explicit values of the chemical potentials $\Delta\tilde{\mu}_+ = \Delta\mu_+^c + \mathcal{F}\,\Delta\psi$ and $\Delta\tilde{\mu}_- = \Delta\mu_-^c - \mathcal{F}\,\Delta\psi$, we find that:

$$\mathcal{F}\,\Delta\psi = -\left(\frac{\frac{1}{R_+}}{\frac{1}{R_+}+\frac{1}{R_-}}\,\Delta\mu_+^c - \frac{\frac{1}{R_-}}{\frac{1}{R_+}+\frac{1}{R_-}}\,\Delta\mu_-^c\right) \tag{4.36}$$

However, it is readily shown that

$$\frac{\frac{1}{R_+}}{\frac{1}{R_+}+\frac{1}{R_-}} = t_+ \tag{4.37}$$

is the transferences number of the cation, while $\dfrac{\frac{1}{R_-}}{\frac{1}{R_+}+\frac{1}{R_-}} = t_-$

is the transference number of the anion, so that

$$\mathcal{F}\,\Delta\psi = -\left(\frac{t_+\Delta\mu_+^c}{(+1)} + \frac{t_-\Delta\mu_-^c}{(-1)}\right), \tag{4.38}$$

which is a special case of the well-known equation for the liquid junction potential.

4.4.3.

In concluding this section, it is worth noting that the flows on the bonds leading to the zero-junction of the electrical capacitor are partial electrical currents, so that, for instance, the junction adjacent to C^1_{elect} carries the flows $I_+^0, I_-^0, I_+^1, I_-^1$ which, by KCL, combine to give the capacitive current I_C:

$$-I_+^0 - I_-^0 + I_+^1 + I_-^1 + I_C = 0$$

or

$$I_C = (I_+^0 + I_-^0) - (I_+^1 + I_-^1).$$

The capacitor equation is

$$C^1_{elect} \frac{d\psi}{dt} = (I^0_+ + I^0_-) - (I^1_+ + I^1_-).$$

Since electroneutrality makes $(I^0_+ + I^0_-) - (I^1_+ + I^1_-)$ approximately zero, the capacitance must be very small, as pointed out at the beginning of the section. It is, however, non-zero; and the insertion of the electrical capacitor into the bond graph is imperative for causal completeness.

4.5. The treatment of real electrolyte solutions

After treating the ideal case, there is no difficulty in dealing with real electrolyte solutions in which both electrostatic and hydrodynamic coupling govern the ionic flows. The bond graph will be a combination of Figs. 4.9 and 4.5, as shown in Fig. 4.10. Following the same alogrithm as before, we apply KCL and obtain

$$-\mu^1_+ - \mathcal{F}\psi_1 + X_+ + \mu^2_+ + \mathcal{F}\psi_2 + \frac{X_C}{r_+} = 0$$

or (4.39)

$$(\mu^1_+ + \mathcal{F}\psi_1) - (\mu^2_+ + \mathcal{F}\psi_2) = \Delta\tilde{\mu}_+ = X_+ + \frac{X_C}{r_+} .$$

Assuming linear dependences between flows and forces $X_+ = R_+J_+$ and $X_C = R_CJ_C$, the coupling flow is as before

$$J_C = \frac{J_+}{r_+} + \frac{J_-}{r_-} . \qquad (4.40)$$

Inserting the last equation into (4.39), we obtain

$$\Delta\tilde{\mu}_+ = \left(R_+ + \frac{R_C}{r_+^2}\right) J_+ + \frac{R_C}{r_+ r_-} J_- , \qquad (4.41)$$

and similarly,

$$\Delta\tilde{\mu}_- = \frac{R_C}{r_+ r_-} J_+ + \left(R_- + \frac{R_C}{r_-^2}\right) J_- .$$

It is worth noting that even if one assumes nonlinear dependence of flows on forces, the Jacobian matrix is symmetric and the system is reciprocal. If we write $X_+ = R_+(J_+)$ and $X_C = R_C(J_C)$, we find with the aid of equation (4.39) that

$$\Delta\tilde{\mu}_+ = R_+(J_+) + \frac{1}{r_+} R_C\left(\frac{J_+}{r_+} + \frac{J_-}{r_-}\right)$$

and

$$\Delta\tilde{\mu}_- = \frac{1}{r_-} R_C\left(\frac{J_+}{r_+} + \frac{J_-}{r_-}\right) + R_-(J_-). \qquad (4.42)$$

Partial differentiation with respect to the flows gives

$$\left(\frac{\partial \Delta\tilde{\mu}_+}{\partial J_-}\right)_{J_+} = \frac{1}{r_+} \frac{\partial R_C}{\partial J_C} \frac{\partial J_C}{\partial J_-} = \frac{1}{r_+ r_-} \frac{\partial R_C}{\partial J_C} = \left(\frac{\partial \Delta\tilde{\mu}_-}{\partial J_+}\right)_{J_-} . \qquad (4.43)$$

4.6. Membrane permeability to electrolytes

Consider the transport of a completeley dissociated binary electrolyte through a membrane. Such a system comprises four components: membrane, water, anions and cations. Using the Gibbs-Duhem relation we can eliminate the membrane component and measure our flows with respect to the membrane as a fixed reference frame. The bond graph representation of a membrane being permeated by an electrolyte will thus consist of three RC diffusion chains, one for the solvent, one for the cations and one for the anions, with an electrical capacitor tying the ionic chains together. If the electrolyte is present at finite dilutions, we must also include hydrodynamic coupling structures between each of the RC chains. This bond graph is complicated and will not be drawn. If the membrane is uncharged, we may regard one section of the bond graph as the membrane phase and assign the appropriate diffusional resistances as in Section II. The electrical capacitor adjacent to the membrane section can be used to represent the double layer; and if one wishes, the unstirred layers adjacent to any membrane may be represented by RC chains adjoining the membrane. In Fig. 4.11, the bond graph for a membrane permeation system in which the solvent flow and hydrodynamic coupling may be neglected has been drawn. If $R_m^+ \neq R_m^-$, the graph predicts the rapid build up of a retarding membrane potential. If $R^+ \neq R^-$ in the bulk solution, a diffusion potential is generated. In general, this representation appears to model all primary bulk electrolyte effects.

V. CHEMICAL PROCESSES

5.1 Bond graph representation of chemical flows

5.1.1

In this section we shall consider chemical processes which occur in a closed reaction vessel with volume V. We shall assume that the reaction vessel is in contact with constant temperature and pressure reservoirs and exchanges thermal and mechanical energy with these reservoirs so as to maintain a constant internal temperature and pressure. The case of an open vessel, in which both diffusion and reaction take place, will be considered in the following section. Further, it is assumed that the reaction mixture is well stirred so that the rate of the reaction, or, as it is sometimes called, the "flow of reaction," is the same at every point in the vessel. The flow of a chemical reaction is thus a scalar quantity and differs in a fundamental way from the vectorial diffusional or electrical flows which represent directed movements through space. In a chemical process, the individual component is not conserved but undergoes a dissipative transformation to a new substance, so that conservation of mass is obeyed only by the reacting system as a whole.

From the point of view of network thermodynamics, the reaction mixture may be considered as a black box. However, since by sampling the contents of the vessel one may determine the chemical potential $\mu_i(t)$ and the rate of change in the number of moles $J_i(t)$ for each component i, the black box may be partially opened. Figure 5.1 illustrates the multiport representation of a chemical transformation in which the molecular species A, B, C and D participate. It will be our goal to open this black box and further reticulate this multiport model.

The relationship between the chemical potential and the number of moles of each chemical species within the reaction mixture may be represented by a capacitor which is discharged if the component is a reactant and charged if the component is a reaction product. In general, μ_i is a function of all the n_j's and, inversely,

$$dn_i = \sum_{j=1}^{N} \frac{\partial n_i}{\partial \mu_j} d\mu_j \qquad i = 1, \cdots, N \tag{5.1}$$

or

$$J_i = \frac{dn_i}{\partial t} = \sum_{j=1}^{N} C_{ij} \frac{d\mu_j}{dt} \quad , \tag{5.2}$$

where C_{ij} is an element of the incremental capacitance matrix for the system. In vector notation, the above equation takes the following form:

$$\underset{\sim}{J} = \underset{\sim}{C} \dot{\underset{\sim}{\mu}} \, , \tag{5.3}$$

where $\underset{\sim}{C}$ represents a multiport capacitor. For ideal solutions, in which the components do not interact, this multiport capacitor may be reticulated into N capacitors, each representing a single species.

If

$$\mu_i = \mu_i^0 + RT\ln \frac{n_i}{V} \quad , \tag{5.4}$$

then we shall attribute the incremental capacitance

$$C_i = \frac{\partial n_i}{\partial \mu_i} = \frac{n_i}{RT} = \frac{c_i V}{RT} \tag{5.5}$$

to the i^{th} component, where c_i is the concentration of the i^{th} species in the reaction vessel, the chemical potential μ_i is regarded as the potential of the i^{th} capacitor, and the capacitor flow is given by:

$$J_i = \frac{dn_i}{dt} = \frac{dn_i}{d\mu_i} \frac{d\mu_i}{dt} = C_i \frac{d\mu_i}{dt} \ . \tag{5.6}$$

5.1.2

The conventional representation of a chemical reaction as

$$\underset{\text{reactants}}{\nu_A A + \nu_B B + \cdot\cdot\cdot} \longrightarrow \underset{\text{reactant products}}{\nu_C C + \nu_D D + \cdot\cdot\cdot} \tag{5.7}$$

assigns to the stoichiometric coefficients of the reactants a negative sign and to those of the reaction products a positive sign. In autocatalytic reactions such as

$$X + Y \rightleftharpoons 2X \tag{5.8}$$

the stoichiometric coefficient of X should be negative on the left-hand side and positive on the right-hand side, while the overall coefficient $\nu_X = -1 + 2 = +1$ would fit equally well the reaction $Y \rightleftharpoons X$. To make explicit such processes, as well as for reasons to be discussed later, we prefer to distinguish forward stoichiometric coefficients ν_i^f from the coefficients of the reverse process ν_i^r, and to assign to all the coefficients a positive sign. Thus, the general reaction scheme for a single process will be

$$\nu_A^f A + \nu_B^f B + \nu_C^f C + \nu_D^f D \rightleftharpoons \nu_A^r A + \nu_B^r B + \nu_C^r C + \nu_D^r D + \cdots \tag{5.9}$$

To be sure, many of the coefficients may be zero, as in scheme (5.7) where $\nu_C^f = \nu_D^f = \cdots = \nu_A^r = \nu_B^r = 0$; while for the autocatalytic process, $\nu_X^f = -1$, $\nu_X^r = +2$, it is readily seen that the conventional stoichiometric coefficient ν_i is given by the expression

$$-\nu_i = \nu_i^f - \nu_i^r \quad . \tag{5.10}$$

5.1.3

For a single reaction such as (5.7),

$$\frac{dn_A}{\nu_A} = \frac{dn_B}{\nu_B} = \cdots \quad \frac{dn_C}{\nu_C} = \frac{dn_D}{\nu_D} \quad ,$$

or, generally,

$$\frac{dn_i}{\nu_i} = d\,\xi, \tag{5.11}$$

where $d\xi$ is independent of i. The common factor ξ is the advancement of the reaction; and its change with time is the reaction rate (Aris, 1969),

$$J^R = \frac{d\xi}{dt} \quad . \tag{5.12}$$

The rate of change in the number of moles of the i^{th} component is then

$$\frac{dn_i}{dt} = \nu_i J^R = -(\nu_i^f - \nu_i^r)\, J^R. \tag{5.13}$$

A substance which participates in several processes, with stoichiometric coefficient in the k^{th} reaction, ν_{ik}, obeys the following:

$$\frac{dn_i}{dt} = \sum_{k=1}^{M} \nu_{ik} J_k^R . \tag{5.14}$$

For the bond graph reticulation of chemical process, it will often be convenient to insert explicitly the forward and reverse stoichiometric coefficient and rewrite equation (5.14) as

$$\frac{dn_i}{dt} = - \sum_{k=1}^{M} \nu_{ik}^f J_k^R + \sum_{k=1}^{M} \nu_{ik}^r J_k^R . \tag{5.15}$$

5.1.4

A comparison of equations (5.6) and (5.13) or (5.14) shows that the reversible flow of the ith chemical capacitor was transformed into the dissipative flow of reaction. Although the amount of substance discharged by the capacitor is equal to that flowing in the reactions, it should be clear that the nature of the capacitive and resistive flows is different, and an explicit representation of the transformation requires the introduction of a transducer (TD) which converts one flow into the other. The transducer is characterized by a scaling factor (r) which, in the present case, is either ν_{ik}^f or $\frac{1}{\nu_{ik}{}^r}$, depending upon the direction of the transformation. In bond graph notation a reactant will be depicted as

$$C_i \xrightarrow[J_i]{\mu_i} \overset{\nu_{ik}^f}{TD} \xrightarrow[J^R]{\nu_{ik}^f \mu_i}$$

while a product will be represented as

$$\xrightarrow[J^R]{\nu^r_{jk}\,\mu_j} \overset{1/\nu^r_{jk}}{\mathrm{TD}} \xrightarrow[J_j]{\mu_j} C_j ,$$

where the constitutive relation of $\xrightarrow{1} \mathrm{TD} \xrightarrow{2}$ is

$$\begin{pmatrix} e_2 \\ f_2 \end{pmatrix} = \begin{pmatrix} r & 0 \\ 0 & 1/r \end{pmatrix} \begin{pmatrix} e_1 \\ f_1 \end{pmatrix} . \tag{5.16}$$

Note that the TD may be viewed as a map between capacitive flow and reaction flow.

For a chemical component participating in several reactions, for instance the i^{th} component being a reactant in the p^{th} reaction and a product of the q^{th} reaction, the capacitor C_i is connected to the two reactions through a zero-junction as shown in Fig. 5.2. The summation of flows at the zero-junction gives $J_i = J_i^q - J_i^p = \nu^r_{iq} \; J^R_q - \nu^f_{ip} \; J^R_p$, as expected; and the chemical potential of component i is the same in both reactions.

While the μ_i's and the J_i's are the externally measured port parameters, the rate of reaction J^R is an internal variable driven by an internal force. The driving forces of chemical processes have been studied extensively in the range close to equilibrium. We shall therefore start our discussion of the further reticulation of the reaction black box with the consideration of affinities in this well investigated domain.

5.2 Chemical kinetics close to equilibrium

5.2.1

The equation of Gibbs for a closed system, as considered in this section, is

$$TdS = dU + pdV - \sum_{i=1}^{N} \mu_i dn_i, \qquad (5.17)$$

where all the dn_i's are due to chemical transformation

$$dn_i = \sum_{k=1}^{M} \nu_{ik} d\xi_k. \qquad (5.18)$$

Inserting (5.18) into (5.17), we obtain

$$TdS = dU + pdV - \sum_{k=1}^{M} (\sum_{i=1}^{N} \nu_{ik}\mu_i) d\xi_k. \qquad (5.19)$$

Following De Donder and Van Rysselberghe (1936), we denote the affinity of the k^{th} reaction by

$$A_k = -\sum_{i=1}^{N} \nu_{ik}\mu_i \qquad (5.20)$$

obtaining

$$TdS = dU + pdV + \sum_{k=1}^{N} A_k d\xi_k. \qquad (5.21)$$

According to the formulation of nonequilibrium thermodynamics, $dS = d_eS + d_iS$, where d_eS is the entropy exchanged with the surroundings (given in the present case by $Td_eS = dU + pdV$), while the entropy produced by chemical change is

$$Td_iS = \sum_{k=1}^{M} A_k d\xi_k. \qquad (5.22)$$

The dissipation function for our system is therefore

$$T\frac{d_iS}{dt} \equiv \phi = \sum_{k=1}^{M} A_k \frac{d\xi_k}{dt} = \sum_{k=1}^{M} A_k J_k^R. \qquad (5.23)$$

From equation (5.23), we see that the driving force conjugate to each chemical flow is the respective affinity (equation 5.20).

5.2.2

The relations between rates of reaction and affinities are not unique, as may be seen in the following consideration. Let us define a forward affinity of a single process

$$A^f \equiv \sum_{i=1}^{N} \nu_i^f \mu_i \tag{5.24}$$

and a reverse affinity

$$A^r \equiv \sum_{i=1}^{N} \nu_i^r \mu_i \, . \tag{5.25}$$

Evidently, the thermodynamic affinity is

$$A = A^f - A^r = \sum_{i=1}^{N} (\nu_i^f - \nu_i^r)\mu_i = -\sum_{i=1}^{N} \nu_i \mu_i \, . \tag{5.26}$$

Similarly, it is advantageous to define a forward reference affinity $A_0^f = \Sigma \nu_i^f \mu_i^0$ and a reverse reference affinity $A_0^r = \sum_{i=1}^{N} \nu_i^r \mu_1^0$, whose difference is , according to classical thermodynamics,

$$A_0^f - A_0^r = \sum_{i=1}^{N} \nu_i \mu_1^0 = RT\ln K_{eq}, \tag{5.27}$$

where K_{eq} is the equilibrium constant of the reaction. Assuming that the rate of the reaction follows a simple mass action constitutive relation, we may write

$$J^R = k_f \prod_{i=1}^{N} c_i^{v_i^f} - k_r \prod_{i=1}^{N} c_i^{v_i^f} \tag{5.28}$$

where k_f is the forward rate constant and k_r is the rate constant of the reverse reaction. The ratio $\frac{k_f}{k_r}$ is

$$K_{eq} = \exp[(A_0^f - A_0^r)/RT] \tag{5.29}$$

or

$$k_f e^{-A_0^f/RT} = k_r e^{-A_0^r/RT} \Delta \kappa \, . \tag{5.30}$$

If we further assume ideal relations between concentration and chemical potential $c_i = e^{(\mu_i - \mu_i^0)/RT}$, we obtain from equations (5.28), (5.30) and (5.24) through (5.26) the following simple relation, used by Van Rysselberghe (1958):

$$J^R = k_f e^{-A_0^f/RT} e^{A^f/RT} - k_r e^{-A_0^r/RT} e^{A^r/RT}$$
$$= \kappa (e^{A^f/RT} - e^{A^r/RT}). \qquad (5.31)$$

If we denote $\kappa \exp \frac{A^f}{RT}$ as the forward velocity v^f and $\kappa \exp \frac{A^r}{RT}$ as the reverse velocity v^r, equation (5.31) assumes the well-known and suggestive form

$$J^R = v^f - v^r. \qquad (5.32)$$

It is now evident that J^R cannot be reduced to a function of the thermodynamic affinity **A** only, but depends on both $\mathbf{A}^f$ and $\mathbf{A}^r$, which comprise all the concentration effects. It is only close to equilibrium that substantial simplification is obtained.*

5.2.3

At equilibrium, $J^R = 0$; and therefore $\overline{A}^f = \overline{A}^r$, as well as $\overline{A} = 0$, where the overbars denote equilibrium values. We may write equation (5.31) in the form

$$J^R = \kappa e^{A^f/RT} (1 - e^{-A/RT});$$

and since close to equilibrium $A/RT \ll 1$,

---

* The nonuniqueness is readily seen, even in the simplest case of $A \rightleftharpoons B$. When c_A and c_B are doubled, J^R is doubled -- the affinity, however, remains unchanged.

$$J^R \simeq \left[\frac{\kappa}{RT} \quad e^{\bar{A}^f/RT}\right] A = L_R A, \tag{5.33}$$

where the phenomenological coefficient

$$L_R = \frac{\kappa}{RT} e^{\bar{A}^f/RT} = \frac{\bar{v}^f}{RT} \tag{5.34}$$

is constant. Thus, at equilibrium, J^R becomes a linear, single-valued of the affinity. This type of functional relationship is characteristic of a linear one-port resistor. Since all one-port elements are reciprocal; and as will be shown in Section VIII, the interconnection of reciprocal elements is reciprocal in the close-to-equilibrium regime discussed above, the multiport representing the reaction mixture is reciprocal and therefore may be characterized by a potential function — the entropy production (Prigogine, 1967).

A necessary and sufficient condition for reciprocity is the symmetry of the Jacobian matrix of the port flows and efforts. In the present case, the Jacobian is the matrix of terms

$$DJ = \left[\frac{\partial J_i}{\partial \mu_i}\right] \quad .$$

Making use of equation (5.13) for J_i, equation (5.26) for the affinity, and equation (5.33) for the reaction rate-affinity relation, we find

$$\frac{\partial J_i}{\partial \mu_j} = \nu_i \frac{\partial J^R}{\partial \mu_j} = \nu_i L_R \frac{\partial A}{\partial \mu_j} = - \nu_i \nu_j L_R$$

while

$$\frac{\partial J_j}{\partial \mu_i} = \nu_j \frac{\partial J^R}{\partial \mu_i} = - \nu_j \nu_i L_R = \frac{\partial J_i}{\partial \mu_j} \quad , \tag{5.35}$$

which is the required relation.

5.2.4

It is now possible to complete the reticulation of the black box which characterizes a chemical process close to equilibrium by utilizing a one-port resistor, with conductance L_R, to describe the dissipation due to the reaction. Figure 5.3 illustrates a causally correct bond graph for a typical chemical reaction.

Examining the bond graph for the reaction $2A + 3B \rightleftharpoons C$, we see that at the zero-junction all the flows are the same: $-\frac{J_A}{2} = -\frac{J_B}{3} = J_C = J_R$, as required by equations (5.11) and (5.12). The sum of the forces at a zero-junction should be zero: $-2\mu_A - 3\mu_B + \mu_C + A = 0$ or $A = 2\mu_A + 3\mu_B - \mu_C$, in accord with equation (5.26).

More complex cases are readily constructed by the same principle; and Fig. 5.4 represents the case of a three-flow system -- close to equilibrium.

5.2.5

Most biochemical reactions are very rapid; consequently, there is little interest in the study of quasi-equilibrium processes. However, the determination of the relaxation times of a chemical process, i.e., the time required for a system perturbed from equilibrium to return to 1/e of its equilibrium value, provides valuable information for the evaluation of the kinetic parameters describing the reaction. It will be shown that the treatment outlined above offers a useful approach to the computation of relaxation times.

all information about their behavior is obtained from measurements of flow-effort relations at external ports. Since it is possible in principle to determine the chemical potentials and the rates of change of concentration of the known constituents, the incremental constitutive relations $\frac{\partial J_i}{\partial \mu_j}$ which constitute the (N × N) conductance matrix for the n-port may be constructed. Earlier we used this Jacobian for consideration of reciprocity in chemical reactions. Now we shall examine in some detail the information provided by this matrix on the nature and number of independent chemical processes in a given system.

In order to examine the significance of the conductance matrix, let us consider three possible reactions of components A, B and C, namely:

(a) $A + B \xrightarrow{1} C$;

(b) $A \xrightarrow{1} B \xrightarrow{2} C$; and

(c) the triangle reaction

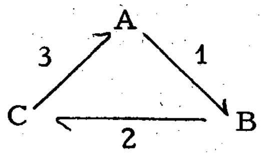

To evaluate the terms in each matrix, we use equation (5.44). Assuming $J_i = J_i(\mu_A, \mu_B, \mu_C)$, $i = 1, 2, 3$, we find the (3 × 3) Jacobian matrices to be:

For case (a) For case (b) For case (c)

$$\frac{1}{RT}\begin{pmatrix} -v^f & -v^f & v^r \\ -v^f & -v^f & v^r \\ v^f & v^f & -v^r \end{pmatrix} - \frac{1}{RT}\begin{pmatrix} v_1^f & v_1^r & 0 \\ v_1^f & v_1^f + v_2^f & v_2^r \\ 0 & v_2^f & v_2^r \end{pmatrix} \frac{1}{RT}\begin{pmatrix} -v_1^f - v_3^r & v_1^f & v_3^f \\ v_1^f & v_1^r - v_2^f & v_2^r \\ v_3^r & v_2^f & -v_2^r - v_3^f \end{pmatrix}$$

The relaxation time of a reaction τ_R is defined by the equation

$$\frac{d\xi}{dt} = \frac{\xi - \bar{\xi}}{\tau_R} , \qquad (5.36)$$

where $\bar{\xi}$ is the advancement of a reaction at equilibrium, and $\xi - \xi$ the small deviation under consideration. Close to equilibrium, equation (5.33) is valid, hence

$$\frac{d\xi}{dt} = J^R = L_R A. \qquad (5.37)$$

Expanding the affinity in a Taylor series close to equilibrium, we find that

$$A = \bar{A} + (\overline{\frac{\partial A}{\partial \xi}})(\xi - \bar{\xi}) + \cdots = (\overline{\frac{\partial A}{\partial \xi}}) \Delta \xi \qquad (5.38)$$

since $\bar{A} = 0$. Inserting equation (5.38) into (5.37) and equating with (5.36) gives

$$- \frac{1}{\tau_R} = L_R (\frac{\partial \bar{A}}{\partial \xi}) . \qquad (5.39$$

The factor $(\overline{\frac{\partial A}{\partial \xi}})$ can be made more explicit in terms of the capacitances of the components (equations 5.5 and 5.11):

$$(\overline{\frac{\partial A}{\partial \xi}}) = - \Sigma \frac{\nu_i^2}{\bar{C}_i} \qquad (5.40)$$

and hence

$$\frac{1}{\tau_R} = L_R \Sigma \frac{\nu_i^2}{\bar{C}_i} . \qquad (5.41)$$

Denoting the "relaxation time of a single component" by

$$\tau_i = \bar{C}_i / L_R = \bar{C}_i R_R , \qquad (5.42)$$

equation (5.41) assumes the suggestive form

$$\frac{1}{\tau_R} = \sum_i \frac{\nu_i^2}{\tau_i} \quad . \qquad (5.43)$$

The significance of equation (5.43) can be shown by the following trivial example: consider the reaction $A \rightleftharpoons B$. Here $L_R = \frac{v^f}{RT} = k_f \frac{\bar{c}_A}{RT}$. By equation (5.5), $\bar{C}_A = \bar{c}_A \cdot V/_{RT}$ and $\bar{C}_B = \bar{c}_B \cdot V/_{RT}$; hence, considering a unit volume for the reaction vessel, $\tau_A = \bar{C}_A/L_R = 1/k_f$, $\tau_B = \bar{C}_B/L_R = 1/k_r$, and $\tau_R = 1/(k_f + k_n)$, as is well-known in chemical kinetics.

5.3 Two-port representation of chemical dissipative processes.

5.3.1

As pointed out in paragraph 5.2.2, chemical processes far from equilibrium cannot be adequately described by a one-port representation for the reaction resistance. Such a representation implies that: a) a unique relationship exists between the reaction rate and affinity; and b) the Jacobian matrix $\underset{\sim}{DJ}$ of the port efforts and flows is symmetrical. We shall show that in the far-from-equilibrium case, this Jacobian is not symmetrical; and only near equilibrium, when the forward reaction velocity v^f approaches that of the reverse reaction v^r, is symmetry regained. That is, there is an additional "dynamical" constraint on the constitutive relation for a chemical reaction: the experimental fact of "nonreciprocity." Perturbations of reactant and product concentrations do not produce symmetric effects far from equilibrium.

Consider the general term $\frac{\partial J_i}{\partial \mu_j}$ of the incremental conductance matrix for any reaction system. Since, on a priori grounds, we regard the system as a black box in which M reactions may take place, J_i should be written, according to equation (5.15), as $J_i = \sum_k \nu_{ik} J_k^R$. Further, the dependence of each reaction rate on the μ_j's is through the forward and reverse affinities, so that

$$\frac{\partial J_i}{\partial \mu_j} = \sum_{k=1}^{M} \nu_{ik} \frac{\partial J_k^R}{\partial \mu_j} = \sum_{k=1}^{M} \nu_{ik} \frac{\kappa}{RT} \left(\frac{\partial A_k^f}{\partial \mu_j} e^{A_k^f/RT} - \frac{\partial A_k^r}{\partial \mu_j} e^{A_k^r/RT} \right)$$

or

$$\frac{\partial J_i}{\partial \mu_j} = \frac{1}{RT} \sum \nu_{ik} (\nu_{jk}^f v_k^f - \nu_{jk}^r v_k^r).$$

It will be observed that $(\nu_{jk}^f v_k^f - \nu_{jk}^r v_k^r) = \frac{\partial J_k^R}{\partial \mu_j} = \omega_{jk}$ is a kind of modified rate of reaction, and

$$\frac{\partial J_i}{\partial \mu_j} = \frac{1}{RT} \sum_k \nu_{ik} \omega_{jk}. \qquad (5.44)$$

Generally, $\partial J_i/\partial \mu_j \neq \partial J_j/\partial \mu_i$; however at equilibrium, when $\bar{v}_k^f = \bar{v}_k^r$, the value of ω_{jk} becomes $\bar{\omega}_{jk} = \bar{v}_k^f (\nu_{jk}^f - \nu_{jk}^r) = -\nu_{jk} \bar{v}_k^f$ which leads to a symmetry of the cross conductances as obtained in 5.2.3:

$$\overline{\left(\frac{\partial J_i}{\partial \mu_j}\right)} = -\frac{1}{RT} \sum_{k=1}^{M} \nu_{ik} \bar{v}_k^f \nu_{jk} = \overline{\left(\frac{\partial J_j}{\partial \mu_i}\right)} . \qquad (5.45)$$

5.3.2

For chemical reactions proceeding far from equilibrium, the incremental conductance of a single chemical reaction $L_R = \frac{\partial J^R}{\partial A}$ is not a well-defined function of the thermodynamic affinity A since J^R depends on both A^f and A^r. Moreover, the extrathermodynamic constraint of nonreciprocity cannot be accommodated by a one-port representation.* Therefore, we must conclude that the dissipation due to a chemical reaction must be represented by a two-port resistor, which cannot be further reticulated except close to equilibrium.

The general bond representation of the dissipation due to a chemical process is shown in Fig. 5.5. The ports are defined by the forward and reverse affinities and an input and output flow of reaction (J^R_{in} and J^R_{out}). Conservation of mass in chemical reactions imposes the further constraint that the port flows are always equal to the rate of reaction: $J^R_{in} = J^R_{out} = J^R$.** The overall force acting "across" the two-port is the thermodynamic affinity $A = A^f - A^r$. Near equilibrium, the two-port may be further reticulated into a one-junction and a one-port resistor driven by A alone.

5.3.3

The general representation of chemical processes is illustrated in Figs. 5.6 through 5.10. The case of a bimolecular reaction is shown in Fig. 5.6. For reactions with a common component, the simplest case of $A \underset{}{\overset{1}{\rightleftharpoons}} B \underset{}{\overset{2}{\rightleftharpoons}} C$ is shown

---

* This constitutive constraint is analogous to the "nonthermodynamic" assumption of homogeneity for fluid systems which leads to the Euler and Gibbs-Duhem relations. (see footnote, p. 14)

**Note that $J^R_{in} \neq v^f$ and $J^R_{out} \neq v^r$.

in Fig. 5.7. A more sophisticated case is the network of dependent reactions disscussed by Pings and Nebecker (1964) and shown in Fig. 5.8.

A very important group of bond graphs are those representing enzymatic processes such as $S + E \rightleftharpoons (ES) \rightleftharpoons E + P$ (Fig. 5.9), where E denotes the enzyme, S the substrate, ES the enzyme-substrate complex, and P the reaction product. Note that in this scheme the enzyme is confined to the portion of the bond graph enclosed by dotted lines, and thus may be viewed as a black box converting substrate into product. In the nonenzymatic reaction $S \rightleftharpoons P$, this black box converter is replaced by a single two-port resistor.

The simple autocatalytic process $X + Y \rightleftharpoons 2X$ is shown in Fig. 5.10. It is worth noting that an autocatalytic reaction appears as a positive feedback loop, suggesting that such reactions may produce dynamic instabilities.

5.3.4 .

The last three figures (5.8, 5.9, 5.10) exhibit in a clear manner the topological properties of a chemical network. Indeed, every bond graph may be viewed as a topological object which may be treated formally from a general mathematical point of view. This approach will be pursued further in Section VIII.

5.4 Analysis of chemical systems

5.4.1

The network approach to reacting systems assumes that where the v_i's represent the forward or reverse velocities of the corresponding reactions. It will be noted that the ranks of these matrices are 1, 2 and 2, respectively. We readily discern the important fact that the number of independent rows equals the number of independent reactions in the system. In case (a), we have only one reaction; in case (b), there are two independent reactions, A ⟶ B and B ⟶ C. Although comprising three processes, case (c) contains only two independent reactions, corresponding to the rank of the conductance matrix.

5.4.2

This important observation leads to a general statement that the rank (ρ) of the incremental conductance matrix equals the number of independent chemical processes proceeding in the reaction vessel. The proof for the general case follows.

It will be recalled that, in equation (5.15), the total change in the number of moles of the i^{th} component was related to the M reaction rates J_k^R through the stoichiometric coefficients ν_{ik}. The coefficients ν_{ik} constitute an N × M stoichiometric matrix. If the rank of this matrix is ρ, then there exist only ρ independent affinities and, as shown by De Groot and Mazur (1962),

$$\frac{dn_i}{dt} = \sum_{k=1}^{\rho} \nu_{ik} \hat{J}_k^R , \tag{5.46}$$

where the $\hat{J}_k^R$ are a set of independent flows conjugate to the independent affinities.

Since the chemical flows $\hat{J}_k^R$ are independent, $\hat{J}_k^R = \phi(A_k)$ is a function only of its conjugate independent affinity. By equation (5.46), the general term of the Jacobian is

$$\frac{\partial J_i}{\partial \mu_j} = \sum_{k=1}^{\rho} \nu_{ik} \frac{\partial \hat{J}_k^R}{\partial \mu_i} = \sum_{k=1}^{\rho} \nu_{ik} \frac{\partial \hat{J}_k^R}{\partial A_k} \frac{\partial A_k}{\partial \mu_i}$$

$$= -\sum_{k=1}^{\rho} \nu_{ik} L_k^R \nu_{jk} \tag{5.47}$$

or, in matrix form, $\underset{\sim}{DJ} = -\underset{\sim}{\nu}\underset{\sim}{L}^R\underset{\sim}{\nu}^T$, (5.48)

where L_k^R is the conductance of the k^{th} independent chemical reaction.

The matrix $\underset{\sim}{\nu}$ for the <u>independent</u> reaction flows is a $n \times \rho$ matrix. The $\rho \times \rho$ matrix $\underset{\sim}{L}^R$ of conductances is diagonal since all the flows are independent. It is a standard result in linear algebra (c.f. Cullis, 1913) that the rank of the product of an $\alpha \times \rho$ matrix $\underset{\sim}{Q}$ and a $\rho \times \beta$ matrix $\underset{\sim}{P}$ has the rank of $\underset{\sim}{Q}$ if rank $(\underset{\sim}{P}) = \rho$, and has the rank of $\underset{\sim}{P}$ if rank $(\underset{\sim}{Q}) = \rho$. Therefore, rank $(\underset{\sim}{\nu}\underset{\sim}{L}^R) = \rho$, since rank $(\underset{\sim}{\nu}) = \rho$, and furthermore, rank $(\underset{\sim}{\nu}\underset{\sim}{L}^R\underset{\sim}{\nu}^T) = \rho$, since rank $(\underset{\sim}{\nu}^T) = \rho$ also. Hence, the rank of the Jacobian: rank $(\underset{\sim}{DJ}) = \rho$.* (5.49)

5.4.3

A straightforward use of the previous result is the elucidation of "hidden" intermediates which increase the number of independent reactions. Consider, for example, the simple reaction $A \underset{v^r}{\overset{v^f}{\rightleftharpoons}} B$, which should be characterized by a Jacobian

---

* Aris and Mah (1963), using a similar argument, developed a kinetic test for the number of independent reactions.

of rank 1, $\underset{\sim}{DJ} = \frac{1}{RT}(-v^f v^r)$. However, if the process passes through an intermediate component X, it comprises two rate processes $A \underset{v_1^r}{\overset{v_1^f}{\rightleftharpoons}} X \underset{v_2^r}{\overset{v_2^f}{\rightleftharpoons}} B$; and its Jacobian, based only on the measurements of the properties of species A and B, has rank two:

$$\underset{\sim}{DJ} = -\frac{1}{RT}\begin{bmatrix} v_1^f & 0 \\ 0 & v_2^r \end{bmatrix}.$$

In many applications, it is important to distinguish between autocatalytic and nonautocatalytic reaction mechanisms. For example, consider the reactions: (a) $X + Y \rightleftharpoons 2X$, and (b) $Y \rightleftharpoons X$. In case (a), the Jacobian is

$$\underset{\sim}{DJ} = \frac{1}{RT}\begin{bmatrix} -v^f & -v^f + 2v^r \\ v^f & v^f - 2v^r \end{bmatrix},$$

while, in case (b),

$$\underset{\sim}{DJ} = \frac{1}{RT}\begin{bmatrix} -v^f & v^r \\ v^f & -v^r \end{bmatrix}.$$

It is evident that with a set of experimentally obtained numerical values one could not distinguish between the two cases. Another test is required.

For each externally measureable flow J_ℓ, the Hessian, i.e., the matrix of second partial derivatives with respect to the chemical potentials, may be computed. Differentiating equation (5.48), we obtain

$$\frac{\partial^2 J_\ell}{\partial \mu_i \partial \mu_j} = \frac{1}{RT}\sum_{k=1}^{M} \nu_{\ell k}\frac{\partial \omega_{jk}}{\partial \mu_i} = \frac{1}{(RT)^2}\sum_k \nu_{\ell k}(\nu_{jk}^f \nu_{ik}^f v_k^f - \nu_{jk}^r \nu_{ik}^r v_k^r), \tag{5.50}$$

where $\ell = 1, 2, \cdots n$.

Thus, in the autocatalytic case (a):

$$\underset{\sim}{D}^2 J_X = \frac{1}{(RT)^2} \begin{bmatrix} -v^f & -v^f \\ -v^f & -v^f + 4v^r \end{bmatrix} ,$$

while in the nonautocatalytic case (b):

$$\underset{\sim}{D}^2 J_X = \frac{1}{(RT)^2} \begin{bmatrix} -v^f & 0 \\ 0 & -v^r \end{bmatrix} .$$

From an experimental determination of the Hessian, it is thus possible to distinguish between autocatalytic and nonautocatalytic reaction mechanisms.

VI. THE COUPLING OF CHEMICAL AND DIFFUSIONAL PROCESSES

6.1. Bond graph representation of coupled chemical and diffusional processes

The interaction of chemical and diffusional processes occurs so ubiquitously in all biological systems that there is no need to stress its importance. If suffices to mention that both facilitated and active transport are typical examples of chemico-diffusional coupling, and there is no doubt that the cybernetic organization of cells and tissues is in part based on the functional relation between metabolic and transport processes. Although facilitated transport has been considered from the point of view of nonequilibrium thermodynamics and analyzed frequently on the basis of different kinetic models, it is advantageous to reconsider the field from another phenomenological point of view, which allows a more general treatment of nonlinear coupled flows.

As discussed previously, one of the principal advantages of the bond graph notation is that it algorithmically accounts for conservation and continuity conditions via the definitions of the zero- and one-junctions. During diffusional flows, the total amount of each chemical species remains constant, and so the conservation condition on the zero-junction (KCL) is clearly satisfied (see Fig. 3.2d). However, if a chemical reaction involving the diffusing substance is proceeding simultaneously, each species is not conserved. The reaction appears as a source or sink term in the conservation equation for each reacting species:

$$\frac{\partial n_i}{\partial t} = -\nabla J_i + \sum_k \nu_{ik}' J_k^R . \qquad (6.1)$$

However, by extending the bond graph representing diffusion to include chemical reactions the terms $\sum_k \nu_{ik} J_k^R$ can be assigned to the appropriate bonds incident on the zero-junction, so as to transform equation (6.1) into KCL form.

We shall introduce the analysis of coupled chemico-diffusional processes by considering the flow of two nonelectrolytes, A and B, through a membrane in which reaction proceeds during the transport process.

The bond graph representing such a system is obtained by combining the structures for diffusion and reaction described previously. For simplicity, we will not include hydrodynamic coupling here, although such an inclusion is trivial. The bond graph structure shown in Fig. 6.1 suggests that an appropriate functional representation of 1-dimensional diffusion-reaction processes would be an x vs ξ plot. The structure shown is a "one-lump" representation where single average concentrations of A and B are taken to represent the true concentration profile within the membrane, and the sources E_A and E_B indicate that the reservoirs bounding the membrane maintain a constant chemical potential. The transition to the continuum profile will be discussed below. We wish to emphasize that, strictly speaking, the bond graph displays only topological relations. The bonds have no geometrical significance in themselves. However, by taking advantage of the obvious similarities between the actual physical system and its bond graph, the bonds joining zero- and one-junctions in many cases may be ascribed an actual length, depending on the number of repeating units one employs to represent the system.

6.2. Port constitutive relations

The one-lump model shown in Fig. 6.1 may be used to represent both uncoupled and coupled diffusion and reaction, depending upon the port variables used to describe the system. This is most easily seen by deriving the Onsager phenomenological equations from the bond graph. Assuming the diffusional resistors are linear,

$$\mu_A^I - \mu_A^m = R_A^1 J_A^1 \tag{6.2a}$$

and

$$\mu_A^m - \mu_A^{II} = R_A^2 J_A^2 . \tag{6.2b}$$

Adding equations (6.2a) and (6.2b) and assuming the bond graph resistances R_A^1 and R_A^2 are each one half the total diffusional resistance R_A, we get

$$\Delta\mu_A = \mu_A^I - \mu_A^{II} = R_A \bar{J}_A, \qquad (6.3)$$

where $\bar{J}_A = \frac{J_A^1 + J_A^2}{2}$ is an average diffusional flow. Similarly,

$$\Delta\mu_B = R_B \bar{J}_B \qquad (6.4)$$

where $\bar{J}_B = \frac{J_B^1 + J_B^2}{2}$. As we have shown in paragraph 5.2, in the near equilibrium the reaction dissipation may be represented by a one-port resistor. Hence,

$$A = A^f - A^r = R_R J^R \qquad (6.5)$$

and the phenomenological equations are uncoupled. DeSimone and Caplan (1972) have shown by a continuum treatment that for a homogeneous membrane, choices other than the average diffusional flow may lead to reaction diffusion coupling. For example, as Katchalsky and Oster (1969) demonstrate, one may choose the diffusional flows on one side of the membrane, say J_A^1 and J_B^1, and the affinity on the opposite side, say A^{II}, to describe the dissipative process. In steady state,

$$J_A^2 = J_A^1 - J^R$$

and

$$J_B^2 = J_B^1 - J^R.$$

Therefore,

$$\Delta\mu_A = R_A J_A^1 - \frac{R_A}{2} J^R$$

and

$$\Delta\mu_B = R_B J_B^1 - \frac{R_B}{2} J^R. \tag{6.6}$$

The affinity on side II of the membrane is given by

$$A^{II} = \mu_A^{II} - \mu_B^{II} = (\mu_A^m - R_A J_A^2) - (\mu_B^m - R_B J_B^2)$$

$$= (\mu_A^m - \mu_B^m) - R_A(J_A^1 - J^R) + R_B(J_B^1 - J^R).$$

Therefore,

$$A^{II} = - R_A J_A^1 + R_B J_B^1 + (R_R + R_A - R_B)J^R; \tag{6.7}$$

and equations (6.6) and (6.7) represent a coupled Onsager scheme.

6.3. Relaxation times for chemico-diffusional processes

6.3.1.

Utilizing the one-lump bond graph model shown in Fig. 6.1, one can calculate the relaxation times for chemico-diffusional processes. In paragraph 2.3 we showed that the pure diffusional relaxation time τ_D equals $\frac{RC}{4}$ (equation 2.30); and in paragraph 5.2.5 we derived the relaxation time τ_R for chemical processes perturbed from their equilibrium state. In this section we will consider a chemical process maintained at a far-from-equilibrium steady state by diffusion.

The general time dependent state equations may be read directly from the bond graph:

$$C_A \frac{d\mu_A}{dt} = J_A^1 - J_A^2 - J^R(A^f, A^r),$$
$$C_B \frac{d\mu_B}{dt} = J_B^1 - J_B^2 + J^R(A^f, A^r). \tag{6.8}$$

Introducing the resistive constitutive relations and assuming

$$R_A^1 = R_A^2 = \frac{R_A}{2} \text{ and } R_B^1 = R_B^2 = \frac{R_B}{2}$$

results in the nonlinear state equations

$$C_A \frac{d\mu_A}{dt} = 2\,\frac{(\mu_A^I + \mu_A^{II} - 2\mu_A)}{R_A} - J^R(A^f, A^r)$$

and

$$C_B \frac{d\mu_B}{dt} = 2\,\frac{(\mu_B^I + \mu_B^{II} - 2\mu_B)}{R_B} - J^R(A^f, A^r). \tag{6.9}$$

6.3.2.

In order to study the relaxation times of the system, we examine the tangent system about the steady state; i.e., let $\mu_A = \mu_A^{ss} + \delta\mu_A$ and $\mu_B = \mu_B^{ss} + \delta\mu_B$, where μ^{ss} denotes the steady state value of the chemical potential. Inserting these perturbations into equation (6.9) yields the following small signal equation

$$\frac{d}{dt}\begin{pmatrix}\delta\mu_A \\ \delta\mu_B\end{pmatrix} = \begin{pmatrix} -\frac{4}{R_A C_A} - \frac{L_R^f}{C_A} & -\frac{L_R^r}{C_A} \\ -\frac{L_R^f}{C_B} & -\frac{4}{R_B C_B} - \frac{L_R^r}{C_B} \end{pmatrix}_{ss} \begin{pmatrix}\delta\mu_A \\ \delta\mu_B\end{pmatrix} \qquad (6.10)$$

or

$$\frac{d}{dt}(\underset{\sim}{\delta\mu}) = \underset{\sim}{Q}\ \underset{\sim}{\delta\mu}, \qquad (6.11)$$

where Q is a constant matrix and $L_R^f = \left(\frac{\partial J^R}{\partial A^f}\right)_{ss}$, $L_R^r = \left(\frac{\partial J^r}{\partial A^r}\right)_{ss}$. Notice that, for the mass action constitutive relation, $L_R^f = \frac{v_{ss}^f}{RT}$ and $L_R^r = \frac{v_{ss}^r}{RT}$, where v_{ss} is a steady state velocity.

The eigenvalues, λ, of Q determine the relaxation times of the system, and are given by the characteristic equation

$$\lambda^2 - \lambda \operatorname{tr} Q + \det Q = 0, \qquad (6.12)$$

where the trace of Q is

$$\operatorname{tr} Q = -\frac{4}{R_A C_A} - \frac{4}{R_B C_B} - \frac{L_R^f}{C_A} - \frac{L_R^r}{C_B} < 0 \qquad (6.13)$$

and the determinant of Q is

$$\det Q = \frac{16}{R_A R_B C_A C_B} + \frac{4L_R^f}{R_B C_A C_B} + \frac{4L_R^r}{R_A C_A C_B} > 0. \qquad (6.14)$$

Since $\operatorname{tr} Q < 0$ and $\det Q > 0$, the steady state is asymptotically stable; and any perturbation will return to the stationary state.

Solving the characteristic equation, we find that

$$\lambda = -\left(\frac{2}{R_A C_A} + \frac{2}{R_B C_B} + \frac{L_R^f}{2C_A} + \frac{L_R^r}{2C_B}\right)$$

$$\pm\sqrt{\left(\frac{2}{R_A C_A} + \frac{2}{R_B C_B} + \frac{L_R^f}{2C_A} + \frac{L_R^r}{2C_B}\right)^2 - \frac{4}{C_A C_B}\left(\frac{4}{R_A R_B} + \frac{L_R^f}{R_B} + \frac{L_R^r}{R_A}\right)} \tag{6.15}$$

and the relaxation times are given by $\tau = -\frac{1}{\lambda}$.

6.3.3.

In the limiting case where there is no reaction, $L_R^f = L_R^r = 0$; and equation (6.15) simplifies to

$$\lambda_A = -\frac{4}{R_A C_A} = -\frac{1}{\tau_A},$$
$$\lambda_B = -\frac{4}{R_B C_B} = -\frac{1}{\tau_B}. \tag{6.16}$$

In the other limiting case, where there is no diffusion, R_A, $R_B \rightarrow \infty$; and the eigenvalues are

$$\lambda_R = -\left(\frac{L_R^f}{C_A} + \frac{L_R^r}{C_B}\right) = -\frac{1}{\tau_R} . \tag{6.17}$$

If will prove to be convenient to define two relaxation times for a chemical process—one for the forward reaction and one for the reverse reaction. Hence, we denote

$$\lambda_f \triangleq -\frac{L_R^f}{C_A} = -\frac{1}{\tau_R^f} ; \quad \lambda_r \triangleq -\frac{L_R^r}{C_B} = -\frac{1}{\tau_R^r} , \tag{6.18}$$

where $$\lambda_R = \lambda_f + \lambda_r .^{*} \qquad (6.19)$$

For the case of mass action kinetics, $L_R^f = \frac{v^f}{RT} = \frac{k_f c_A}{RT}$ and $L_R^r = \frac{v^r}{RT} = \frac{k_r c_B}{RT}$; while, for ideal solutions of unit volume, $C_A = \frac{c_A}{RT}$ and $C_B = \frac{c_B}{RT}$. Under these restrictions, $\lambda_f = -k_f$ and $\lambda_r = -k_r$; hence, $\tau_R = \frac{1}{k_f + k_r}$, which is the usual kinetic result.

6.3.4.

Let us now reconsider the general case where both reaction and diffusion occur. Rewriting equation (6.15), we find:

$$\lambda = \frac{(\lambda_A + \lambda_B + \lambda_f + \lambda_r) \pm (\lambda_A + \lambda_f - \lambda_B - \lambda_r)}{2} \sqrt{1 + \frac{4\lambda_f \lambda_r}{(\lambda_A + \lambda_f - \lambda_B - \lambda_r)^2}} . \qquad (6.20)$$

In the case when the diffusion constants of A and B are equal, i.e., when $\lambda_A = \lambda_B = \lambda_D$, equation (6.20) simplifies, and

$$\lambda_1 = \lambda_D = -\frac{1}{\tau_D},$$

$$\lambda_2 = \lambda_D + \lambda_r + \lambda_f = -\left(\frac{1}{\tau_D} + \frac{1}{\tau_R}\right). \qquad (6.21)$$

We may also consider the case of unequal diffusion coefficients, when the reaction is much faster than diffusion, i.e., when $|\lambda_f + \lambda_r| \gg |\lambda_A|, |\lambda_B|$. For this case, it is advantageous to

---

[*] In the case of nonunit stoichiometry, $\lambda_f = -\frac{(\nu_A^f)^2 L_R^f}{C_A}$ and $\lambda_r = -\frac{(\nu_B^f)^2 L_R^r}{C_B}$; the rest of the analysis remains the same.

rewrite equation (6.15) in the form

$$\lambda = \frac{(\lambda_A + \lambda_B + \lambda_f + \lambda_r) \pm (\lambda_f + \lambda_r)}{2} \sqrt{1 + \frac{2(\lambda_A - \lambda_B)(\lambda_f - \lambda_r)}{(\lambda_f + \lambda_r)^2} + \frac{(\lambda_A - \lambda_B)^2}{(\lambda_f + \lambda_f)^2}} \; . \tag{6.22}$$

Neglecting the term $\left(\frac{\lambda_A - \lambda_B}{\lambda_f + \lambda_r}\right)^2$ and expanding the square root in a Taylor series to first order yields

$$\lambda_1 = (\lambda_f + \lambda_r) + \frac{\lambda_A \lambda_f + \lambda_B \lambda_r}{\lambda_f + \lambda_r}$$

and

$$\lambda_2 = \frac{\lambda_A \lambda_r + \lambda_B \lambda_f}{\lambda_f + \lambda_r} , \tag{6.23}$$

which reduce to equation (6.21) when $\lambda_A = \lambda_B$. In terms of relaxation times, inserting equation (6.16) and (6.17) into (6.23) yields

$$\tau_1^{-1} = \tau_R^{-1} + \tau_R \left(\tau_A^{-1} \tau_R^{f\,-1} + \tau_B^{-1} \tau_R^{r-1} \right),$$

$$\tau_2^{-1} = \tau_R \left(\frac{1}{\tau_A \tau_R^r} + \frac{1}{\tau_B \tau_R^f} \right) . \tag{6.24}$$

6.4. Continuum equations

6.4.1.

The bond shown in Fig. 6.1 is a one-lump model of reaction and diffusion processes. In this section, we will show that as the number of lumps in the model becomes very large, the bond graph equations reduce to the usual continuum equations for simultaneous reaction and diffusion processes.

Considering a bond graph composed of a large number of lumps, a typical subunit of length dx is the asymmetric lump shown in Fig. 6.2, where $\tilde{C}$ and $\tilde{R}$ denote the specific capacitance and resistance. For a sufficiently large number of lumps, the chemical potential and flow on the right-hand side of the lump may be expressed as a Taylor expansion of μ, and of J on the left-hand side. Keeping only the first-order terms in the expansion, we see from the bond graph that on the diffusional resistors

$$-\frac{d\mu_A}{dx}\,dx = \tilde{R}_A dx \left(J_A + \frac{dJ_A}{dx}\,dx\right)$$

$$-\frac{d\mu_B}{dx}\,dx = \tilde{R}_B dx \left(J_B + \frac{dJ_B}{dx}\,dx\right),$$

or to first order in dx

$$-\frac{d\mu_A}{dx} = \tilde{R}_A\, J_A, \qquad -\frac{d\mu_B}{dx} = \tilde{R}_B\, J_B\,. \tag{6.25}$$

Equations (6.25) are the conventional nonequilibrium thermodynamic continuum equations for diffusional flow. Considering the bond graph equations for the capacitors, we have

$$\begin{aligned}\tilde{C}_A dx\,\frac{d\mu_A}{dt} &= J_A - \left(J_A + \frac{dJ_A}{dx}\,dx\right) - \tilde{L}_R\left(A^f,\ A^r\right) dx\\ \tilde{C}_B dx\,\frac{d\mu_B}{dt} &= J_B - \left(J_B + \frac{dJ_B}{dx}\,dx\right) + \tilde{L}_R\left(A^f,\ A^r\right) dx,\end{aligned} \tag{6.26}$$

where we have used the constitutive relation

$$J^R = \tilde{L}_R(A^f, A^r)\,dx\ .$$

Rewriting equations (6.26), we find

$$\begin{aligned}\tilde{C}_A \frac{d\mu_A}{dt} &= -\frac{dJ_A}{dx} - \tilde{L}_R(A^f, A^r)\\ \tilde{C}_B \frac{d\mu_B}{dt} &= -\frac{dJ_B}{dx} + \tilde{L}_R(A^f, A^r).\end{aligned} \qquad (6.27)$$

Identifying $\tilde{L}_R(A^f, A^r)$ with the local reaction rate $\tilde{J}^R$, and noting that $\tilde{C}_A = \frac{\partial c_A}{\partial \mu_A}$, we see that equations (6.27) are nothing more than the continuity equations for the reaction diffusion system

$$\frac{\partial c_i}{\partial t} = -\frac{dJ_i}{dx} + \nu_i \tilde{J}^R. \qquad (6.28)$$

Thus the lumped bond graph representation reduces to the basic equations of continua when driven to the limit of infinitesimal lump size. Notice that, as one would expect, this derivation was independent of the form of the constitutive assumption for the chemical reaction.

We can combine these local equations in the standard fashion by differentiating equations (6.25) and inserting dJ/dx into equations (6.27), obtaining

$$\begin{aligned}
\tilde{R}_A \tilde{C}_A \frac{d\mu_A}{dt} &= \frac{d^2\mu_A}{dx^2} - \frac{d\ln\tilde{R}_A}{dx}\frac{d\mu_A}{dx} - \tilde{R}_A\tilde{L}_R\,(A^f, A^r) \\
\tilde{R}_B \tilde{C}_B \frac{d\mu_B}{dt} &= \frac{d^2\mu_B}{dx^2} - \frac{d\ln\tilde{R}_B}{dx}\frac{d\mu_B}{dx} + \tilde{R}_B\tilde{L}_R\,(A^f, A^r).
\end{aligned} \tag{6.29}$$

Equations (6.29) adequately describe the relaxation behavior of A and B in a membrane with reaction.

Friedlander and Keller (1965) and Katchalsky and Oster (1969) have shown that in the near equilibrium regime, assuming constant diffusional resitances, equations (6.29) take a particularly simple form. Under conditions of steady flow, a field equation of the Helmholz type for the affinity is obtained:

$$\lambda^2 \nabla^2 A = A, \tag{6.30}$$

where $\lambda = [\tilde{L}_R(\tilde{R}_A + \tilde{R}_B)]^{-1/2}$ is a characteristic reaction diffusion length proportional to the Thiele modulus for near equilibrium reactions. For membranes of thickness Δx,

$$\left(\frac{\lambda}{\Delta x}\right)^2 = \frac{\tau_R}{2\langle \tau_D \rangle}, \tag{6.31}$$

where τ_R is the relaxation time of the reaction,

$$\langle \tau_D \rangle = \frac{\sum_{i=1}^{n} \nu_i^2 \bar{\mu}_{ii} \tau_D^i}{\sum_{i=1}^{n} \nu_i^2 \bar{\mu}_{ii}} \tag{6.32}$$

is an average diffusional relaxation time, and $\bar{\mu}_{ii} = \overline{\frac{\partial \mu_i}{\partial c_i}}$ is the change in chemical potential with concentration evaluated at equilibrium (Perelson and Katchalsky, 1972). When $\lambda << \Delta x$, $\tau_R << \langle \tau_D \rangle$; and the reaction will come to equilibrium near the surface of the membrane. On the other hand, for $\lambda >> \Delta x$, $\langle \tau_D \rangle << \tau_R$; and the components diffuse through the membrane without coming to equilibrium. Hence λ is a measure of the distance a reactant must penetrate the membrane before coming to equilibrium.

The average diffusional relaxation time, which was derived from a continuum treatment, contains the unusual weighting factors $\nu_i^2 \bar{\mu}_{ii}$. However, from the network viewpoint, this average may be interpreted in a natural way. By removing the reaction resistance R_R from Fig. 6.1 and adding a one-junction so that the flows on the adjoining bonds remain equal, we can create a port through which one can view the diffusional portion of the network. The resulting bond graph is illustrated in Fig. 6.3. At steady state, when there is no flow into the capacitor, the incremental resistance as seen from this new port is $R_D^{TOT} = \dfrac{\nu_A^2 R_A + \nu_B^2 R_B}{4}$. At equilibrium, when the diffusional flows are zero, the total capacitance seen from this new port is $\dfrac{1}{C^{TOT}} = \dfrac{\nu_A^2}{C_A} + \dfrac{\nu_B^2}{C_B}$. For a reaction diffusion system in which more than two components participate in a single reaction,

$$R_D^{TOT} = \frac{\sum_{i=1}^{n} \nu_i^2 R_i}{4}$$

$$C^{TOT} = \left(\sum_{i=1}^{n} \frac{\nu_i^2}{C_i}\right)^{-1} . \qquad (6.33)$$

Noting that $\bar{\mu}_{ii} = \frac{\Delta x}{C_i}$ and that $\tau_D^i = \frac{R_i C_i}{4}$ (c. f. equation 2.30), we may rewrite equation (6.31) as

$$\langle \tau_D \rangle = \frac{\sum_{i=1}^{n} \nu_i^2 \left(\frac{\Delta x}{C_i}\right) \frac{R_i C_i}{4}}{\sum_{i=1}^{n} \nu_i^2 \left(\frac{\Delta x}{C_i}\right)} = \frac{\sum_{i=1}^{n} \frac{\nu_i^2 R_i}{4}}{\sum_{i=1}^{n} \frac{\nu_i^2}{C_i}} = R_D^{TOT} C^{TOT} . \qquad (6.34)$$

The average diffusional relaxation time is thus simply the total steady state resistance multiplied by the total equilibrium capacitance as seen from the reaction resistance.

6.5. Facilitated transport

As a slightly more complex example of the bond graph technique, let us consider the case of facilitated transport through a membrane. The conventional model for facilitated transport assumes that the membrane contains a carrier C which reacts with a permeant substrate S to form a complex CS. Both S and CS diffuse through the membrane. The CS complex then dissociates releasing C and S at the other side of the membrane. S exits from the membrane and C is free to diffuse back across the membrane and combine with more substrate.

The bond graph representing this process, shown in Fig. 6.4, is a combination of the previously examined bond graphs for reaction and diffusion. We have chosen for illustrative purposes a two-lump model, which is the simplest representation that allows one to include chemical reactions occurring at different points in space. For greater accuracy we could, of course, represent the interior of the membrane by many lumps with a reaction occurring in each. The compartments external to the membrane are represented by the effort (chemical potential) sources E_s^I and E_s^{II}; R_s^I and R_s^{II} are the resistances the substrate sees in entering lump 1 and exiting from lump 2 of the membrane model, respectively. R_s, R_c and R_{cs} are resistances to diffusion within the membrane; R_R^1 and R_R^2 are the reaction resistances; and C_s^1, C_s^2, C_c^1, C_c^2, C_{cs}^1, C_{cs}^2 are the capacitances of the substrate, carrier and carrier substrate complex on sides 1 and 2 of the membrane. In this model, we have assumed that the forward chemical reaction

$$C + S \underset{k_r}{\overset{k_f}{\rightleftharpoons}} CS$$

occurs on side 1 and that the reverse reaction takes place on side 2 of the membrane. These two chemical reactions, plus the diffusion of the carrier and the carrier substrate complex, form a cycle which is characteristic of facilitated transport and which is clearly visible in the bond graph model.

The steady state and the dynamical equations describing the transport system may be read directly from the bond graph. First consider the equations describing the steady state of this system when the reactions are assumed to be close to equilibrium. Under this assumption, we may use the one-port representation for the dissipation due to a chemical process, as shown in Fig. 6.5. In order to be completely general, we shall assume nonlinear constitutive relations for the resistors. In the steady state analysis we concern ourselves only with the driving force across the membrane, the diffusional flow of A alone (called the shunt flow), and the flow of S due to the carrier circulation. The variables characterizing the circulation of the carrier may not be experimentally accessible; therefore, we lump this portion of the bond graph into a new two-port element, -CIR-, called a circulation two-port. This new two-port element represents the structure enclosed by dotted lines in Fig. 6.5.

The steady state relationship between the input and output variables of -CIR- is easily read from the bond graph:

$$J_s^1 = J_s^2 = J_{cir}, \qquad (6.35)$$

$$\mu_s^1 - \mu_s^2 = R_{cir}(J_{cir}), \tag{6.36}$$

where $$R_{cir} = R_R^1 + R_R^2 + R_c + R_{cs} . \tag{6.37}$$

Also notice that $J_{cir} = J_c = J_{cs}$, a result derived kinetically by Katchalsky and Spangler (1968). As one might expect, at steady state there is only one flow through the circulation two-port, which we have denoted J_{cir}; and the driving force in the linear case is equal to the total series resistance, R_{cir} multiplied by J_{cir}.

One of the goals in analyzing a facilitated transport model is to determine the relationship between the diffusional flow of S alone, J_{shunt}, and the flow of the CS complex, J_{cir}. The bond graph in Fig. 6.5 shows that -CIR- is in parallel with the shunt resistance R_s. Hence, the driving forces across both elements are equal and

$$R_{cir}(J_{cir}) = R_s(J_{shunt}). \tag{6.38}$$

If either of these resistance characteristics is invertible, equation (6.38) yields the desired relationship between the flows. In the linear case we simply have

$$\frac{J_{cir}}{J_{shunt}} = \frac{R_s}{R_{cir}} . \tag{6.39}$$

The steady state force-flow relations observable in the compartments surrounding the membrane are also obtained directly from the diagram:

$$\Delta\mu_s = (R_s{}^{I} + R_s{}^{II} + R_s{}^{-1} + R_{cir}{}^{-1})\,(J_s)^{*} \tag{6.40}$$

and, in the linear case,

$$\Delta\mu_s = J_s\left(R_s{}^{I} + R_s{}^{II} + \frac{R_s\,R_{cir}}{R_s + R_{cir}}\right), \tag{6.41}$$

where $\Delta\mu_s = \mu_s{}^{I} = \mu_s{}^{II}$ and $J_s = J_s{}^{I} = J_s{}^{II}$; thus, we retrieve the intuitive feeling that the substrate "sees" some resistance in entering and leaving the membrane, and that the carrier provides a parallel method of substrate transport. From the diagram, it is clear that maximum diffusion enhancement occurs as $R_R \longrightarrow 0$, i.e., for the equilibrium reaction (Friedlander and Keller, 1965).

The bond graph not only gives us information about the steady state behavior of facilitated diffusion, but also generates the state equations for the system. Since not much attention has been given to the dynamics of facilitated transport, we will derive the general nonlinear equations that hold far from equilibrium from the bond graph in Fig. 6.4:

---

[*] Care must be taken in formulating nonlinear equations since all constitutive relations do not have inverses; e.g., for an autocatalytic reaction $J^R = f(A)$ does not have an inverse. Equation (6.40) is valid only when R_s^{-1} and R_{cir}^{-1} exist.

$$
\begin{aligned}
C_s^1 \dot{\mu}_s^1 &= J_s^1 - J_{shunt} - J_1^R = L_s^I(\mu_s^I - \mu_s^1) - L_s(\mu_s^1 - \mu_s^2) \\
&\qquad - L_R^1(\mu_s^1 + \mu_c^1, \mu_{cs}^1) \\
C_s^2 \dot{\mu}_s^2 &= J_2^R + J_{shunt} = J_s^2 = L_R^2(\mu_{cs}^2, \mu_s^1 + \mu_c^1) + L_s(\mu_s^1 - \mu_s^2) \\
&\qquad - L_s^{II}(\mu_s^2 - \mu_s^{II}) \\
C_c^1 \dot{\mu}_c^1 &= J_c - J_1^R = L_c(\mu_c^1 - \mu_c^2) - L_R^1(\mu_s^1 + \mu_c^1, \mu_{cs}^1) \\
C_c^2 \dot{\mu}_c^2 &= J_2^R - J_c = L_R^2(\mu_{cs}^2, \mu_s^2 + \mu_c^2) - L_c(\mu_c^1 - \mu_c^2) \\
C_{cs}^1 \dot{\mu}_{cs}^1 &= J_1^R - J_{cs} = L_R^1(\mu_s^1 + \mu_c^1, \mu_{cs}^1) - L_{cs}(\mu_{cs}^1 - \mu_{cs}^2) \\
C_{cs}^2 \dot{\mu}_{cs}^2 &= J_{cs} - J_2^R = L_{cs}(\mu_{cs}^1 - \mu_{cs}^2) - L_R^2(\mu_{cs}^2, \mu_s^2 + \mu_c^2),
\end{aligned}
\tag{6.42}
$$

where $L_s(\cdot)$, $L_c(\cdot)$, $L_{cs}(\cdot)$, and $L_R(\cdot)$ denote arbitrary conductance functions. In the case of linear diffusion, $L_s^I(\mu_s^I - \mu_s^1)$, for example, reduces to $\frac{\mu_s^I - \mu_s^1}{R_s^I}$. The reaction conductance for far-from-equilibrium reactions has the form $J^R = L_R(A^f, A^r) = \kappa(e^{A^f/RT} - e^{A^r/RT})$, as was shown in Section V.

VII. SIGNAL FLOWS AND CONTROL PROCESSES

7.1 Unilateral energy transmission and activated bonds

One of the most important aspects of network thermodynamics is the possibility of treating control processes. In biological systems, it is common for an event to exert an influence out of all proportion to its energetic level. The minute energetic influence of an allosteric modifier on an enzyme can affect the entire energetic operation of a cell. The effects exerted by a hormone or neuromuscular transmitter substance are in no way related to the energetics of its interactions. In general, there may be no relation between the energy investment in a control mechanism and the energy released or inhibited by the controlling agent.

Regulation and control of energetic processes therefore requires the ability to amplify signals. This, in turn, implies the necessity of introducing unilateral energy flows. For example, at a neuromuscular junction a small amount of energy is expended to produce transmitter substance; however, there is little or no back effect exerted on the nerve by the controlled muscular contraction. The nerve transmits energy unilaterally to the muscle, in contrast to the bilateral energy flows encountered previously. Similar phenomena characterize most control systems.

To distinguish unilateral energy transmission from ordinary signals, we shall append an arrow to the bond. This is not to be confused with the half-arrow employed for sign conventions (Fig. 7.1). An energy bond with an arrow appended is called activated, since it appears as an active device, or source, to the downstream side of the bond.

7.2 Signal flow bonds

In many instances the power level on an activated bond is negligible compared with the other energy flows of interest. In such cases the unilateral energy flow may be considered a pure signal flow. This is indicated by drawing the activated bond as a broken line (Fig. 7.1). Such bonds are called signal flow bonds.

The way a control signal usually exerts its influence on energetic flows is by parametrically modulating the constitutive relation of an energetic n-port. For example, consider a chemical reaction catalyzed by the allosteric enzyme malate : TPN^+ oxidoreductase from Escherichia coli, which is activated by NH_3^+ ions (Sanwal & Smando, 1969). The constitutive relation for the reaction, velocity versus affinity curves, is modulated by the concentration of the allosteric modifier. Figure 7.2 shows the effect of varying the NH_3^+ concentration on the velocity of the malic enzyme reaction.

In many cases the parametric modulation of a constitutive curve can be represented explicitly with the aid of a transducer. If, for example, we let R_0 denote the constitutive curve for malic enzyme when no NH_3^+ is present, we can approximate the whole family of curves shown in Fig. 7.2 by $f(NH_3^+) \cdot R_0$ where $f(\cdot)$ is some function of the NH_3^+ concentration. This type of multiplicative modulation can be represented in the bond graph for a near equilibrium reaction by letting $\sqrt{f(\cdot)}$ be the transducer modulus and connecting the TD to the resistor port, as shown in Fig. 7.3. The signal flow bond incident on the TD indicates that the modulus is a function of the NH_3^+ concentration.

7.3 Unilateral energy transmission and reciprocity

Another important aspect of unilateral energy transmission and signal flow concerns reciprocity. The constitutive relation of a reciprocal device can be characterized by a potential function; consequently, as we will show in Section VIII, the system will decay to a unique equilibrium set. The introduction of unilateral control processes, however, precludes the possibility of analyzing systems solely in terms of potential functions. Hence, in biological systems, where control processes presumably play a preeminent role, reciprocity is probably the exception rather than the rule, and potential functions lose their preeminent position in thermodynamics.

7.4 Unilateral energy flow and dissipation

Unilateral energy flows also arise in connection with dissipation as a consequence of the second law of thermodynamics. Every n-port resistive element operating isothermally can be viewed as an (n+1)-port "converter," transforming work unilaterally into heat (= temperature × entropy flow). Figure 7.4 illustrates this for a one-port resistor. The energy dissipated as heat usually passes from our universe of discourse because the system is considered to be either at constant temperature or temperature insensitive.

There are, however, instances in which the heat generated during the operation of a process does, in fact, feed back and influence the dynamic behavior of the system. This can come about, as mentioned above, by the parametric modulation of a constitutive relation. Indeed, all constitutive relations implicitly contain temperature as a parameter! An elementary example of this effect is the thermistor. This is an electrical resistance whose material properties are such that its resistance is of the form $R(T) = R_0 \exp(-B/T)$, i.e., with increasing temperature the electrical resistance decreases, contrary to most electrical conductors. (This effect is due to the thermal excitation of additional electronic charge carriers within the thermistor material.) An electrical circuit containing this parametric feedback, which has been described elsewhere (Oster and Auslander, 1971), is shown in Fig. 7.5.

Without the parametric thermal feedback this circuit would exhibit only monotone behavior. The unilateral coupling of the electrical and thermal systems, however, enables the entire system to perform limit cycle oscillations about an operating point (Smith, 1950).

A similar situation can arise in a continuous flow stirred tank reactor (CFSTR). The rate constants k for a chemical reaction are temperature sensitive since by the Arrhenius equation $k = A \exp(-E/RT)$, where E is the activation energy.

Consequently, the behavior of a CFSTR will resemble that of a thermistor circuit. Aris (1969), for example, demonstrates the existence of instabilities and the possibility of oscillations in such reactors.

7.5 Nonlinear oscillations

A more interesting example of parametric modulation is a device first constructed by Teorell (1962) as a model for certain biological periodicities. The system shown in Fig. 7.6 consists of a negatively charged membrane separating two salt solutions of unequal concentration. A current is imposed across the membrane via reversible electrodes, and at a critical value of the current density the system exhibits a pronounced instability manifested by relaxation oscillations in the transmembrane potential and the hydrostatic pressure head in the two reservoirs (Oster and Auslander, 1971).

The electrical current flow I, under conditions of constant pressure, is related to the volume flow J_v (~ water flow) by β, the electroosmotic permeability: $J_v = \beta I$. Consequently, under conditions of equal hydrostatic head across the membrane, the transmembrane potential $\Delta \psi$ acts as a driving force for the volume flow $J_v = L_0 \Delta\psi$. In the bond graph of Fig. 7.6 (b), this effect is represented as a source of pressure head on the water system whose magnitude is modulated from the electrical system. The electrical system, in turn, sees a resistance whose magnitude depends in part on the amount of salt in capacitance C_m^S. This effect is represented by resistance R_m^0 in the electrical system modulated from the membrane capacitance.

At this level of description we have abandoned, to some extent, purely energetic considerations in representing the coupling phenomena. The dotted modulation lines represent pure signal, or information flows; and the complete energy bookkeeping implied in a true thermodynamic analysis has been surrendered. A more detailed analysis would consider, among other things, the ionic flows of the anion and cation, the electrode reactions and the membrane charges. Many of the nonenergetic modulation couplings could then be eliminated, and a totally thermodynamic model constructed. Needless to say, the large number of physical interactions might tend to obscure the key control mechanism.

For the case under consideration, the "first order" phenomenological model shown in Fig. 7.6 suffices to understand the parametric feedback mechanism giving rise to the oscillation. Fortunately, the differential equations obtained from this model reproduce the experimentally observed magnitudes with sufficient accuracy so that an expanded model is not required.

The operation of the system can be understood by considering the following sequence of events: (i) Assume that at t=0 the salt has established a steady-state diffusion profile within the membrane. (Here represented as a single average concentration). With the electrode polarity shown, when the current is applied across the membrane, the electroosmotic force E_{eo} induces a flow of solvent from the low concentration side (2) to the high concentration side (1). (ii) This relatively large solvent flow distorts the concentration profile within the membrane, reducing the amount of salt in C_m^S. (iii) With a smaller amount of electrolyte in the membrane, the voltage drop across the membrane increases (R_m increases via TD_1), thus inducing an even higher electroosmotic force on the solvent (via TD_2), which tends to drive the water level in C_1^W still higher. (iv) Ultimately, a steady head is obtained across the membrane depending on the strength of the electrical source. After a while, however, the much slower diffusion process from C_2^S to C_1^S will tend to restore the salt concentration in C_m to its original level. (v) As electrolyte gradually reaccumulates in C_m^S, R_m drops; therefore the electroosmotic force also decreases, initiating a flow of solvent from C_1^W to C_2^W that is driven by the accumulated pressure head. (vi) As the solvent flow proceeds, salt from the high concentration side (C_2^S) is carried into C_m^S, decreasing R_m and the electroosmotic force still further. This positive feedback effect continues until a static head is built up on the other side. The relaxation of the new salt profile and pressure head begins the cycle again, the salt profile in the membrane beginning to decrease again as the salt is dragged by solvent flow from C_2^W into C_1^W.

Relaxation oscillators frequently have the common property of possessing competing energetic processes that occur with widely separated time scales. In this case, the diffusion of salt is much slower than the hydrodynamic flow of solvent.

Figures 7.7 and 7.8 show the liquid pressure-head difference and the membrane electrical resistance as measured by Teorell (1962), as well as the results computed from the bond graph (Oster and Auslander, 1971). Considering the simplicity of the model, the results are surprisingly good. Inclusion of a true salt profile within the membrane by introducing several more C_m^S greatly improves the fit. Our purpose here, however, was to illustrate how signal flows could be utilized in the network approach.

VIII. THEORETICAL CONSIDERATIONS

8.1. Introduction

In this section, we shall briefly outline some technical aspects of network thermodynamics. It is intended that this section be read in parallel with Section I for those readers of a more theoretical bent. Some concepts previously introduced will be restated in a broader context, and the mathematical level necessarily will be somewhat higher. A more detailed treatment of the matters discussed herein will be presented in a later publication.

8.2. Duality

8.2.1.

In Section I, we classified all thermodynamic quantities as either KCL or KVL variables, based on requirements of conservation and continuity. These definitions corresponded to the operational notions of through and across measurements based on the recognition that most physical measurements can be classified as either 2-point measurements, like voltage, or 1-point measurements, like current. We noted that it was frequently the case that the inner product of the through and across variables had some physically meaningful interpretation, e.g. dimensions of power or energy.*

---

*This is by no means a logical requirement for the formalism. Conjugate variables whose products have no such interpretation are frequently employed in traffic flow networks and economics.

The notion of conjugate variables appears throughout the realm of classical physics, e.g. force and flow in irreversible thermodynamics, extensive and intensive in equilibrium thermodynamics, position and momentum in mechanics, etc. (see Table 1).

The clue to this ubiquitous duality lies in noticing that the conjugate variables transform either covariantly or contravariantly under coordinate changes, suggesting that the distinction between the KCL and KVL variables is the distinction between a vector space V and its dual V^*, i.e., the space of all linear real-valued functions on V (Loomis and Sternberg, 1968). We shall briefly indicate the nature of this duality, since it plays a central role in the mathematical structure of our model.

For capacitive n-ports, conjugacy arises quite naturally. In Section I, we defined an n-port as the constitutive map $\underset{\sim}{\mathbb{F}}: \mathbb{R}^n \to \mathbb{R}$, $\underset{\sim}{x} \to \underset{\sim}{y}(\underset{\sim}{x})$, where the pair (x_i, y_i) is associated with the ith port. Since equilibrium systems are presumed reciprocal, the constitutive relations may be summarized by a potential function, $U: \mathbb{R}^n \to \mathbb{R}$, as described in paragraph 1.3. Then, for example, if the intensive variables y_i are defined as the coordinate functions of $\underset{\sim}{DU}$, the gradient vector field generated by the potential function, they transform contravariantly while the x_i transform covariantly (Killingbeck and Cole, 1971). (i.e., the gradient vector itself is covariant).

It is a simple generalization to maintain this duality between the x_i and y_i when we drop the assumption of reciprocity for arbitrary n-ports. We may redefine the constitutive relation for an n-port as a covector field, i.e., a differential form: (Fleming, 1966)

$$\omega : \mathbb{R}^n \to \mathbb{R}^{n*}, \ \underset{\sim}{x} \to \omega(\underset{\sim}{x}),$$

where $(x_i, \omega(x_i))$ are the pair of variables associated with the ith port. Although it may seem pedantic to maintain the distinction between vector and covector fields on $\mathbb{R}^n$ (especially in view of the global canonical isomorphism between $\mathbb{R}^n$ and $(\mathbb{R}^n)^*$ given by the Euclidean metric), confusion of the two spaces obscures the logical structure and ultimately leads to difficulties when dealing with nonlinear systems. Moreover, the distinction is crucial for the definition of reciprocity given in paragraph 8.3.

8.2.2.

The construction of a linear graph representation for systems composed of 1-port elements was demonstrated in paragraph 2.1. This construction may be easily extended to n-port systems in the following way.

The port variables come in pairs (e_i, f_i), so the 2n-dimensional state space for each n-port may be decomposed into the direct sum of constitutive planes:
$\mathbb{R}^n \times (\mathbb{R}^n)^* = \mathbb{R}^1 \times (\mathbb{R}^1)^* \oplus \cdots \oplus \mathbb{R}^1 \times (\mathbb{R}^1)^*$. We associate with each constitutive plane of the n-port a single branch of a linear

graph which carries the port variables as branch variables. The collection of branches so formed is called the terminal graph for the n-port (Koenig et al., 1969; Martens and Allen, 1969). Figure 8.2 illustrates this for several n-ports. Note that, when each port represents a different energy mode, the terminal graph is disconnected, forming a forest of 1-branch graphs.

We may now interconnect the ports of an n-port system in the usual way, as if each port were a separate circuit, as shown in Fig. 8.2b. The resulting system graph is disconnected, and the coupling between the ports is not explicitly represented. In some earlier treatments, port coupling was depicted by a dotted line, or loop, joining the ports. This is clearly unsatisfactory for large systems; and the bond graph, which is mathematically equivalent, is a much clearer representation.

A particularly important class of n-ports are the zero-junction and the one-junction. From the linear graph viewpoint, these may be defined as connection n-ports, i.e., black boxes containing only connections, as shown in Fig. 8.3. The terminal graphs corresponding to the zero- and one-junctions are also shown in Fig. 8.3.

Tellegen's Theorem for an n-port network is obtained from each terminal graph separately:

$$\underset{\sim}{e}^T \underset{\sim}{f} = \sum_{\gamma} \underset{\sim}{e}_{\gamma}^T \underset{\sim}{f}_{\gamma} = \sum_{\gamma} 0 = 0 \qquad (8.1)$$

where the sum γ is taken over each graph of the forest.

8.3. Reciprocity

8.3.1

The definition of reciprocity given in Section I, i.e., the symmetry of the Jacobian matrix $\underset{\sim}{DF}(\underset{\sim}{x})$ at every point $\underset{\sim}{x} \in \mathbb{R}^n$, is both a local condition and one that depends on the coordinate system used to describe the constitutive relation. In the following paragraphs, we will generalize our definition of reciprocity and indicate the role that coordinate choices play in reciprocity.

8.3.2.

In paragraph 8.1, we modified our definition of an n-port constitutive relation to accomodate the notion of intrinsic duality between the port KCL and KVL variables. An n-port was <u>defined</u> as a covector field ω on $\mathbb{R}^n$, i.e., a map $\omega : \mathbb{R}^n \to (\mathbb{R}^n)^*$. In terms of this definition, the condition for reciprocity is that ω be closed, i.e., $d\omega = 0$, where d is the exterior derivative (Fleming, 1966). Since ω is defined on $\mathbb{R}^n$, $d\omega = 0$ implies ω is exact, $\omega = dU$, for some potential function $U : \mathbb{R}^n \to \mathbb{R}$. Note, however, that this definition of an n-port is overly restrictive since we may be forced to employ hybrid coordinates for the n-port. For example, the constitutive relation for a TD, $(e_1, f_1) \to (e_2, f_2)$, has no impedance or admittance representation. Therefore, a more general definition of an n-port would be to view the constitutive relation as a submanifold of $\mathbb{R}^n \times (\mathbb{R}^n)^* \approx \mathbb{R}^{2n}$, the graph of ω. In this section, we will employ this interpretation to obtain a more general definition of reciprocity as a prelude to deriving the canonical equations of motion for nonlinear n-port systems.

Remark: Classical thermodynamics usually considers relatively simple system configurations, e.g. a system connected to one or more reservoirs. When we allow more complex interconnections, certain pathologies can arise, whereupon the constitutive relation does not form a submanifold. For example, Chua has shown that interconnecting only rather elementary resistive elements can produce a composite 1-port whose constitutive relation may consist of either a single point on the e-f plane, a dense set in the e-f plane, several disconnected components, or even characteristics with "self-crossings" like a figure eight! (Chua, 1971).

8.3.3.

The principal reason for viewing the constitutive relation as a submanifold of $\mathbb{R}^{2n}$ lies in the fact that the embedding space can be endowed with a certain canonical structure as a consequence of its even dimensionality. The identical situation is encountered in classical mechanics. Recall that Hamilton's equations are also defined on an even-dimensional manifold modeled on $\mathbb{R}^{2n}$, where they take the form $\underset{\sim}{J}\underset{\sim}{x} = \underset{\sim}{DH}$, where $\underset{\sim}{x} = (\underset{\sim}{q}, \underset{\sim}{p})^T$, H is the Hamiltonian and $\underset{\sim}{J}$ the "symplectic" matrix: $\underset{\sim}{J} = \begin{pmatrix} 0 & I_n \\ -I_n & 0 \end{pmatrix}$, $\underset{\sim}{J}^2 = \underset{\sim}{I}_{2n}$ (Arnold and Avez, 1969).

The ordinary Euclidean inner product structure on $\mathbb{R}^{2n}$ is simply $(\underset{\sim}{x}, \underset{\sim}{y}) = \underset{\sim}{x}^T \underset{\sim}{I} \underset{\sim}{y}$, where $\underset{\sim}{x}$ and $\underset{\sim}{y}$ are 2n-vectors and $\underset{\sim}{I}$ equals the identity matrix. We may define the symplectic (antisymmetric, or Hamiltonian) inner product by (Arnold and Avez, 1969):

$$(\underset{\sim}{x}, \underset{\sim}{y})_H \triangleq \underset{\sim}{x}^T \underset{\sim}{J} \underset{\sim}{y}. \tag{8.2}$$

Linear transformations which preserve this inner product are called symplectic (canonical) transformations for the Euclidean inner product:*

$$\begin{array}{ll} \underline{\text{Orthogonal}} & \underline{\text{Symplectic}} \\ \underset{\sim}{I} = \underset{\sim}{0}^T \underset{\sim}{I} \underset{\sim}{0} & \underset{\sim}{J} = \underset{\sim}{S}^T \underset{\sim}{J} \underset{\sim}{S} \\ \underset{\sim}{0}^{-1} = \underset{\sim}{I}^{-1} \underset{\sim}{0}^T \underset{\sim}{I} & \underset{\sim}{S}^{-1} = \underset{\sim}{J}^{-1} \underset{\sim}{S}^T \underset{\sim}{J} \end{array} \tag{8.3}$$

Now, just as we can define a quadratic surface to be the zero set of a symmetric bilinear function, $\{\underset{\sim}{x} \mid \underset{\sim}{x}^T \underset{\sim}{Q} \underset{\sim}{x} = 0,\ \underset{\sim}{Q} = \underset{\sim}{Q}^T > 0\}$, we define an <u>isotropic</u> subspace of a vector space to be the set of $\underset{\sim}{x}, \underset{\sim}{y}$, which annihilate $\underset{\sim}{J}$: $\{\underset{\sim}{x}, \underset{\sim}{y} \mid \underset{\sim}{x}^T \underset{\sim}{J} \underset{\sim}{y} = 0,\ \underset{\sim}{J} = -\underset{\sim}{J}^T\}$ (Malcev, 1963). A <u>Lagrangian subspace</u> of a vector space V is just an isotropic subspace with dimension = 1/2 dim V (Arnold, 1967). Finally, we define a submanifold $M \subset \mathbb{R}^{2n}$ to be <u>Lagrangian</u> if the tangent plane at each point $p \in M$, $T_p M$, is a Lagrangian subspace, i.e.,

$$\underset{\sim}{x}^T \underset{\sim}{J} \underset{\sim}{y} = 0 \qquad \underset{\sim}{x}, \underset{\sim}{y} \in T_p M, \quad p \in M. \tag{8.4}$$

---

*The Poisson bracket of two functions is just the Hamiltonian inner product of the Jacobians: $\{f, g\} = \underset{\sim}{Df}^T \underset{\sim}{J} \underset{\sim}{Dg}$.

Having defined an n-port as a submanifold, we make the following definition of a reciprocal n-port.

DEFINITION:* A reciprocal n-port is a Lagrangian submanifold $M \subset [R^n \times (R^n)^*]$. In the following paragraph we will show that this definition reduces to the previous definitions when coordinates are introduced.

8.3.4.

Let us now interpret this definition geometrically. Consider the thermomechanical two-port in Fig. 1.1 with port variables (T, S, -p, V). We introduce the port sign conventions in the following way. Cycles traced clockwise on the constitutive planes correspond to energy delivered <u>to</u> the system ports, while cycles traced counterclockwise represent energy delivered <u>by</u> the port. Since we have taken energy into the port as positive by convention, this is tantamount to introducing an <u>orientation</u> onto the constitutive planes (Spivak, 1965). We can conveniently keep track of these orientations by introducing the antisymmetric (exterior) product of coordinate differentials:

$$dx^i \wedge dy_1 = - dy_1 \wedge dx^i. \qquad (8.5)$$

That is, if $\underset{\sim}{X} = (X_1, X_2)$ and $\underset{\sim}{Y} = (Y_1, Y_2)$ are any two vectors on a constitutive plane,

---

*In Desoer and Oster (1972), it is shown that M may also be characterized as the extremal <u>set</u> of a certain real-valued function on R^{2n}. This function generalizes the free-energy functions of classical thermodynamics and gives necessary and sufficient conditions for <u>global</u> reciprocity.

$$dx^i \wedge dy_i(\underset{\sim}{X}, \underset{\sim}{Y}) = \det\begin{pmatrix} X_1 & Y_1 \\ X_2 & Y_2 \end{pmatrix}$$

$$= \underline{\text{oriented}} \text{ area spanned by } \underset{\sim}{X} \text{ and } \underset{\sim}{Y}.^{*} \qquad (8.6)$$

Since this n-port is reciprocal, $\omega = dU$, which when expanded in the coordinate differentials is

$$dU = \sum \frac{\partial U}{\partial x^i}\, dx^i \triangleq \sum_{\text{ports}} y_i(\underset{\sim}{x})\, dx^i\,, \qquad (8.7)$$

i.e., the Gibbs form

$$dU = TdS + (-p)\, dV + \cdots\,. \qquad (8.8)$$

Applying the exterior derivative once again,[**] we obtain

$$d \cdot dU = 0 = dT \wedge dS + d(-p) \wedge dV. \qquad (8.9)$$

The two-form on the right is just the coordinate differential expression for the bilinear form $\underset{\sim}{J}$. Thus, in general, the condition for the constitutive manifold M to be reciprocal (Lagrangian) is the vanishing of the two-form on the tangent planes of M,[***]

$$\rho \triangleq \sum_{\text{ports}} dy_i \wedge dx^i = 0. \qquad (8.10)$$

---

[*] Note that $dx^i \wedge dx^i = 0$.

[**] The Poincaré identity $d \cdot d = 0$ generalizes to the usual vector identities div · curl = curl · grad = 0, and is related to Tellegen's Theorem.

[***] This definition was first proposed by Brayton (1969).

The two-form ρ measures the area spanned by pairs of vectors on T_pM. For any two such vectors

$$\rho(\underset{\sim}{X}, \underset{\sim}{Y}) = \sum dy_i \wedge dx^i (\underset{\sim}{Y}, \underset{\sim}{X}) = \underset{\sim}{X}^T \underset{\sim}{J} \underset{\sim}{Y} \tag{8.11}$$

= sum of projected areas on constitutive planes.

This is clearly an orientation requirement on the tangent planes to M. That is, M must be sitting "just right" in R^{2n} such that the algebraic sum of the tangent projections just cancel. Moreover, from this definition it is clear that reciprocity is not an intrinsic property of the n-port, in the usual sense, but rather depends on the choice of coordinate system for M. Arbitrary coordinate transformations will not preserve reciprocity. For example, a commonly employed coordinate set in network theory is the set of scattering parameters:

$$\xi_i \triangleq \frac{x^i + y_i}{2}, \quad \eta_i \triangleq \frac{x^i - y_i}{2}. \tag{8.12}$$

A short computation shows that $\Sigma\, d\xi_i \wedge d\eta_i \neq 0$. In order to consider reciprocity as an intrinsic property, we must always refer the system back to some physically "preferred" coordinate set. (However, we must recognize that no coordinate system has any special mathematical status.) From the discussion in paragraph 8.3.2, it is clear that the class of coordinate transformations (i.e., transforms of the embedding space R^{2n}) which preserve the property of reciprocity are the canonical transformations. It is just this class of transformations that will also preserve the form of the equations of motion derived in paragraph 8.4.

Although the definition of a reciprocal system as a Lagrangian submanifold is independent of coordinates, it is easy to verify that for various coordinate choices, it reduces to the more familiar expressions.

EXAMPLE: Let $(\hat{\underset{\sim}{x}}, \hat{\underset{\sim}{y}}) = (x_1, \cdots, x_k, y_{k+1}, \cdots, y_n)$ be any set of coordinate variables. The constitutive relation is then:

$$\begin{pmatrix} \hat{\underset{\sim}{x}} \\ \hat{\underset{\sim}{y}} \end{pmatrix} \xmapsto{F} \begin{pmatrix} F_1(\hat{\underset{\sim}{x}}) \\ F_2(\hat{\underset{\sim}{y}}) \end{pmatrix} = \begin{pmatrix} \tilde{\underset{\sim}{y}} \\ \tilde{\underset{\sim}{x}} \end{pmatrix}$$

where $(\tilde{\underset{\sim}{y}}, \tilde{\underset{\sim}{x}}) = (y_1, \cdots, y_k, x_{k+1}, \cdots x_n)$. Then equation 8.10 becomes:

$$\underset{\sim}{DF}_1{}^T \underset{\sim}{DF}_2 - \underset{\sim}{DF}_2{}^T \underset{\sim}{DF}_1 = 0.$$

If the n-port has an impedance representation, (i.e., if $k = 0$), $\underset{\sim}{DF}_1 = \underset{\sim}{I}$ and $\underset{\sim}{DF}_2{}^T = \underset{\sim}{DF}_2$, so that

$$\left(\frac{\partial \underset{\sim}{y}}{\partial \underset{\sim}{x}}\right)^T = \left(\frac{\partial \underset{\sim}{y}}{\partial \underset{\sim}{x}}\right) \tag{8.13}$$

and the Jacobian of the constitutive relation is symmetrical at each point of M.

EXAMPLE: A transducer has no impedance or admittance representation, i.e., (e_1, e_2) and/or (f_1, f_2) are not admissible coordinate sets on the characteristic manifold. The constitutive relation is:

$$\begin{pmatrix} x_1 \\ y_1 \end{pmatrix} \longrightarrow \begin{pmatrix} r & 0 \\ 0 & -\frac{1}{r} \end{pmatrix} \begin{pmatrix} x_1 \\ y_1 \end{pmatrix} = \begin{pmatrix} r x_1 \\ -\frac{1}{r} y_1 \end{pmatrix} = \begin{pmatrix} x_2 \\ y_2 \end{pmatrix}.$$

Clearly $\rho = (dx^1 \wedge dy_1 + dx^2 \wedge dy_2) = 0$ when r is a constant. Viewed as a map from the input port to the output port, the constitutive relation is area (i.e., power) preserving. That is, the TD is a canonical coordinate transformation.

EXAMPLE: The two-port capacitance in Fig. 1.1 may also be viewed as a map from one constitutive plane to another,

$$\begin{pmatrix} T \\ S \end{pmatrix} \xmapsto{\mathbb{F}} \begin{pmatrix} -p \\ V \end{pmatrix} .$$

This map is also area (energy) preserving, i.e., $\det (F) = \frac{\partial(-p, V)}{\partial(T,S)} = 1$; and hence the two-port is reciprocal. This reduces to the familiar thermodynamic identity $c_p - c_v = T\mathcal{V}\beta/\kappa$, where $\mathcal{V}$ is the specific volume and β and κ are the isobaric and isothermal compressibilities, respectively.*

EXAMPLE: The zero- and one-junctions, defined as connection three-ports, have the terminal graph representation shown in Fig. 8.3. Sequences of connected junctions then become connection n-ports. Substituting the port relations (Kirchhoff's laws) into the reciprocity two-form verifies that connection n-ports are

---

*Notice that $\rho = dy_i \wedge dx^i = 0$ for the two-port case is equivalent to requiring that $dx^i \wedge dy_i$ be invariant under F. In classical mechanics, F is a canonical transformation with generating function U, and $dx^i \wedge dy_i$ is the Poincaré integral invariant.

reciprocal. Note that we must choose our sign convention such that all bonds are oriented into the junctions. This corresponds to choosing associated reference directions for the linear graph representation.

EXAMPLE: All one-ports are trivially reciprocal, since $y = y(x)$, and $\rho = dy \wedge dx = \frac{\partial y}{\partial x}(x)\, dx \wedge dx = 0$.

8.4. Potential functions for reciprocal n-ports

The potential functions for one-ports may be represented graphically, as shown in Fig. 8.4. For reciprocal n-ports, these definitions generalize in a straightforward manner.

The reversible elements, capacitors and inductors, are reciprocal according to the Maxwell relations of equilibrium thermodynamics:

$$\sum_{\text{ports}} dq^i \wedge de_i = 0, \tag{8.14}$$

as shown in the examples above. By substituting the terminal characteristics of a reversible multiport, $\underset{\sim}{e} = \underset{\sim}{\psi}(\underset{\sim}{q})$, into equation 8.14, the above reciprocity condition may be written

$$\underset{\sim}{D\psi} = \underset{\sim}{D\psi}^T, \tag{8.15}$$

where $\underset{\sim}{D\psi}$ is the Jacobian matrix of $\underset{\sim}{\psi}$.

For reciprocal irreversible elements, we may define another state function, the <u>content</u>, by

$$G(\underset{\sim}{f}) = \int \underset{\sim}{e}^T d\underset{\sim}{f} = \int \underset{\sim}{\psi}_R^T(\underset{\sim}{f})\, d\underset{\sim}{f}, \tag{8.16}$$

where $\underset{\sim}{e} = \underset{\sim}{\psi}_R(\underset{\sim}{f})$ is the constitutive relation (Cherry, 1951); e.g. for a one-port resistor, $G(f) = \int_0^f e\,df$. For linear constitutive relations, $G(\underset{\sim}{f})$ is just one half the dissipation function (see Fig. 8.4).

$G(\underset{\sim}{f})$ is a state function for the irreversible elements; and the reciprocity condition is trivially satisfied for $D^2\underset{\sim}{G} = D^2\underset{\sim}{G}^T$, or $D\underset{\sim}{\psi}_R = D\underset{\sim}{\psi}_R^T$. A one-port R is trivially reciprocal, since its Jacobian is a scalar.*

Another point to bear in mind is that reciprocity has nothing to do with passivity. A transistor or thermistor (see Section VII) are passive, but not reciprocal. Conversely, it is easy to synthesize reciprocal systems containing active elements.

8.5 Interconnection of n-ports

8.5.1.

Using the definition of reciprocity, equation 8.21, Brayton

---

*For the reversible elements the coenergy, or free energy, is defined via the Legendre transform, i.e.,

$$E(\underset{\sim}{q}) = \int_0^q \underset{\sim}{e}(\underset{\sim}{q})^T d\underset{\sim}{q},$$

$$E^*(\underset{\sim}{e}) = \underset{\sim}{e}^T \underset{\sim}{q} - E(\underset{\sim}{q}).$$

Similarly, for the irreversible processes, we may define the cocontnet by a Legendre transform on the content:
$G^*(\underset{\sim}{e}) = \underset{\sim}{e}^T \underset{\sim}{f} - G(\underset{\sim}{e})$.

proved the following important result:

THEOREM 8.1: (Brayton, 1969): Any n-port obtained by the interconnection of reciprocal n-ports is reciprocal.*

PROOF: Define the reciprocity two-form for the α^{th} n-port,

$$\rho_\alpha = \sum_{k=1}^{n} dx_\alpha^k \wedge dy_k^\alpha . \quad \text{Then, clearly,} \quad \sum_\alpha \rho_\alpha = 0,$$

since each n-port is assumed reciprocal. Using the notion of a connection n-port introduced in paragraph 8.3.4, this sum can be decomposed into a sum over those ports which remain after the interconnection, and those which do not (Fig. 8.5):

$$\text{(a)} \quad \sum\nolimits_{\text{remain}} + \sum\nolimits_{\text{connected}} = 0;$$

if the interconnections create new ports, then

$$\text{(b)} \quad \sum\nolimits_{\text{connected}} + \sum\nolimits_{\text{new}} = 0,$$

since connection n-ports are reciprocal. Since we have taken our positive sign convention into each n-port, when two ports are interconnected, there is a sign change on one set of port variables. Therefore, adding (a) and (b):

$$\sum\nolimits_{\text{remain}} + \sum\nolimits_{\text{new}} = 0$$

QED.

---

*As discussed in paragraph 8.3.2, the interconnection of n-ports may give rise to pathological situations; under such circumstances this theorem is not valid.

Note that we have assumed that all of the connections are compatible. This may not be the case if, for example, an interconnection couples two effort sources with different effort variables in parallel, i.e., violates causality.

The entire network may be represented schematically as shown in Fig. 8.5, where we have lumped all reversible, irreversible and junction elements. Note that the TD is defined with reciprocal constitutive relations; and since it neither stores nor dissipates, it is equivalent to a (possibly) nonlinear constraint equation and so may be considered a junction structure. By construction, therefore, we have demonstrated that for thermodynamic systems representable by reciprocal elements

$$\sum_{\text{ports}} de_i \wedge df_i + \sum_{\text{cap.}} de_j \wedge df_j + \sum_{\text{res.}} de_k \wedge df_k = 0. \tag{8.17}$$

An important special case of the above theorem is an interconnection of one-ports. Most of the bond graph models developed in Sections II and III were assembled from only one-ports and TD's. The reciprocity of the overall system is assured by the above theorem; consequently, such systems possess potential functions.

8.5.2.

Several authors have noted that Onsager reciprocity may be derived from the Kelvin postulate of independent processes (Li, 1958; Pitzer, 1961). That is, if one postulates that there exist noninteracting "kinetically independent" processes,

$$J'_J = g_J(X'_j), \tag{8.18}$$

and that any arbitrary flux J_i is a linear combination of the <u>independent</u> fluxes,

$$J_i = \sum_j \alpha_{ij} J'_j , \tag{8.19}$$

then a reciprocity condition may be derived in terms of J_i and its conjugate force X_i. Substitution of equation 8.19 into the dissipation function $\Phi = \sum_i X_i J_i$ shows that the force conjugate to J'_j is given by

$$X'_j = \sum_i \alpha_{ij} X_i \tag{8.20}$$

and hence that

$$J_i = \sum_j \alpha_{ij} g_j\left(\sum_k \alpha_{kj} X_k\right). \tag{8.21}$$

Testing for reciprocity, we note

$$\frac{\partial J_i}{\partial X_k} = \sum_j \alpha_{ij} g'_j \alpha_{kj} = \frac{\partial J_k}{\partial X_i} ,$$

which is the nonlinear generalization of Pitzer's condition for reciprocity. Notice, however, that the assumption of noninteracting independent processes, equation 8.18, is equivalent to constructing the system out of one-port elements. Brayton's theorem than assures us that the total system will be reciprocal. Both this proof and Pitzer's, however, would not be valid for a system containing chemical reactions since, being nonreciprocal, chemical reactions cannot be reticulated into one-port elements.

8.6. Canonical form for the equations of motion

8.6.1.

One of the convenient aspects of Hamiltonian mechanics, from a theoretical viewpoint, is that the equations of motion may be expressed as a symplectic gradient vector field, i.e., $\underset{\sim}{J}\dot{\underset{\sim}{x}} = \underset{\smile}{DH}$, (see paragraph 8.3.3). That is, the vector field propelling the state point is derivable from a scalar potential function, $H(\underset{\sim}{q}, \underset{\sim}{p})$.

For a large class of reciprocal n-ports, Brayton and Moser (1964) have shown that the equations of motion may be cast into a canonical form. We will restrict our attention to RC networks in which the capacitor efforts can be varied independently without violating Kirchhoff's laws, and in which they determine either the effort or flow on each resistive port bond. We refer the reader to the literature for treatment of more general cases. We begin with Tellegen's Theorem:

$$O = e^T f = \langle \underset{\sim}{e}, \underset{\sim}{f} \rangle_R + \langle \underset{\sim}{e}, \underset{\sim}{f} \rangle_C = \sum_R e_i f_i + \sum_C e_i f_i \qquad (8.22)$$

where we denote by $\sum\limits_R$ and $\sum\limits_C$ summation over the resistive and capacitive ports, respectively.[*]

Since $\underset{\sim}{e}$ and $\underset{\sim}{f}$ lie in fixed orthogonal subspaces,

$$\sum_R f_i\, de_i + \sum_C f_i\, de_i = 0. \qquad (8.23)$$

Introducing the capacitor constitutive relations,

$$\sum_C C_{ij}(\underset{\sim}{e}_C)\, \dot{e}_j\, de_i = - \sum_R f_i\, de_i , \qquad (8.24)$$

where $\underset{\sim}{e}_C$ is the vector of capacitor effects. Recalling the definition of cocontent for the irreversible elements, we may define a potential function

$$\mathcal{P}(\underset{\sim}{e}_C) = - \sum_R \int_0^{e_i} f_i\, de_i = - G^*, \qquad (8.25)$$

so that equation (8.24) becomes

$$\sum C_{ij}(\underset{\sim}{e}_C)\, \dot{e}_j\, de_i = d\mathcal{P}. \qquad (8.26)$$

Operating on both sides with the unit vectors $(0, \cdots, 1, \cdots, 0)$, we may write equation 8.26 in component form as[**]:

---

[*] We regard sources (reservoirs) as nonlinear resistors with constant e vs f characteristics.

[**] In the above treatment, we have employed associated sign conventions throughout; therefore, we differ in sign from the equations derived by Brayton and Moser (1964).

$$\sum_{C} C_{ij}(\underset{\sim}{e}_C)\,\dot{e}_j = \partial\mathcal{P}/\partial e_i \qquad (8.27)$$

or

$$\underset{\sim}{C}(\underset{\sim}{e}_C)\,\dot{\underset{\sim}{e}}_C = \underset{\sim}{D\mathcal{P}}\ . \qquad (8.28$$

The fact that the equations of motion for a reciprocal system may be derived from a potential function is a useful theoretical result for discussing system stability, as we will see in the next paragraph.

Smale (1972) has given the following geometric interpretation of the canonical equations. The complete state space is first restricted by Kirchhoff's laws to a linear submanifold. Then the algebraic constraints of the resistive constitutive relations define a (nonlinear) submanifold of the Kirchhoff subspace. The energy storage elements then provide a metric, just as in classical mechanics (MacLane, 1968), which is semidefinite when both capacitive and inductive energy storage are present. The vector field propelling the state point on this manifold, $\underset{\sim}{C}(\underset{\sim}{e})^{-1}\underset{\sim}{DP}$, is a gradient flow in the reciprocal case.

As mentioned in Section VII, reciprocity is the exception rather than the rule in biological systems; so, in general, the equations of motion will take the form

$$\underset{\sim}{C}\,\dot{\underset{\sim}{e}} = \alpha,$$

where α is a nonintegrable differential form (Smale, 1972). These equations will be dealt with more fully in a further publication. A more detailed treatment of the canonical equations, including the extension to nonreciprocal systems with inductive effects, can be found in Smale (1972), Desoer and Wu (1972), Brayton (1969), Brayton and Moser (1964).

8.7. Stability of the steady state

8.7.1.

In this paragraph we will illustrate how the canonical form of the equations of motion and Tellegen's Theorem may be employed to derive in a unified manner various dynamic stability criteria proposed by Glandsdorff and Prigogine. For simplicity, we will continue to neglect inertia-like effects (inductances) and consider only systems with resistive and capacitive multiports. Furthermore, in the following treatment, we shall always assume that the capacitive constitutive relations conform to the conditions of local thermodynamic stability i.e., $\underset{\sim}{C} > 0$.

8.7.2.

Glansdorff and Prigogine (1954) showed that if the time variation of the entropy production $\frac{d_iS}{dt} = \int_V \Sigma X_i J_i \, dv$ is split into two parts,

$$\frac{\partial}{\partial t}\left(\frac{d_iS}{dt}\right) = \int_V \sum \dot{J}_i X_i \, dv + \int_V \sum J_i \dot{X}_i \, dv, \qquad (8.29$$

then

$$\int_V \sum J_i \dot{X}_i \, dv \leq 0 \qquad (8.30)$$

for time independent boundary conditions. This inequality, called a general evolutionary criterion by Prigogine and Glandsdorff, can also be proven for discrete systems via the network approach.

The following theorem does not require the dissipative constitutive relations to be reciprocal (Oster and Desoer, 1971).

<u>THEOREM</u> 8.2: Assume that we are given a bond graph, a) which is driven by constant sources (time independent boundary reservoirs), and b) whose capacitive constitutive relations obey the thermodynamic stability requirement $\underset{\sim}{C} > 0$.

Then, along the state trajectory

$$\sum_R \dot{e}_i f_i \leq 0, \qquad (8.31)$$

equality holding only at the steady state.

PROOF: From Tellegen's Theorem,

$$0 = \langle \underset{\sim}{e}, \underset{\sim}{f} \rangle = \langle \underset{\sim}{e}, \underset{\sim}{f} \rangle_R + \langle \underset{\sim}{e}, \underset{\sim}{f} \rangle_C ; \qquad (8.32)$$

therefore,

$$\langle \underset{\sim}{e}, \underset{\sim}{f} \rangle_R = - \langle \underset{\sim}{e}, \underset{\sim}{f} \rangle_C . \qquad (8.33)$$

Since Kirchhoff's laws restrict the efforts and flows to fixed orthogonal subspaces, $\langle \dot{\underset{\sim}{e}}, \underset{\sim}{f} \rangle = 0$ and

$$\langle \underset{\sim}{e}, \underset{\sim}{f} \rangle_R = - \langle \dot{\underset{\sim}{e}}, \underset{\sim}{f} \rangle_C . \qquad (8.34)$$

The capacitive constitutive relations are $\underset{\sim}{q} = \mathbb{F}(\underset{\sim}{e})$, when differentiated with respect to time, yield

$$\dot{\underset{\sim}{q}} = \underset{\sim}{f}_C = \underset{\sim}{D\mathbb{F}}(\underset{\sim}{e}_C)\dot{\underset{\sim}{e}}_C .$$

Therefore,

$$\langle \dot{\underset{\sim}{e}}, \underset{\sim}{f} \rangle_R = - \langle \dot{\underset{\sim}{e}}, \underset{\sim}{D\mathbb{F}}(\underset{\sim}{e})\dot{\underset{\sim}{e}} \rangle_C . \qquad (8.35)$$

By assumption (b),

$$D\mathbb{F}(\underset{\sim}{e}) = \underset{\sim}{C}(\underset{\sim}{e}) > 0$$

so

$$\langle \dot{\underset{\sim}{e}}, \underset{\sim}{f} \rangle_R \leq 0. \qquad (8.36)$$

8.7.3.

The quantity $\langle \delta \underset{\sim}{e}, \delta \underset{\sim}{f} \rangle$ has been called the *excess entropy production* by Glansdorff and Prigogine (1970, 1971).* Intuitively, it would seem that variations about a stationary state that produce a net entropy reduction would not be favored in a thermodynamically stable system. For instance, in the one-port case, the instability associated with tunnel diode-like constitutive relations is familiar (Fig. 3.3). In the region where $\delta e \, df < 0$, we find unstable steady states (Katchalsky and Spangler, 1968). Glansdorff

---

*This is perhaps a misnomer since:

$$(\underset{\sim}{\bar{e}} + \underset{\sim}{\delta e})^T (\underset{\sim}{\bar{f}} + \underset{\sim}{\delta f}) - \underset{\sim}{\bar{e}}^T \underset{\sim}{\bar{f}} = \underset{\sim}{\delta e}^T \underset{\sim}{\delta f} + \underset{\sim}{\delta e}^T \underset{\sim}{f} + \underset{\sim}{e}^T \underset{\sim}{\delta f}.$$

and Prigogine (1970, 1971) have shown that $\int_V \delta J_i \delta X_i dV$ can be used to determine the stability of a steady state in a continuous system. Here we will show that this result holds for multiport systems (Oster and Desoer, 1971).

Let $\underset{\sim}{\delta e}$ and $\underset{\sim}{\delta f}$ be tangent vectors to the constitutive manifold at the steady state to be investigated. We assume that the perturbations $\underset{\sim}{\delta e}$, $\underset{\sim}{\delta f}$ obey KCL, KVL and the constitutive relations.

<u>THEOREM</u> 8.3: (i) If, for any pertubation about the steady state conforming to KCL and KVL,

$$\sum_R \delta e_k \delta f_k > 0, \tag{8.37}$$

the steady state is stable; (ii) if, for some such perturbation,

$$\sum_R \delta e_k \delta f_k < 0, \tag{8.38}$$

the steady state is unstable.

PROOF: We present here a simplified proof using Tellegen's Theorem. A more rigorous proof is given in Oster and Desoer, (1971). For the tangent system,

$$\underset{\sim}{\delta e}^T \underset{\sim}{\delta f} = \sum_R \delta e_j \delta f_j + \sum_C \delta e_j \delta f_j = 0. \tag{8.39}$$

Inserting the small signal constitutive relations, $\underset{\sim}{\delta e} = \underset{\sim}{R} \underset{\sim}{\delta f}$ for the resistors and $\underset{\sim}{\delta e} = \underset{\sim}{S} \underset{\sim}{\delta q}$ for the capacitors, where $\underset{\sim}{S} = \underset{\sim}{C}^{-1}$

is the incremental susceptance matrix,

$$(\underset{\sim}{\delta f}^T \underset{\sim}{R}\ \underset{\sim}{\delta f})_R + (\underset{\sim}{\delta q}^T \underset{\sim}{S}\ \underset{\sim}{\delta f})_C = 0$$

or

$$(\underset{\sim}{\delta \dot{q}}^T \underset{\sim}{R}\ \underset{\sim}{\delta \dot{q}})_R + \frac{d}{dt}\left[\frac{1}{2}\ \underset{\sim}{\delta q}^T \underset{\sim}{S}\ \underset{\sim}{\delta q}\right] = 0;$$

and

$$(\delta \dot{q}^T \underset{\sim}{R}\ \delta \dot{q})_R = -\frac{d}{dt}\ \mathcal{E}_C \tag{8.40}$$

where $\mathcal{E}_C(\underset{\sim}{q}, \underset{\sim}{\delta q}| = \frac{1}{2}\ \underset{\sim}{\delta q}^T \underset{\sim}{S}\ \underset{\sim}{\delta q}$ is the "small-signal energy" about the steady state.

If the steady state is unstable, the trajectory initially moves away from the origin $\underset{\sim}{\delta q} = 0$. Therefore, $\mathcal{E}_C$ is increasing and

$$(\underset{\sim}{\delta \dot{q}}^T \underset{\sim}{R}\ \underset{\sim}{\delta \dot{q}})_R < 0$$

or

$$\sum_R \delta e_i\, \delta f_i < 0 \tag{8.41}$$

Q. E. D.

This result has been used by Katchalsky and Spangler (1968) to study the bistable properties of membranes, and by Glansdorff and Prigogine (1971) in discussing chemical instabilities. Moreover, in Oster and Desoer (1971), it is shown that the dissipative processes dominate the local stability properties, i. e., an unstable steady state cannot be stabilized by altering the capacitive constitutive relations.

8.7.4.

Glansdorff and Prigogine (1971) show that the second variation of the entropy, $\delta^2 S$, is a Liapunov function for the linearized system. In the discrete case, this can also be rigorously proven.

The convexity assumption on the capacitive constitutive relations (local thermodynamic stability) means we can use the incremental capacitance (or its inverse) as a metric. For example, the Hessian of the entropy, $\underset{\sim}{S}$, for a diffusion system is

$$S_{ij} = \frac{\delta^2 S}{\partial n_i \, \partial n_j} = \frac{\partial \mu_i}{\partial n_j} > 0, \tag{8.42}$$

inducing a positive-definite bilinear form on T(M)

$$\delta^2 S \triangleq \sum S_{ij} dn_i \otimes dn_j \, . \tag{8.43}$$

If we contract this bilinear form with two tangent vectors at the steady state, whose stability is to be determined, we obtain a real-valued function on the characteristic manifold M:

$$\phi(\cdot) = \underset{\sim}{\delta q}^T \underset{\sim}{S} \, \delta q, \quad \underset{\sim}{\delta q} \in T_p M. \tag{8.44}$$

Then, differentiating along the trajectory in the tangent system, we get

$$\frac{d\phi(\cdot)}{dt} = 2 \underset{\sim}{\delta q}^T S \, \underset{\sim}{\delta \dot{q}} \tag{8.45}$$

$$= 2(\underset{\sim}{\delta e}^T \, \underset{\sim}{\delta f})_C \, . \tag{8.46}$$

But, from Tellegen's Theorem, equation 8.39,

$$\frac{1}{2}\,\frac{d\phi}{dt} = -\,(\delta e^{T}\delta f)_R .$$

When the system is stable, the right-hand side is negative definite, which is just the result obtained previously. Therefore, the curvature of the entropy is a physically meaningful Liapunov function for local stability.

8.7.5.

So far, we have dealt only with local stability conditions. However, if the resistive constitutive relations are reciprocal, then the Brayton-Moser mixed potential is a Liapunov function for the system. The equations of motion may be written

$$\underset{\sim}{C}(\underset{\sim}{e})\,\dot{\underset{\sim}{e}} = \underset{\sim}{D\mathcal{P}}(\underset{\sim}{e}) . \tag{8.47}$$

Taking the inner product with $\dot{\underset{\sim}{e}}$,

$$\frac{d\mathcal{P}}{dt} = \langle\, \dot{\underset{\sim}{e}},\ \underset{\sim}{D\mathcal{P}}(\underset{\sim}{e})\rangle \tag{8.48}$$

$$= \langle\, \dot{\underset{\sim}{e}},\ \underset{\sim}{C}(\underset{\sim}{e})\,\dot{\underset{\sim}{e}}\,\rangle$$

$$\geqslant 0 \tag{8.49}$$

since $\underset{\sim}{C}(\underset{\sim}{e}) > 0$.

Now, if $\mathcal{P}$ tends radially to minus infinity as $|\underset{\sim}{e}| \to \infty$ (which it usually does at large values of thermodynamic efforts and flows as can be seen from equation(8.25), then following Liapunov, no solution is unbounded, and all initial conditions generate solutions which lead to the equilibrium set of the potential $\mathcal{P}$.

In general, nonlinear systems exhibit complex behavior — they may settle down into one of several equilibrium sets, or they may tend asymptotically toward certain oscillatory trajectories (limit cycles), or they may grow without bound. It is an important piece of qualitative information to choose between these classes of behavior, and not a trivial task for nonlinear systems.

For the case of reciprocal systems, we see that the mixed potential function can be used to deduce the existence of a constant limiting set, which eliminates the possibility of oscillatory behavior or unbounded solutions. That is, we can guarantee that the equilibrium set is globally asymptotically stable (Brayton, 1969).

8.8. Extremal principles

As mentioned in Section I, computation of the equilibrium configuration of an n-port with specified port (boundary) constraints is considerably simplified if the system is reciprocal. The solution of a set of nonlinear algebraic equations may then be replaced by a more tractable minimization problem. That is, one may minimize the appropriate potential function subject to the port constraint of KCL and obtain the conjugate equilibrium condition, KVL, as an alternative to merely solving the set of nonlinear constitutive equations subject to both KCL and KVL constraints.

It is an easy exercise to show that of the three conditions, KCL, KVL, and U extremal, any two imply the third. In our treatment, we have encountered nonreciprocal thermodynamic systems. In such cases, it is imperative to choose the algebraic criterion for equilibrium, i.e., the equilibria of the constitutive vector field, rather than the extremal formulation which depends on reciprocity.

For example, in paragraph 8.4, the state function called content was shown to characterize the dissipative processes:

$$G = \int_0^f \underset{\sim}{e}^T d\underset{\sim}{f} .$$

We may investigate the extremal properties of this function for a network operating at a steady state* by introducing variations in the branch flows, $\underset{\sim}{f} = \underset{\sim}{\bar{f}} + \delta \underset{\sim}{f}$, where $\bar{f}$ is the steady state flow. If we require these variations to obey KCL, then from Tellegen's Theorem, $\underset{\sim}{e}^T \underset{\sim}{f} = 0$, and $\underset{\sim}{e}^T (\underset{\sim}{f} + \delta \underset{\sim}{f}) = 0$. Subtracting, we find $\underset{\sim}{e}^T \delta \underset{\sim}{f} = 0$; i.e., the variations in the flows are also orthogonal to the efforts. Therefore, $\delta G = \underset{\sim}{e}^T \delta \underset{\sim}{f} = 0$; the total content is stationary in a steady state (Millar, 1951). For the special case of linear constitutive relations, the above equation is equivalent to the familiar minimum entropy production principle proposed by Prigogine (1947), or Maxwell's minimum heat theorem. Although there is no new information contained in

---

*Note that in a steady state the network is purely dissipative; therefore, the content characterizes the system.

such extremal principles that is not contained in KCL, KVL and the constitutive relations, they often simplify numerical analysis and have a certain esthetic appeal. A complete summary of such extremum principles in network theory can be found in MacFarlane (1970).

This work was done under the auspices of the U. S. Atomic Energy Commission.

One of us (A. S. P.) would like to thank the National Science Foundation for support in the form of a Graduate Traineeship.

IX. REFERENCES

Aris, R. and Mah, R. H. S. (1963). Independence of chemical reactions. Ind. Eng. Chem. Fund. 2, 901.

Aris, R. (1969). Elementary Chemical Reactor Analysis. Englewood Cliffs, New Jersey: Prentice-Hall.

Arnold, V. I. (1967). Characteristic class entering in quantization conditions. Functional Anal. Appl. 1, 1.

Arnold, V. I. and Avez, A. (1968). Ergodic Problems of Classical Mechanics. New York: Benjamin.

Bearman, R. J. and Kirkwood, J. G. (1958). Statistical mechanics of transport processes: XI. Equations of transport in multi-component systems. J. Chem. Phys. 28, 136.

Berge, C. (1962). The Theory of Graphs and Its Applications. New York: Wiley.

Berge, C. and Ghouila-Houri, A. (1965). Programming, Games, and Transportation Networks New York: Wiley.

Blackwell, W. A. (1968). Mathematical Modeling of Physical Networks. New York: Macmillan

Blumenthal, R. and Katchalsky, A. (1969). The effect of the carrier association-dissociation rate on membrane permeation. Biochim. Biophys. Acta 173, 357.

Branin, F. (1962). Machine analysis of networks and its applications. IBM Tech. Rept. TR 00.855.

Branin, F. (1966). The algebraic-topological basis for network analogies and the vector calculus. In Proceedings of the Symposium on Generalized Networks. Brooklyn, New York: Polytechnic Press of the Polytechnic Institute of Brooklyn.

Brayton, R, K. and Moser, J. K. (1964). A theory of nonlinear networks, I and II. Quart. Appl. Math. **22**, 1; **22**, 81.

Brayton, R. K. (1969). Nonlinear reciprocal networks. IBM Research Rept. RC 2606 (#12427).

Callen, H. (1960). Thermodynamics. New York: Wiley.

Cherry, C. (1951). Some general theorems for nonlinear systems possessing reactance. Phil. Mag. **42**, 1161.

Chua, L. (1971). Memristor-the missing circuit element. IEEE Trans. Circuit Theory **CT-18**, 507.

Chua, L. O. and Lam, Y. F. (1971). Nonlinear n-ports. I: Characterization, classification, and representation. Univ. of Calif., Berkeley, Electronics Research Laboratory Memorandum ERL-M307.

Chua, L. (1972). Foundations of Circuit Theory. (In preparation).

Cole, K. (1968). Membranes, Ions and Impulses. Berkeley: Univ. of California Press.

Cullis, C. E. (1913). Matrices and Determinoids, Vol. 2, p. 165. London: Cambridge University Press.

De Donder, Th. and Van Rysselberghe, P. (1930). Affinity. Stanford, California: Stanford University Press.

De Groot, S. (1951). Thermodynamics of Irreversible Processes. Amsterdam: North-Holland.

De Groot, S. R. and Mazur, P. (1962). Nonequilibrium Thermodynamics. Amsterdam: North-Holland.

De Simone, J. A. and Caplan, S. R. (1972). Symmetry and the stationary state behavior of enzyme membranes. J. Theoret. Biol. (in press).

Desoer, C. and Kuh, E. (1969). Basic Circuit Theory. New York: McGraw-Hill.

Desoer, C. (1970). Notes for a Second Course on Linear Systems. New York: Van Nostrand-Reinhold.

Desoer, C. and Oster, G. (1972). Globally reciprocal stationary systems. Intl. J. Eng. Sci. (in press).

Desoer, C. and Wu, F. (1972). Networks viewed as flows on manifolds. (To be published).

Fleming, W. (1965). Functions of Several Variables. Reading, Mass.: Addison-Wesley.

Friedlander, S. K. and Keller, K. H. (1965). Mass transfer in reacting systems near equilibrium. Chem. Eng. Sci. 20, 121.

Glansdorff, P. and Prigogine, I. (1954). Sur le propriétés différentielles de la production d'entropie. Physica 20, 773.

Glansdorff, P. and Prigogine, I. (1964). On a general evolution criterion in macroscopic physics. Physica 30, 351.

Glansdorff, P. and Prigogine, I. (1970). Nonequilibrium stability theory. Physica 46, 344.

Glansdorff, P. and Prigogine, I. (1971). Thermodynamic Theory of Structure, Stability and Fluctuations. London: Wiley-Interscience.

Harary, F. (1969). Graph Theory. Reading, Mass.: Addison-Wesley.

Harned, H. S. and Owen, B. B. (1950). The Physical Chemistry of Electrolyte Solutions, 2nd edition. New York: Reinhold.

Hermann, R. (1971). Vector Bundles in Mathematical Physics, Vols. I and II. New York: Benjamin.

Karnopp, D. and Rosenberg, R. (1968). Analysis and Simulation of Multiport Systems. Cambridge, Mass.: MIT Press.

Katchalsky, A. and Curran, P. (1965). Nonequilibrium Thermodynamics in Biophysics. Cambridge, Mass.: Harvard Univerity Press.

Katchalsky, A. and Oster, G. (1969). Chemico-diffusional coupling in biomembranes. In The Molecular Basis of Membrane Function, ed. D. C. Tosteson. Englewood Cliffs, New Jersey: Prentice-Hall.

Katchalsky, A. and Spangler, R. (1968). Dynamics of membrane processes. Quart. Rev. Biophys. **1**, 127.

Kedem, O. and Katchalsky, A. (1961). A physical interpretation of the phenomenological coefficients of membrane permeability. J. Gen. Physiol. **45**, 143.

Killingbeck, J. and Cole, G. H. A. (1971). Mathematical Techniques and Physical Applications. New York: Academic Press.

Koenig, H., Tokad, Y., and Kevasan, H. K. (1969). Analysis of Discrete Physical Systems. New York: McGraw-Hill.

Kron, G. (1943). Equivalent circuits to represent the electromagnetic field equations. Phys. Rev. **64**, 126.

Kron, G. (1944a). Equivalent circuits of the field equations of Maxwell. *Proc. Inst. Radio Engrs.* **32**, 289.

Kron, G. (1944b). Equivalent circuits of the elastic field. *J. Appl. Mech.* **11**, 149.

Kron, G. (1945a). Equivalent circuit models of the Schrodinger equation. *Phys. Rev.* **67**, 39.

Kron, G. (1945b). Equivalent circuits of compressible and incompressible fluid flow fields. *J. Aeron. Sci.* **12**, 221.

Kron, G. (1946). Electric circuit models for the vibration spectrum of polyatomic molecules. *J. Chem. Phys.* **14**, 19.

Kron, G. (1948). Electric circuit models of partial differential equations. *Elec. Eng.* **67**, 672.

LaMer, V. K., Foss, O., and Reiss, H. (1949). Some new procedures in the thermodynamic theory inspired by the recent work of J. N. Brφnsted. *Ann. N. Y. Acad. Sci.* **51**, 605.

Li, J. C. M. (1958). Thermodynamics for nonisothermal systems. The classical formulation. *J. Chem. Phys.* **29**, 747.

Loomis, L. H. and Sternberg, S. (1968). *Advanced Calculus.* Reading, Mass.: Addison-Wesley.

MacFarlane, A. G. J. (1970). Dynamical System Models. London: Harrap.

MacLane, S. (1968). Geometrical Mechanics. (Lecture Notes) Department of Mathematics, Univ. of Chicago.

Mal'cev, A. I. (1963). Foundation of Linear Algebra. San Francisco: Freeman.

Martens, H. and Allen D. (1969). Introduction to Systems Theory. Columbus, Ohio: Merrill.

Meixner, J. (1941). Zür thermodynamik der thermodiffusion. Ann Physik. **39**, 333.

Meixner, J. (1942). Reversible bewegungen von flüssigkeiten und gasen. Ann. Physik **41**, 409.

Meixner, J. (1943). Zür thermodynamik der irreversiblen prozesse in gasen mit chemisch reagierenden, dissoziierenden und anregbaren komponenten. Ann. Physik **43**, 244.

Meixner, J. (1963). Thermodynamics of electrical networks and the Onsager-Casmir reciprocal relations. J. Math. Phys. **4**, 154.

Meixner, J. (1964). On the theory of linear passive systems. Arch. Rational Mech. Anal. **17**, 278.

Meixner, J. (1965). Linear passive systems. In Proceedings of the International Symposium on Statistical Mechanics and Thermodynamics, pp. 52-68. Amsterdam: North-Holland.

Meixner, J. (1966a). Consequences of an inequality in non-equilibrium thermodynamics. J. Appl. Mech. 33, 481.

Meixner, J. (1966b). Network theory in its relation to thermodynamics. In Proceedings of the Symposium on Generalized Networks, pp. 13-25. New York: Polytechnic Press of the Polytechnic Institute of Brooklyn.

Millar, W. (1951). Some general theorems for nonlinear systems possessing resistance. Phil. Mag. 42, 1150.

Morowitz, H. J., Higinbotham, W. A., Matthysse, S. W., and Quastler, H. (1964). Passive stability in a metabolic network. J. Theoret. Biol. 7, 98.

Munster, A. (1970). Classical Thermodynamics. New York: Wiley-Interscience.

Newman, S. and Rice, S. (1971). Model for constraint and control in biochemical networks. Proc. Natl. Acad. Sci. (U.S.) 68, 92.

Olson, H. (1958). Dynamical Analogies, 2nd ed. Princeton, New Jersey: D. Van Nostrand.

Onsager, L. (1931). Reciprocal relations in irreversible processes, I and II. Phys. Rev. 37, 405; 38, 2265.

Oster, G. and Auslander, A. (1971). Topological representations of thermodynamic systems: I. Basic concepts. J. Franklin Inst. 292, 1; II. Some elemental subunits for irreversible thermodynamics. ibid. 292, 77.

Oster, G. and Desoer, C. (1971). Tellegen's theorem and thermodynamic inequalities. J. Theoret. Biol. 32, 219.

Oster, G., Perelson, A., Katchalsky, A. (1971). Network thermodynamics. Nature 234, 393.

Othmer, H. G. and Scriven, L. E. (1969). Interactions of reaction and diffusion in open systems. Ind. Eng. Chem. Fund. 8, 32.

Othmer, H. G. and Scriven, L. E. (1971). Instability and dynamic pattern in cellular networks. J. Theoret. Biol. 32, 507.

Paynter, H. (1961). Analysis and Design of Engineering Systems. Cambridge, Mass.: MIT Press.

Penfield, P. and Haus, H. (1967). Electrodynamics of Moving Media. Cambridge, Mass.: MIT Press.

Penfield, P., Spence, R., and Duinker, S. (1970). Tellegen's Theorem and Electrical Networks. Cambridge, Mass.: MIT Press.

Perelson, A. and Katchalsky, A. (1972). The relationship between the thermodynamic and kinetic reaction diffusion parameters. Chem. Eng. Sci. (in press).

Pings, C. J. and Nebeker, E. B. (1964). Thermodynamics of chemical coupling. *Ind. Eng. Chem. Fund.* **4**, 376.

Pitzer, K. S. (1961). Irreversible thermodynamics. *Pure Appl. Chem.* **2**, 207.

Prigogine, I. (1947). *Étude Thermodynamique des Phenomenes Irreversibles*. Liege: Desoer.

Prigogine, I. (1967). *Thermodynamics of Irreversible Processes*, 3rd ed. New York: Wiley–Interscience.

Redlich, O. (1970). Intensive and extensive properties. *J. Chem. Educ.* **47**, 154.

Roth, J. P. (1955). An application of algebraic topology to numerical analysis: On the existence of a solution to the network problem. *Proc. Natl. Acad. Sci. (U.S.)* **41**, 518.

Sanwal, B. D. and Smando, R. (1969). Malic enzyme of *Escherichia coli*. *J. Biol. Chem.* **244**, 1817.

Seshu, S. and Reed, M. (1961). *Linear Graphs and Electrical Networks*. Reading, Mass.: Addison-Wesley.

Shearer, J., Murphy, A. and Richardon, H. (1967). *Introduction to System Dynamics*. Reading, Mass.: Addison-Wesley.

Smale, S. (1972). On the mathematical foundations of circuit theory. *J. Diff. Geom.* (in press).

Smith, O. J. M. (1950). Thermistors: I. Static characteristics. *Rev. Sci. Instr*. **21**, 344; II. Dynamic characteristics *ibid*. **21**, 351.

Spiegler, K. S. (1958). Transport processes in ionic membranes. *Trans. Faraday Soc*. **54**, 1408.

Spivak, M. (1965). *Calculus on Manifolds*. New York: Benjamin.

Sudarshan, E. C. G. (1962). The structure of dynamical theories. *Brandeis Summer Institute, 1961. Lectures in Theoretical Physics*. Vol. 2. New York: Benjamin.

Takakashi, Y., Auslander, D. and Rabins, M. (1970). *Control*. Reading, Mass: Addison-Wesley.

Tellegen, B. D. H. (1952). A general network theorem, with applications. *Phillips Res. Rept.* **7**, 259.

Teorell, T. (1962). Excitability phenomena in artificial membranes. *Biophys. J.* **2**, (2), part 2, 27.

Trent, H. M. (1955). Isomorphisms between oriented linear graphs and lumped physical systems. *J. Acoust. Soc. Am.* **27**, 500.

Truesdell, C. (1970). *Rational Thermodynamics*. New York: McGraw-Hill.

Vaidhyanathan, V. S. (1966). Some theoretical aspects of biological transport. In Intracellular Transport, ed. K. B. Warren, pp. 153-165. New York: Academic Press.

Van Rysselberghe, P. (1958). Reaction rates and affinities. J. Chem. Phys. **29**, 640.

Table 1. Common through and across variables.

Energy domain	Through variable	Across Variable	Integrated through variable (generalized displacement)	Integrated across variable (generalized momentum)
Electrical	Current i	Voltage v	Charge q	Flux ϕ
Fluid	Volume flow Q	Pressure p	Volume V	Pressure momentum Γ
Diffusion	Mass flow J_i (or molar flow)	Chemical potential μ_i	Mass m_i No. of moles n_i	-
Chemical reaction	Reaction rate J^r	Affinity $A = -\Sigma \nu_i \mu_i$	Advancement ξ	-
Mechanical (translational)	Force F	Velocity v	Momentum p	Displacement x
Mechanical (rotational)	Torque τ	Angular velocity ω	Angular momentum H	Angular displacement θ

Table 2. Ideal system elements.

Element	Symbol	Defining equations	Remarks
0-junction	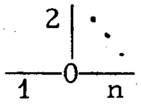	$\Sigma\sigma_1 f_i = 0, e_1 = e_2 = \cdots = e_n$	Generalized "parallel" connection
1-junction	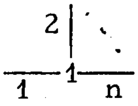	$\Sigma\sigma_i e_i = 0, f_1 = f_2 = \cdots = f_n$	Generalized "series" connection
Resistance[1]	$\rightharpoonup R$	$\phi_R(e, f) = 0$	Ideal dissipative element
Capacitance[2]	$\vdash\!\rightharpoonup C$	$\phi_C(e, q) = 0$	Capacitive (displacement) energy storage
Inductance[3]	$\rightharpoonup\!\mid L$	$\phi_L(p, f) = 0$	Inductive (kinetic) energy storage
Memristance	$\rightharpoonup M$	$\phi_M(p, q) = 0$	Displacement-dependent dissipation
Transducer	$\rightharpoonup TD \leftharpoondown$	$\begin{bmatrix} e_1 \\ f_1 \end{bmatrix} = \begin{bmatrix} r & 0 \\ 0 & -r \end{bmatrix} \begin{bmatrix} e_2 \\ f_2 \end{bmatrix}$	Energy conversion and signal modulation
Effort source	$E \rightharpoonup\!\mid$	$e = \text{constant}$	Ideal energy source(effort)
Flow source	$F \vdash\!\rightharpoonup$	$f = \text{constant}$	Ideal energy source (flow)

---

[1] The half-arrow is the sign convention: power is considered positive into all elements.

[2] The causal stroke $\vdash\!\rightharpoonup C$ indicates that the natural input (independent) variable is the flow variable, since for C, the dynamic equation is $C \frac{de}{dt} = f$, and the physical restriction $P = ef < \infty$ prohibits step inputs of effort.

[3] The natural input (independent) variable for L is e. All other elements are causally neutral.

FIGURE CAPTIONS

Fig. 1.1. Thermodynamic multiports.

Fig. 1.2. Relation of the state variables.

Fig. 2.1. Topological graph for a mechanical system. The KCL requirement for the system gives $F_1+F_2+F_4+F_5 = 0$ for node A and $F_4+F_5-F_3 = 0$ for node B, which is equivalent to the equations $k_1x_A+m_2x_A+k_4(x_B-x_A)+b(\dot{x}_B-\dot{x}_A) = 0$ and $k_4(x_B-x_A)+b(\dot{x}_B-\dot{x}_A) - m_3\ddot{x}_B= 0$.

Fig. 2.2 Membrane transport system. In (b) the processes of dissipation and storage are separated.

Fig. 2.3. Assignment of linear graph elements to transport across a membrane.

Fig. 2.4. Topological graph representation of nonelectrolyte transport across a simple membrane.

Fig. 3.1. (a) Two-terminal element with associated reference directions for current and voltage; (b) nonassociated reference directions.

Fig. 3.2. Bond graph representation of nonelectrolyte transport through a simple membrane.

Fig. 3.3. The constitutive relation for a tunnel diode.

Fig. 3.4. The causality convention in bond graph representation.

Fig. 3.5. Diffusion chain and transmission matrices.

Fig. 4.1. An angle dependent transducer.

Fig. 4.2. Bond graph representation of coupled hydrodynamic flows.

Fig. 4.3. The structure of the coupling element (CPL) in hydrodynamic flow.

Fig. 4.4. Stationary state hydrodynamic coupling between flows in a membrane.

Fig. 4.5. Coupled nonstationary flows.

Fig. 4.6. Bond graph representation of coupled diffusional flows within a volume element of length dx for a membrane of unit area.

Fig. 4.7. Arrangement of concentration and electrical capacitors at point x and $x + \Delta x$ of an electrolyte solution.

Fig. 4.8. Transport of a univalent cation.

Fig. 4.9. Bond graph representing the electrostatically coupled flow of a univalent anion and cation.

Fig. 4.10. Bond graph representation of an electrolyte solution in which both electrostatic and hydrodynamic couplings govern the ionic flows.

Fig. 4.11. Bond graph representation for the permeation of a binary electrolyte through a membrane. Solvent flow and hydrodynamic coupling not shown.

Fig. 5.1. Multiport representation of a chemical transformation.

Fig. 5.2. Component i is a reactant in the p^{th} reaction and a product in the q^{th} reaction.

Fig. 5.3. A causally correct bond graph for the near equilibrium chemical reaction $2A + 3B \rightleftharpoons C$.

Fig. 5.4. Bond graph representation of a system of near-equilibrium reactions:

$$A + B \rightleftharpoons C$$
$$C \rightleftharpoons 2D$$
$$D + B \rightleftharpoons E$$

Fig. 5.5. The dissipation due to a chemical process may be represented by a two-port resistor.

Fig. 5.6. Bond graph for the reaction $A + B \rightleftharpoons C + D$.

Fig. 5.7. Representation of two reactions with a common component: $A \rightleftharpoons B \rightleftharpoons C$.

Fig. 5.8. Representation of the coupled system of reactions:

$$NO + \frac{1}{2}\,Cl_2 \overset{1}{\rightleftharpoons} NOCl$$
$$NOCl + \frac{1}{2}\,I_2 \overset{2}{\rightleftharpoons} NO + ICl$$
$$\frac{1}{2}\,I_2 + \frac{1}{2}\,Cl_2 \overset{3}{\rightleftharpoons} ICl$$

Fig. 5.9. Representation of an enzymatic reaction $S + E \overset{1}{\rightleftharpoons} ES \overset{2}{\rightleftharpoons} E + P$.

Fig. 5.10. Representation of the autocatalytic reaction $X + Y \rightleftharpoons 2X$.

Fig. 6.1. Chemical diffusional coupling in the flow of two nonelectrolytes through a membrane.

Fig. 6.2. A subunit of length dx of the reaction diffusion bond graph.

Fig. 6.3. Bond graph used to evaluate average diffusional relaxation time.

Fig. 6.4. Facilitated diffusion.

Fig. 6.5. Facilitated diffusion with near-equilibrium reactions.

Fig. 7.1. Active, bilateral and signal flow bonds.

Fig. 7.2. The effect of NH_4^+ on the activity of malic enzyme with malate as the varied substrate. Concentrations of TPN^+ and $MNCl_2$ were 0.15 MM and 1 MM, respectively. The pH of the mixture was 7.5. (From Sanwal and Smando, 1969).

Fig. 7.3. Modulation of constitutive relation for allosteric enzyme.

Fig. 7.4. One-port resistor as a two-port thermal converter. Note the active bond on the thermal port, as required by the second law of thermodynamics.

Fig. 7.5. (a) Thermistor circuit

(b) Bond graph

Fig. 7.6. (a) Schematic diagram of the Teorell membrane oscillator.

(b) One-lump bond graph representation.

Fig. 7.7. Experimental and simulated liquid head difference for the Teorell oscillator.

Fig. 7.8. Experimental and simulated membrane electrical resistance for the Teorell oscillator.

Fig. 8.1. Potential function for capacitive n-port and its associated gradient vector field.

Fig. 8.2. (a) A two-port capacitor represented as a terminal graph and as a bond graph.

(b) Interconnection of multiports with bond graph and terminal graph representations.

Fig. 8.3. Junctions, their connection n-port representations and terminal graphs.

Fig. 8.4. One-port potential functions.

Fig. 8.5. N-port structure.

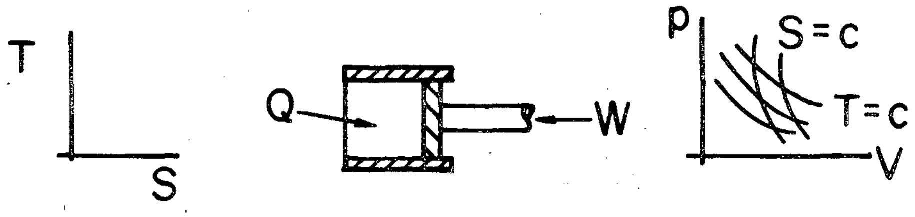

(a) Thermomechanical 2-port

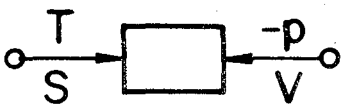

(b) 2-port schematic

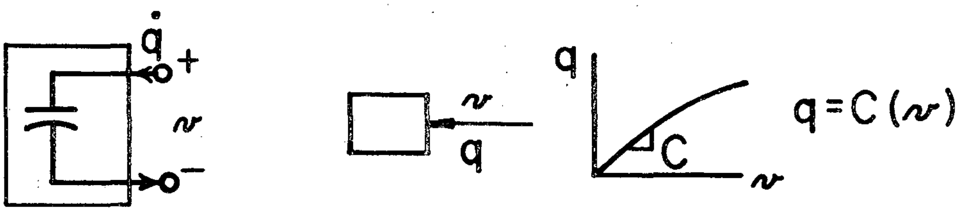

(c) Electrical 1-port capacitor

XBL722-2291

Fig 1.1

$$\begin{tikzcd}
f \arrow[r, "\phi_R"] \arrow[d, "\int"'] \arrow[dr, "\phi_L"] & e \arrow[d, "\int"] \arrow[dl, "\phi_C"] \\
q & \wp \arrow[l, "\phi_M"]
\end{tikzcd}$$

$$\begin{tikzcd}
\text{KCL} \arrow[r, leftrightarrow, "\text{Constitutive relations}"'] & \text{KVL}
\end{tikzcd}$$

XBL722-2292

Fig. 1.2

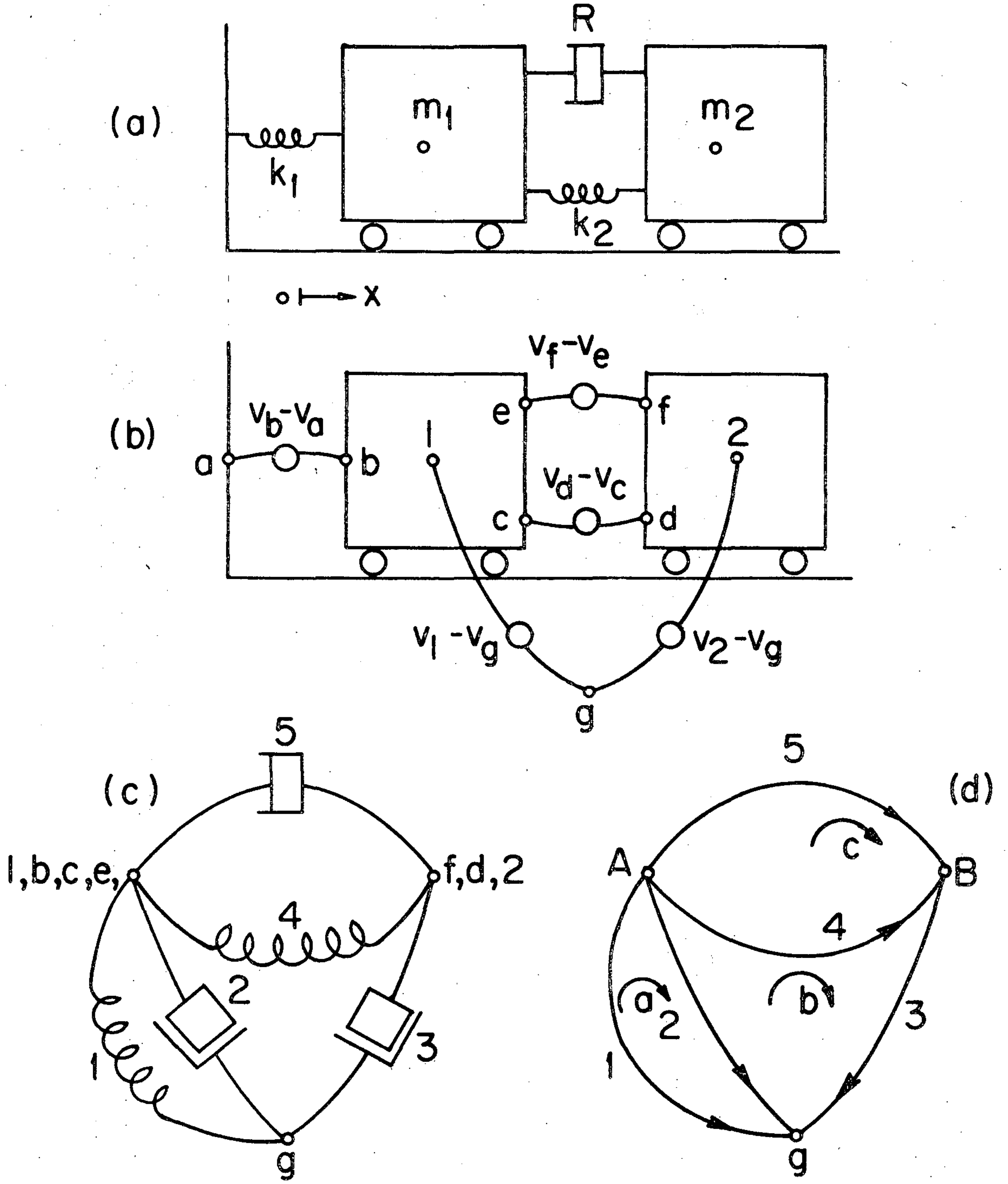

XBL723-2585

Fig. 2.1

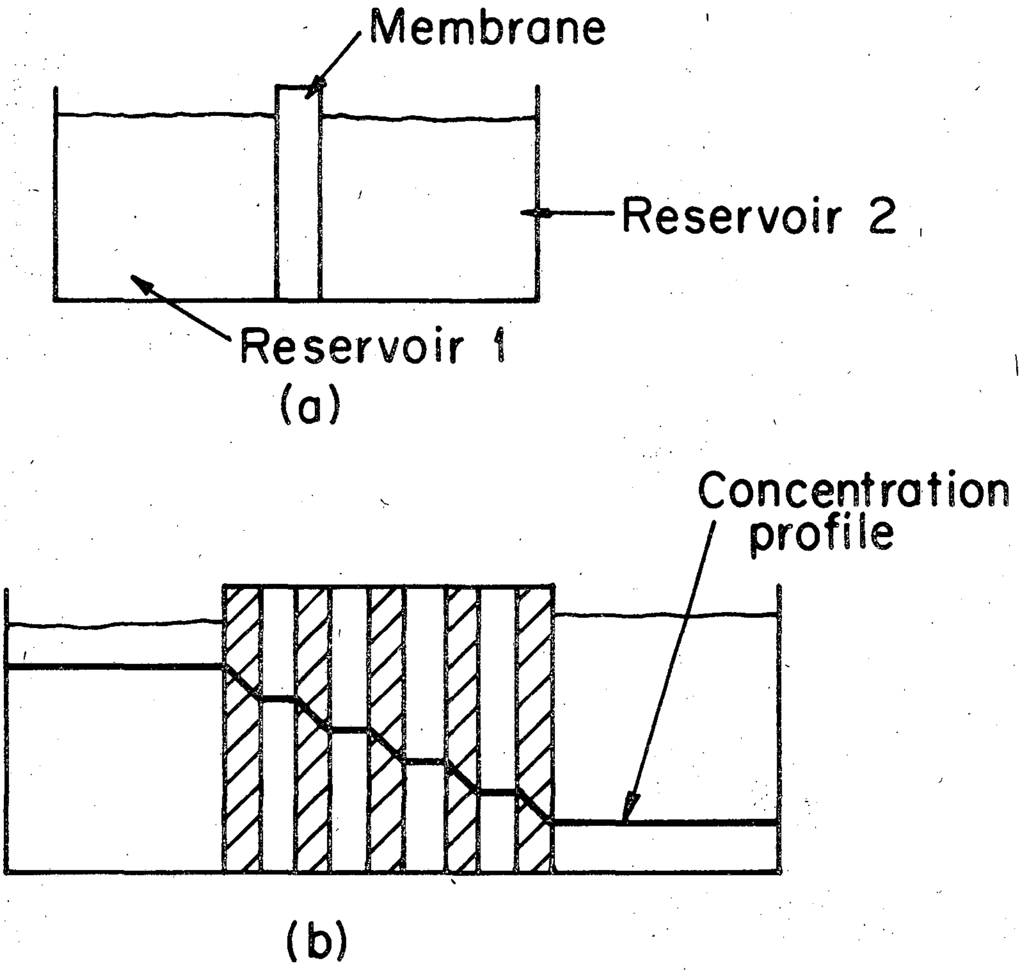

XBL722-2293

Fig. 2.2

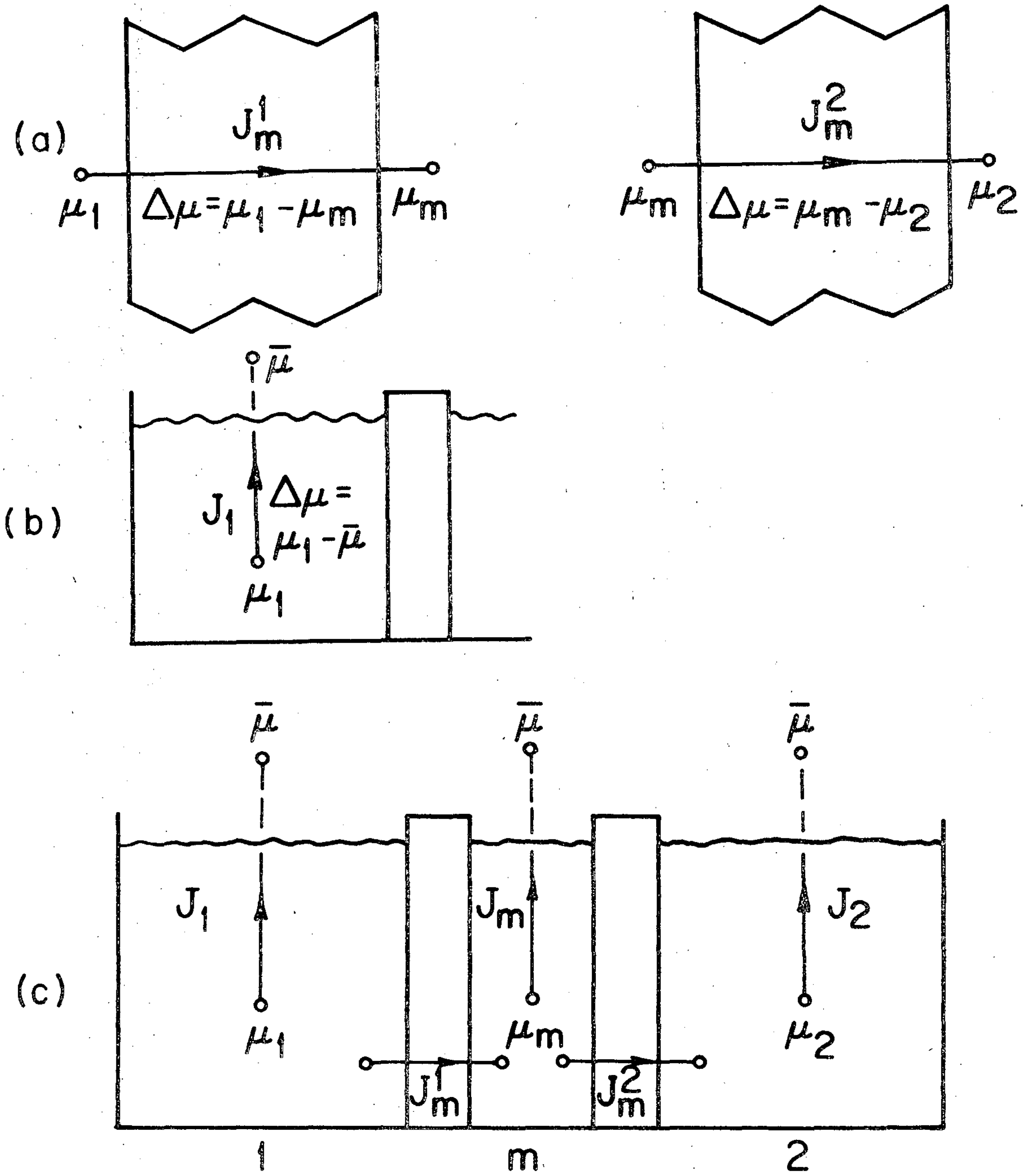

XBL722-2294

Fig. 2.3

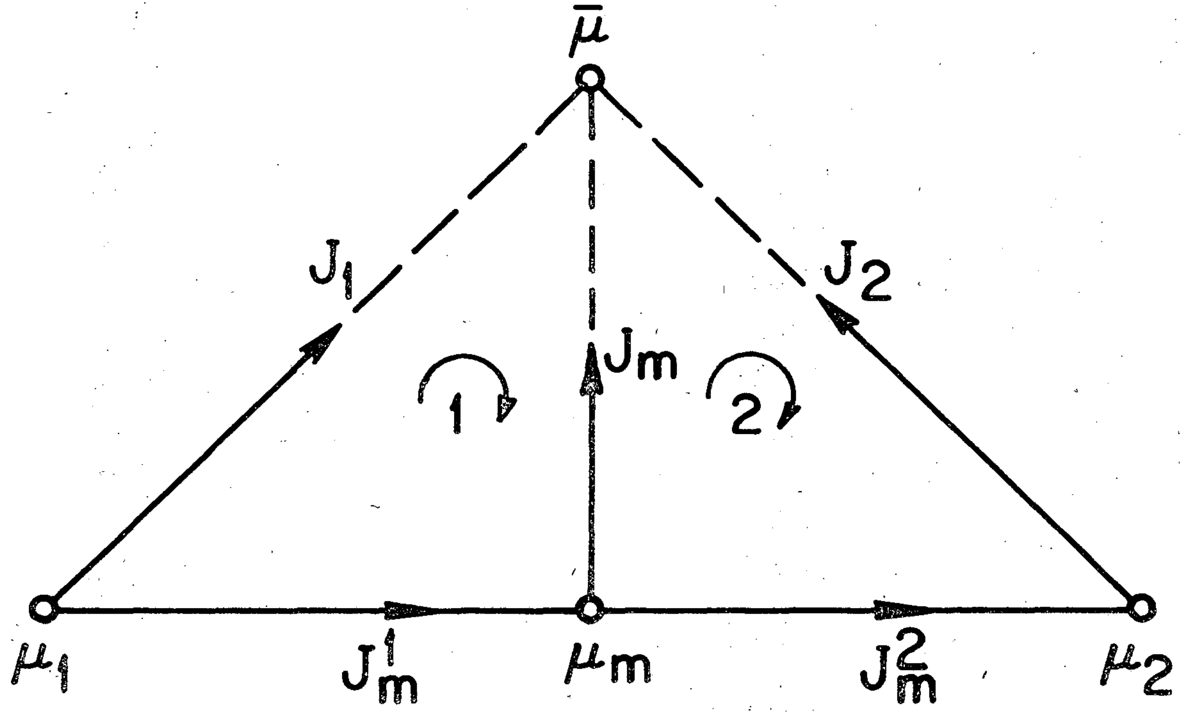

XBL722-2295

Fig. 2.4

(a)

(b)

XBL722-2297

Fig. 3.1

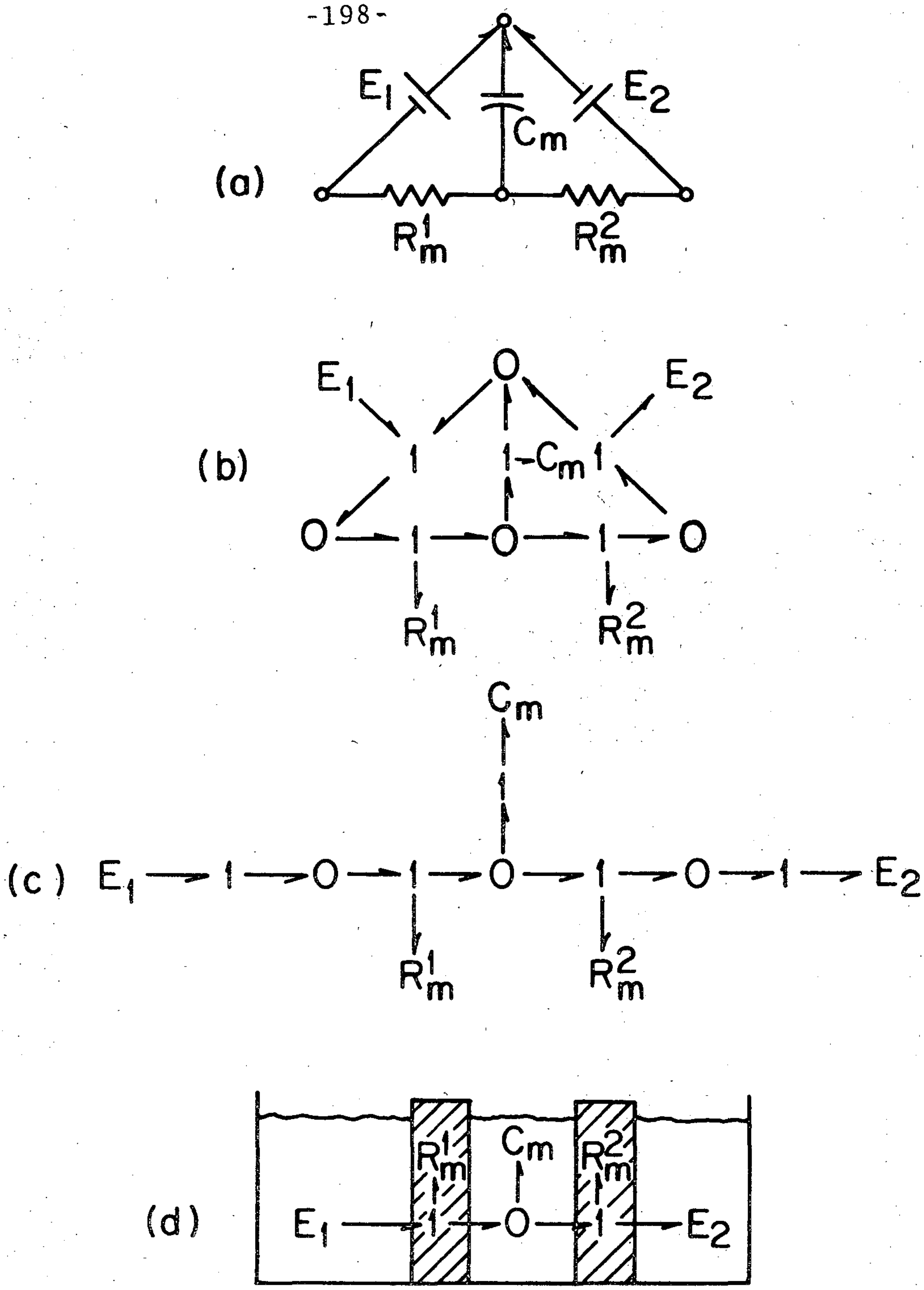

XBL722-2298

Fig. 3.2

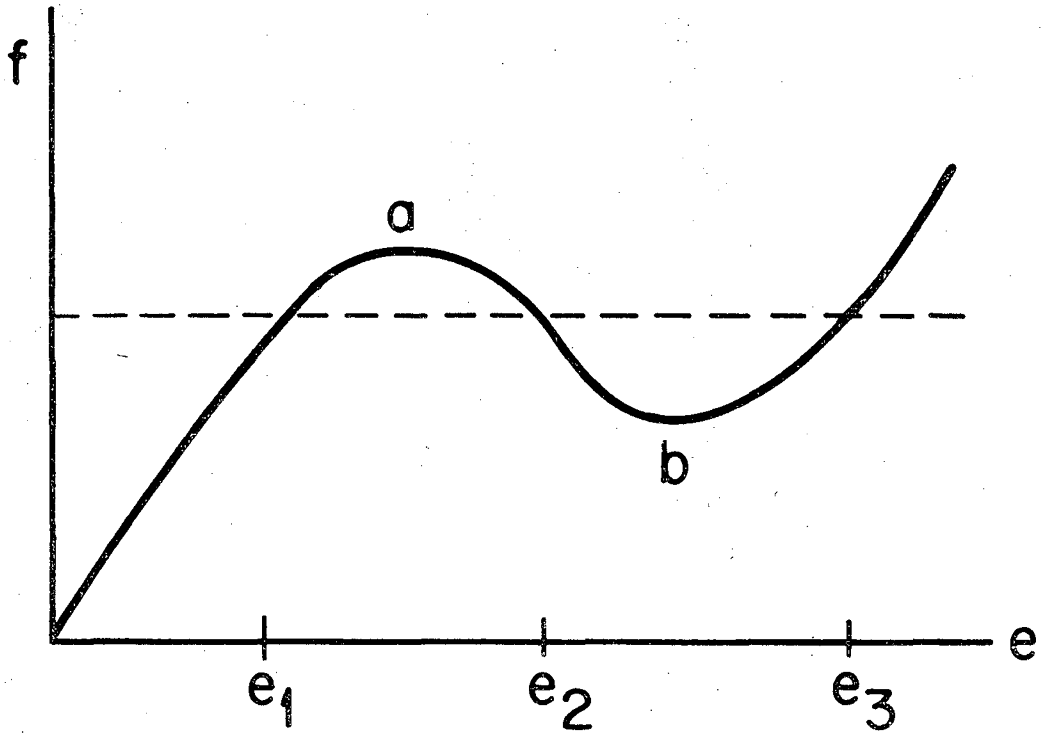

XBL722-2299

Fig. 3.3

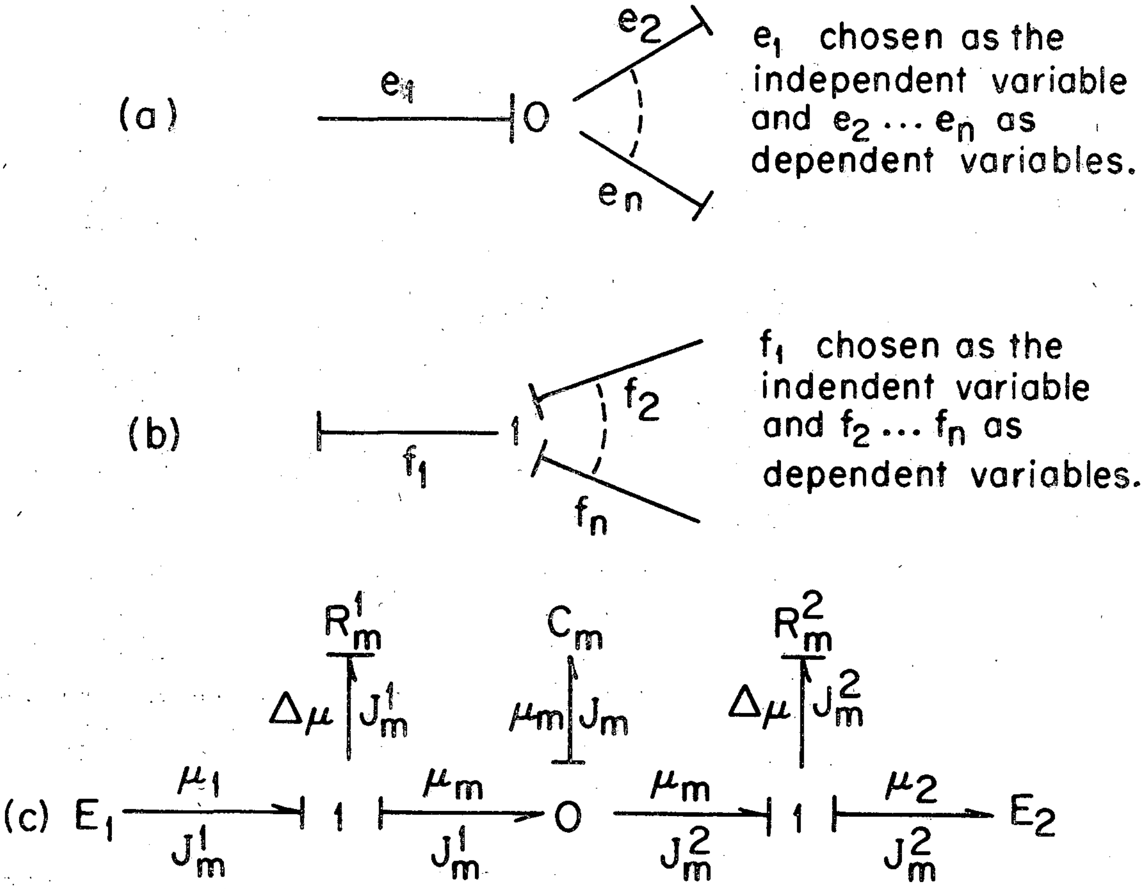

XBL722-2300

Fig. 3.4

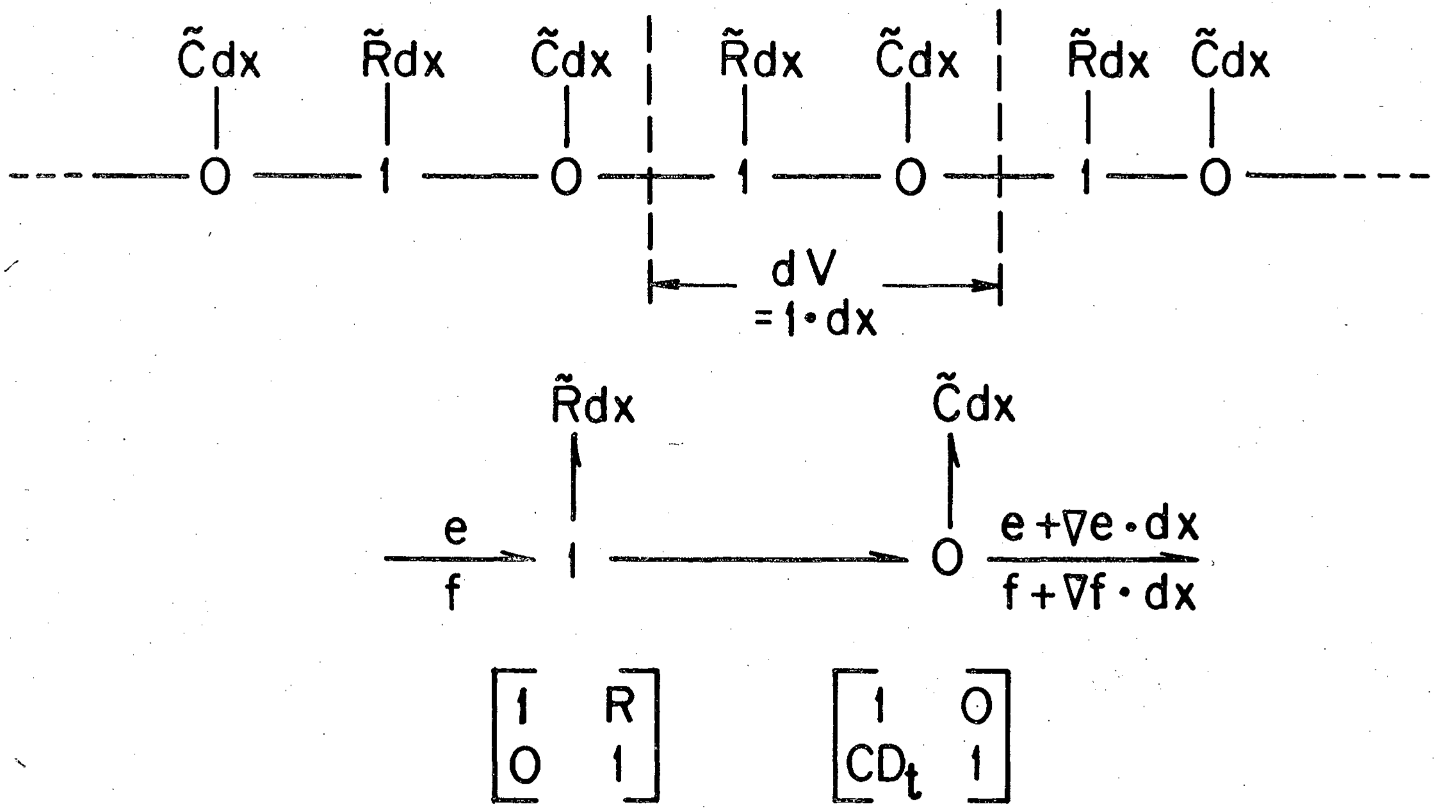

XBL722-2301

Fig. 3.5

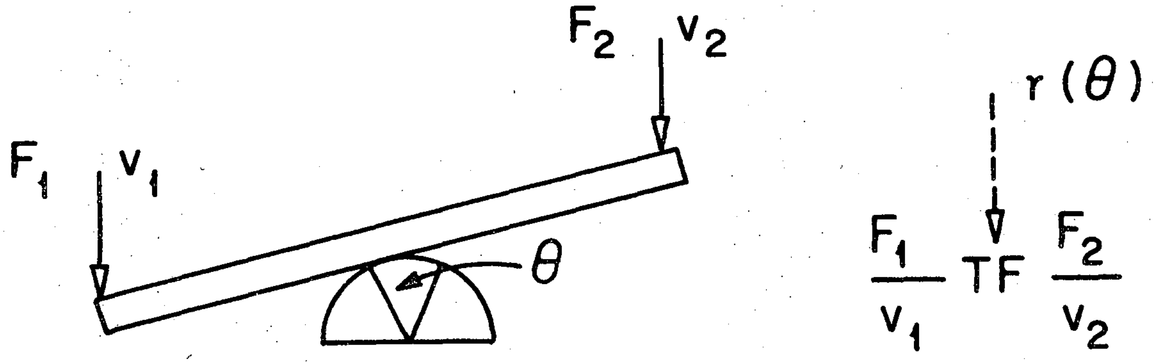

XBL722-2335

Fig. 4.1

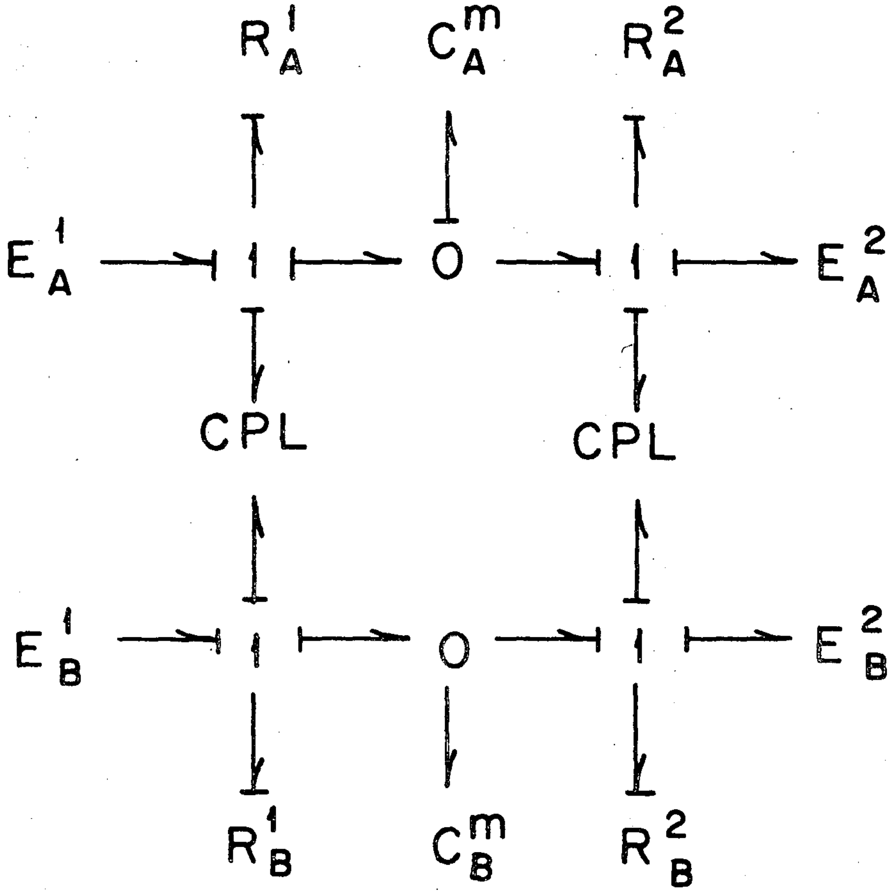

XBL722-2336

Fig 4.2

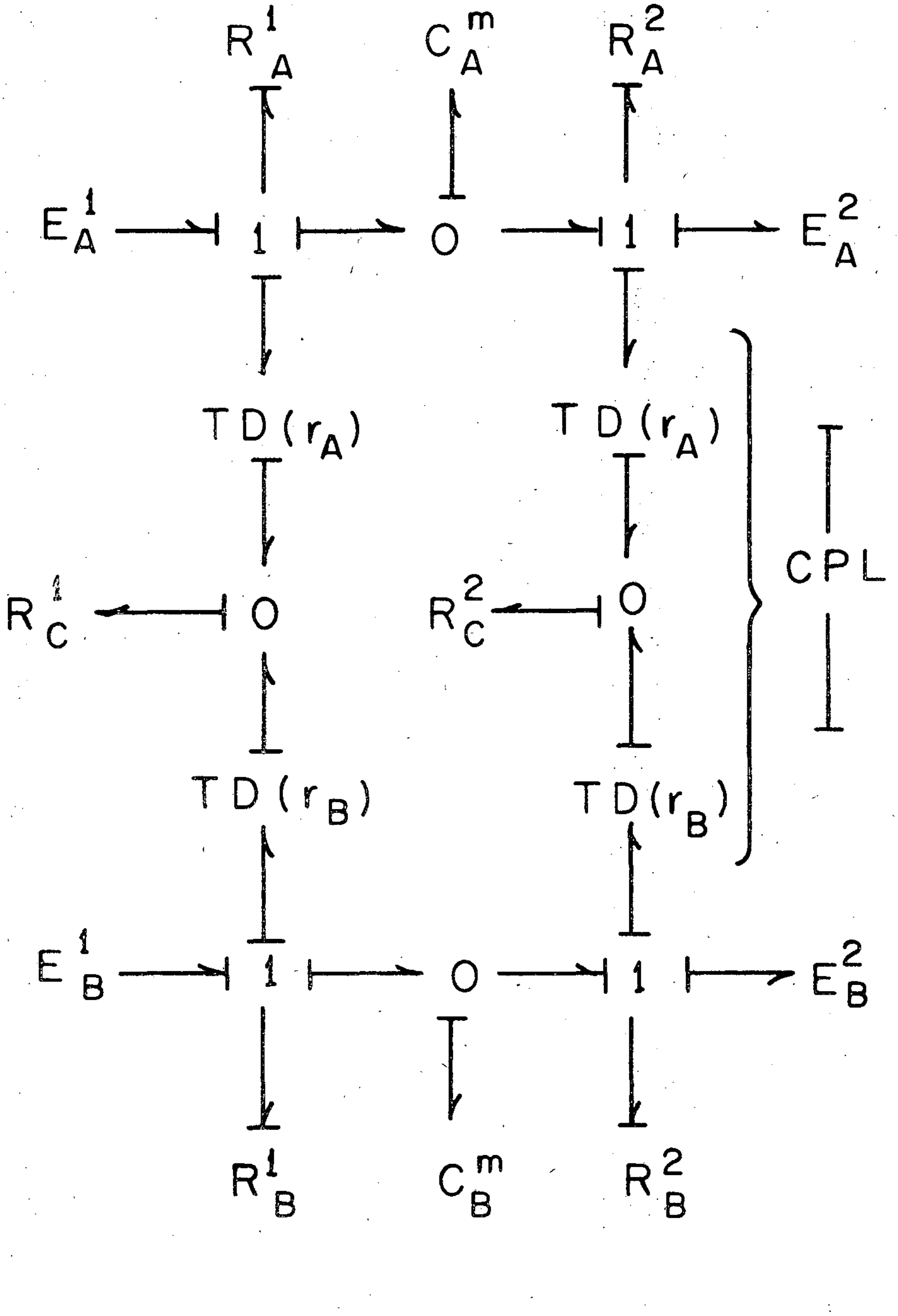

XBL 722-2337

Fig. 4.3

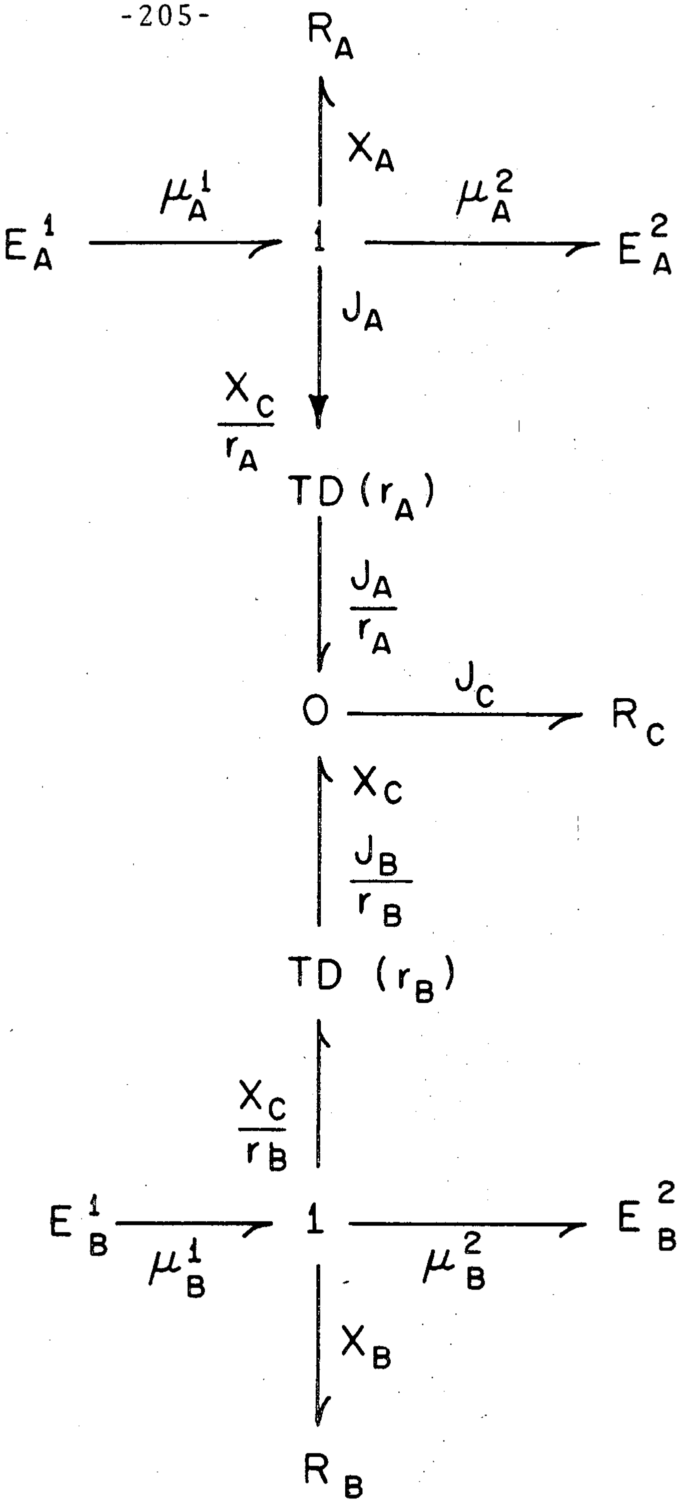

XBL722-2338

Fig. 4.4

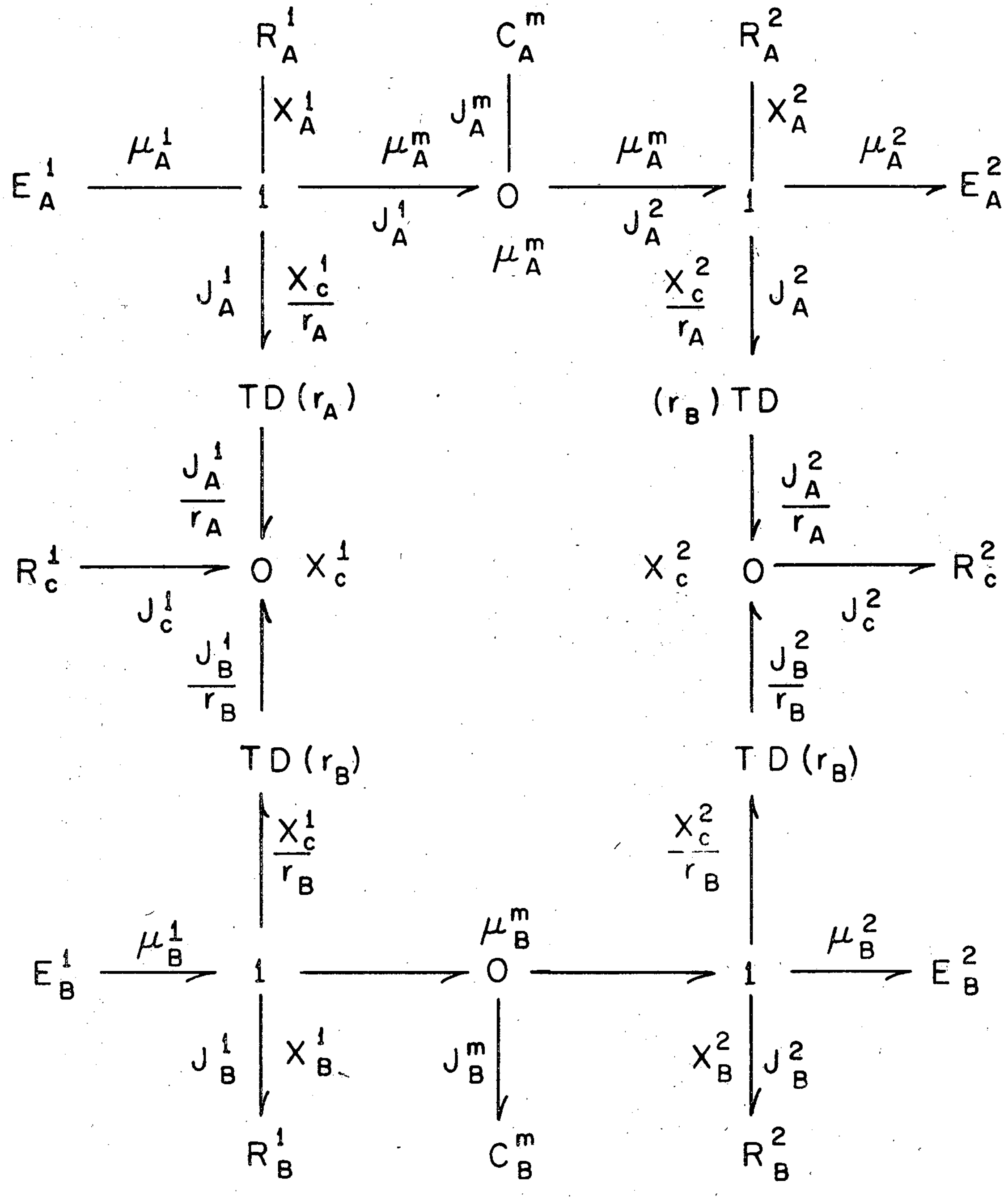

Fig. 4.5

XBL722-2339

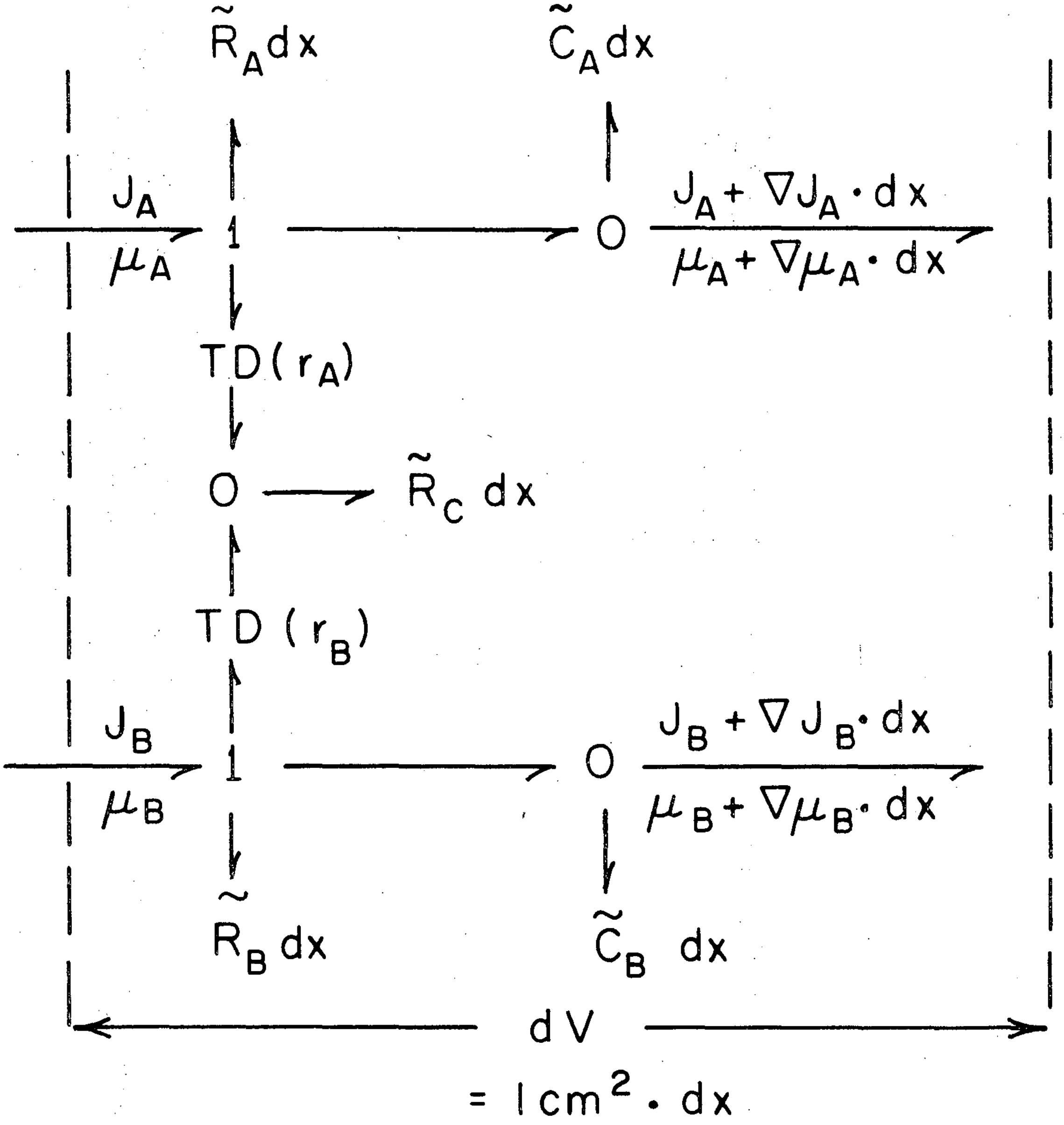

Fig. 4.6

XBL722-2340

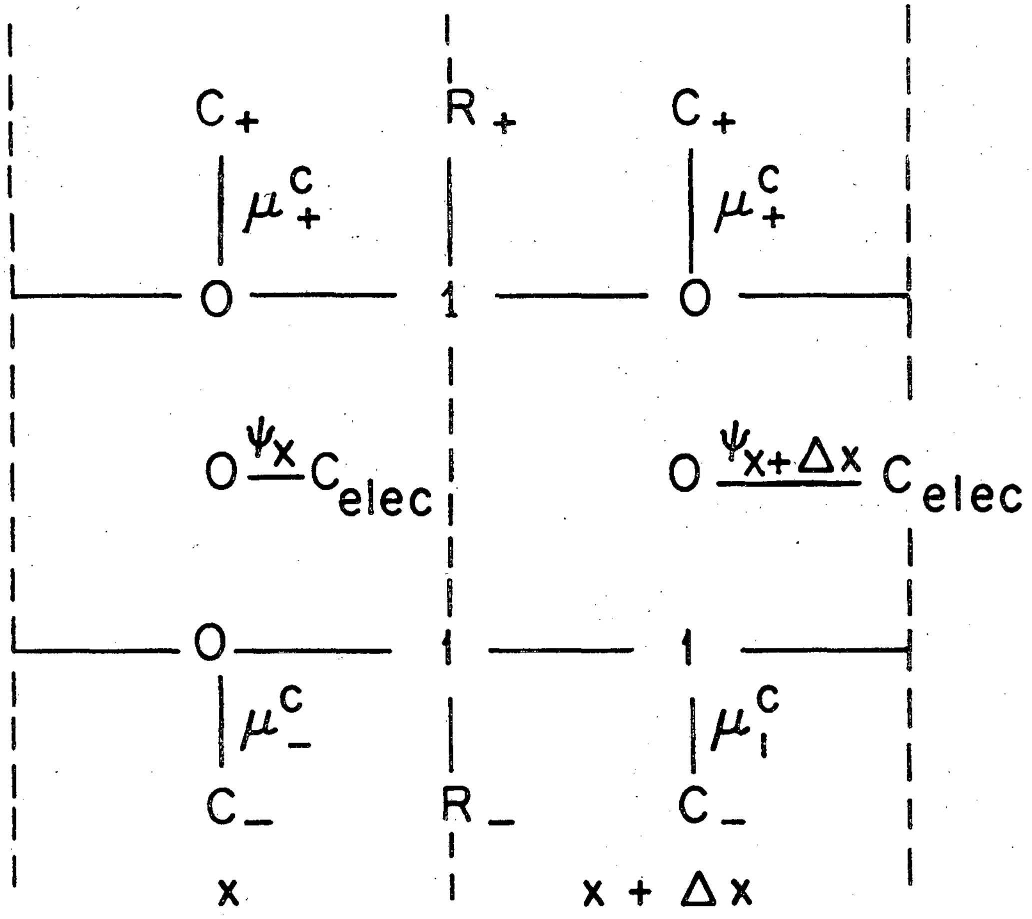

Fig. 4.7

XBL722-2341

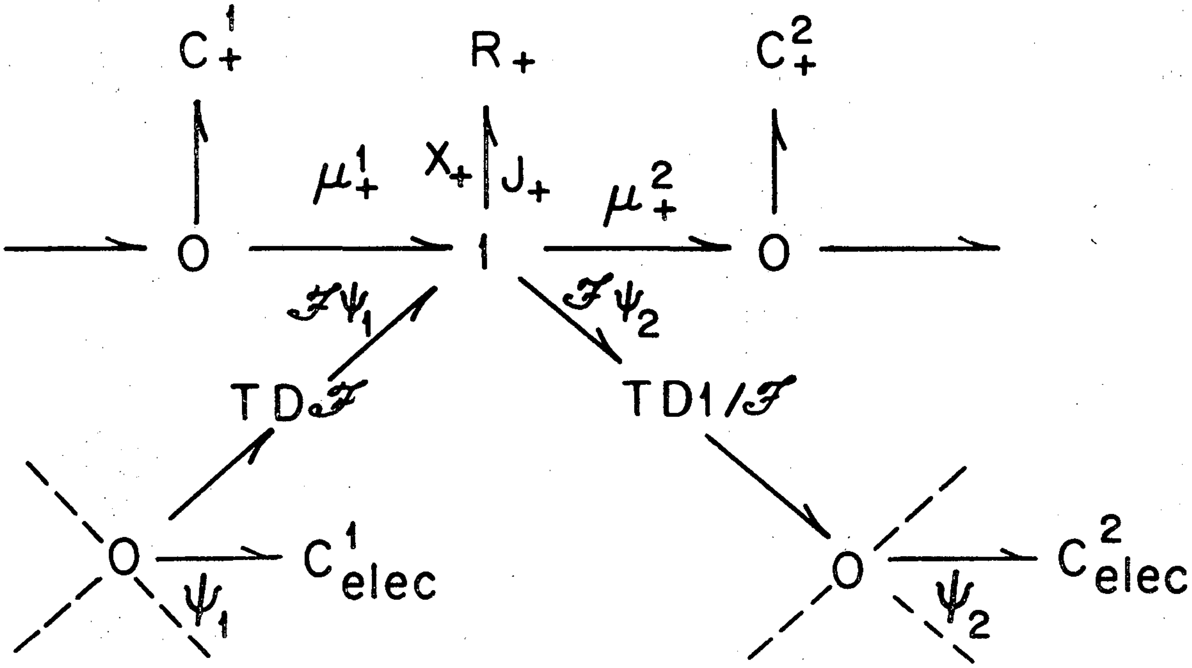

XBL722-2342

Fig. 4.8

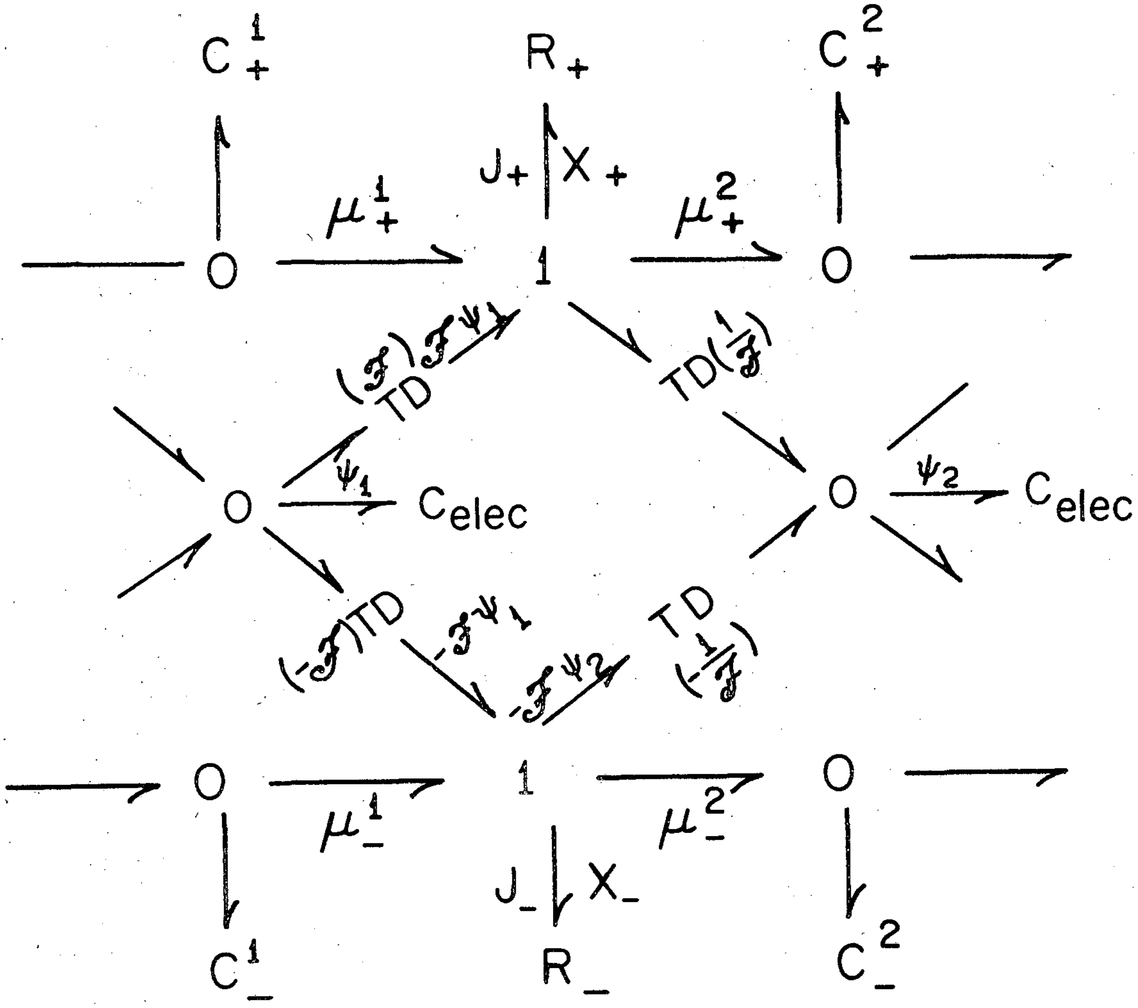

XBL722-2343

Fig. 4.9

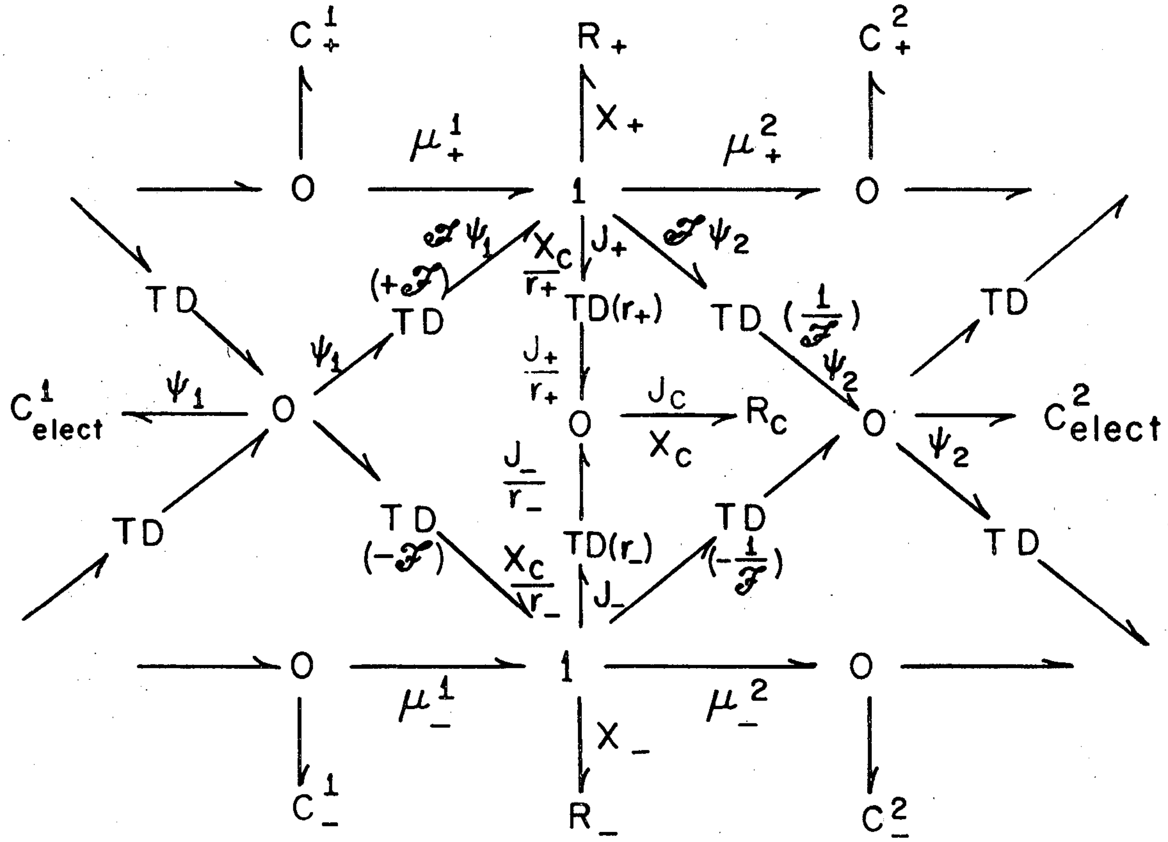

XBL722-2344

Fig. 4.10

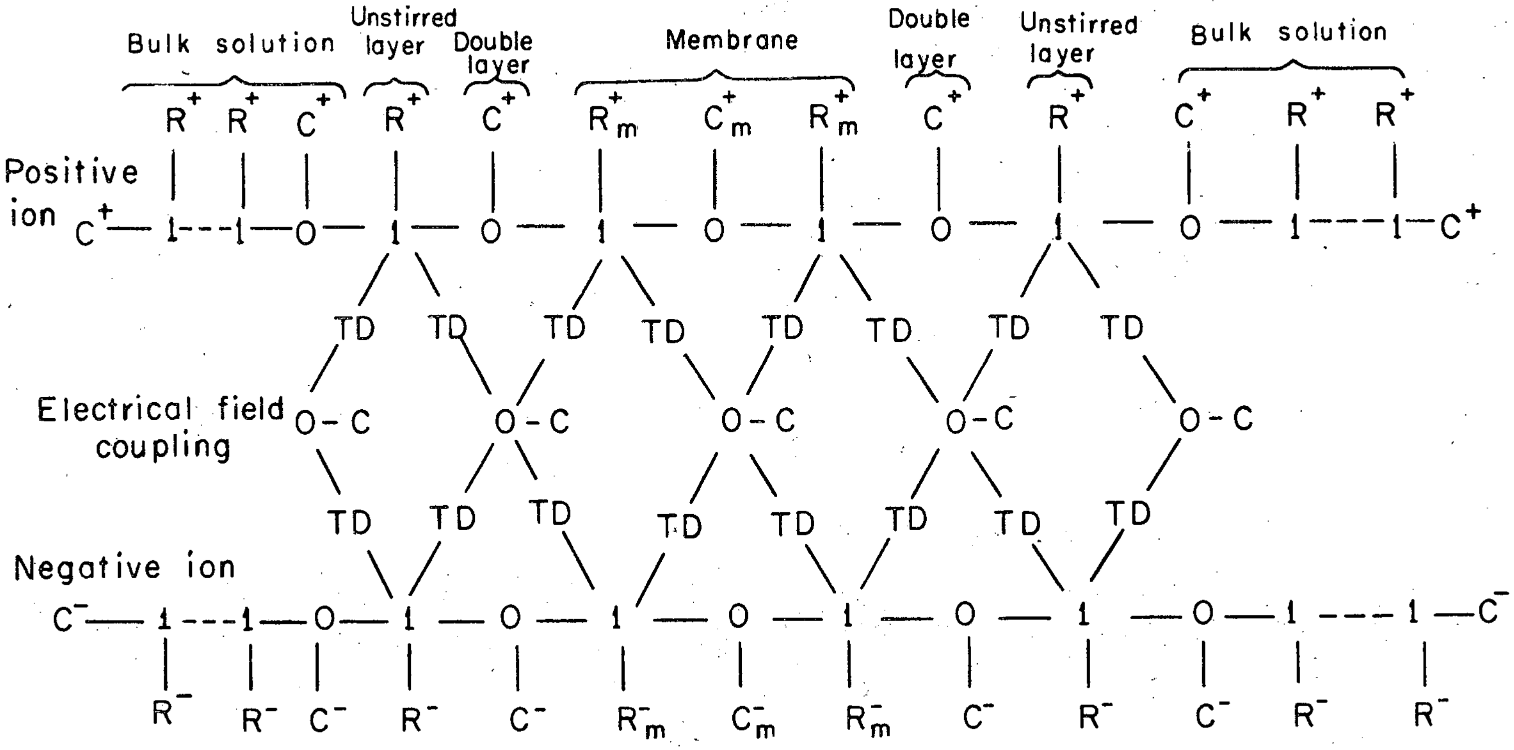

Fig. 4.11

XBL722-2345

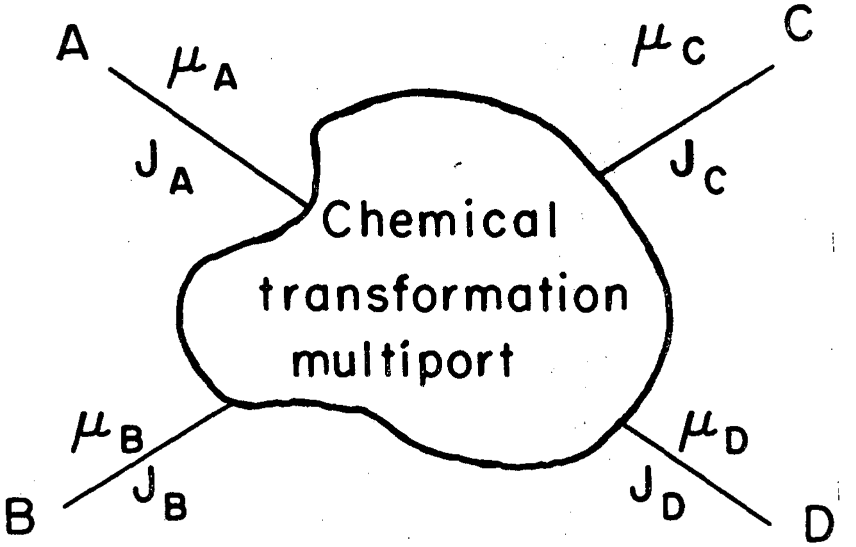

XBL722-2369

Fig. 5.1

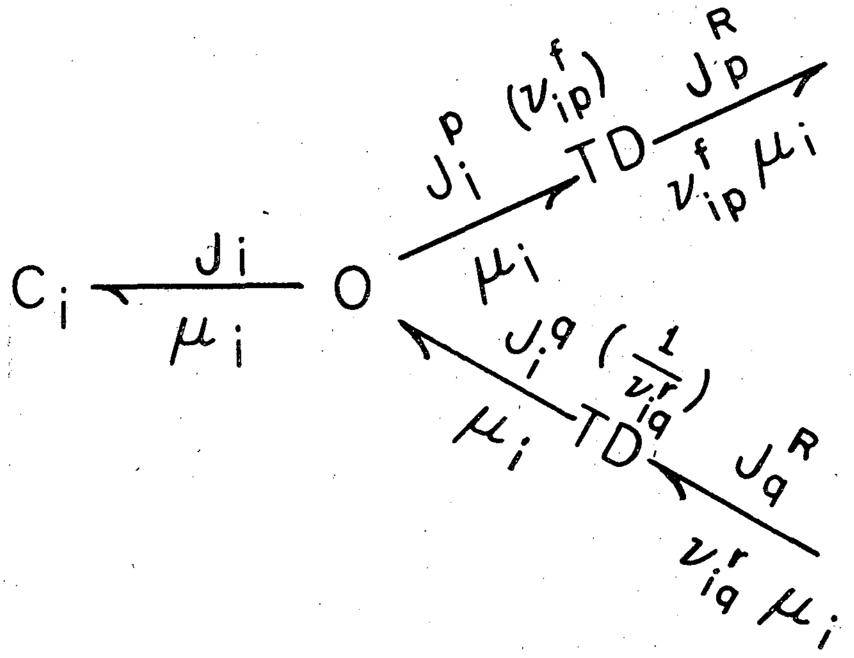

XBL722 - 2370

Fig. 5.2

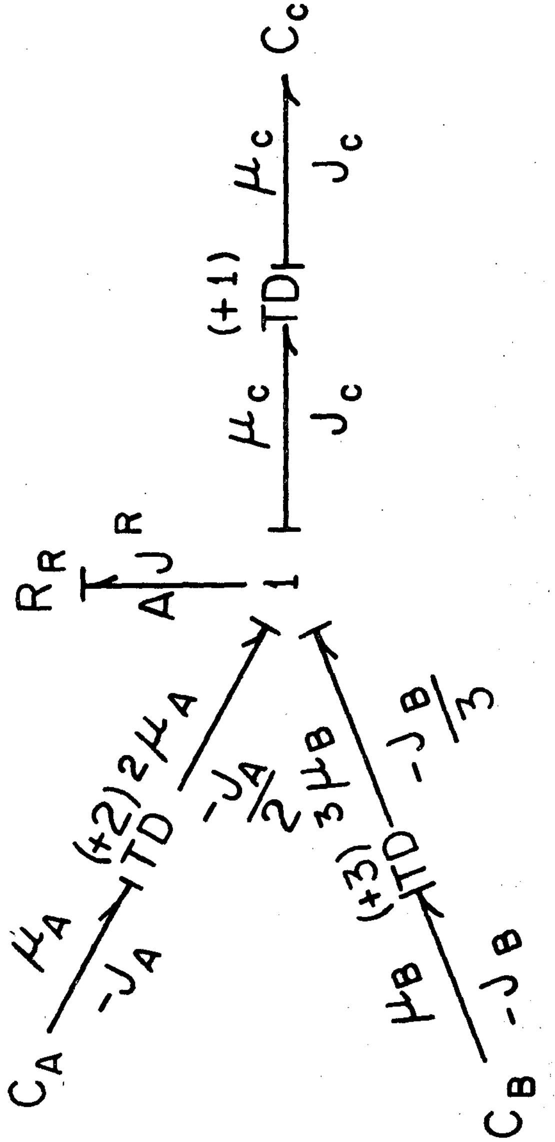

XBL722-2371

Fig. 5.3

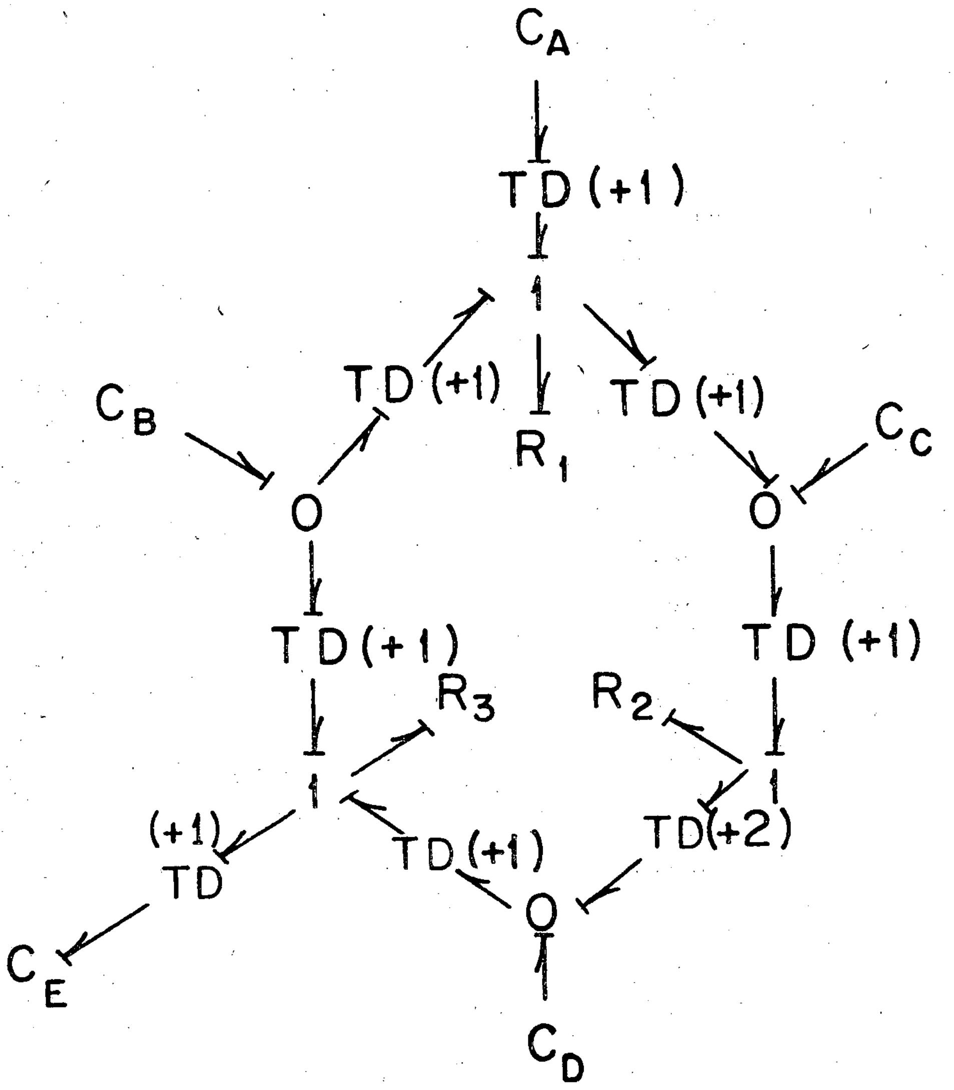

XBL722-2372

Fig. 5.4

$$\xrightarrow[J^{R}_{in}]{A^{f}} R_{R} \xrightarrow[J^{R}_{out}]{A^{r}}$$

XBL722-2373

Fig. 5.5

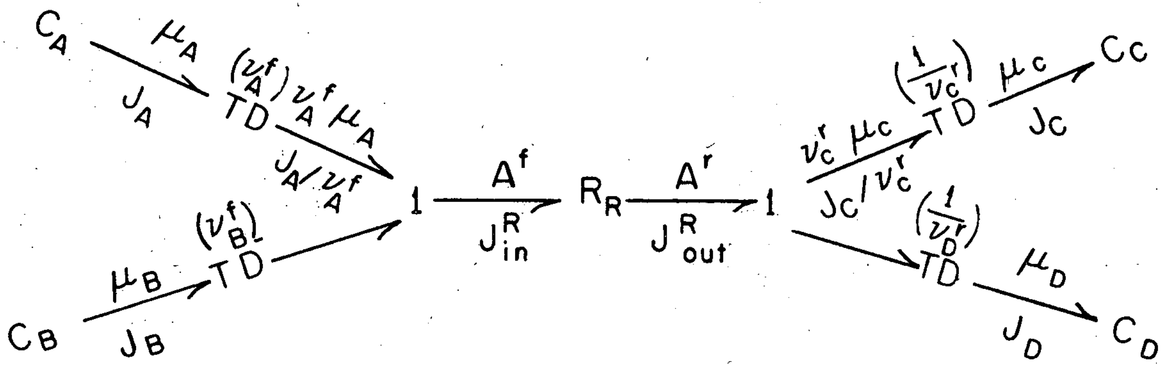

XBL722-2374

Fig. 5.6

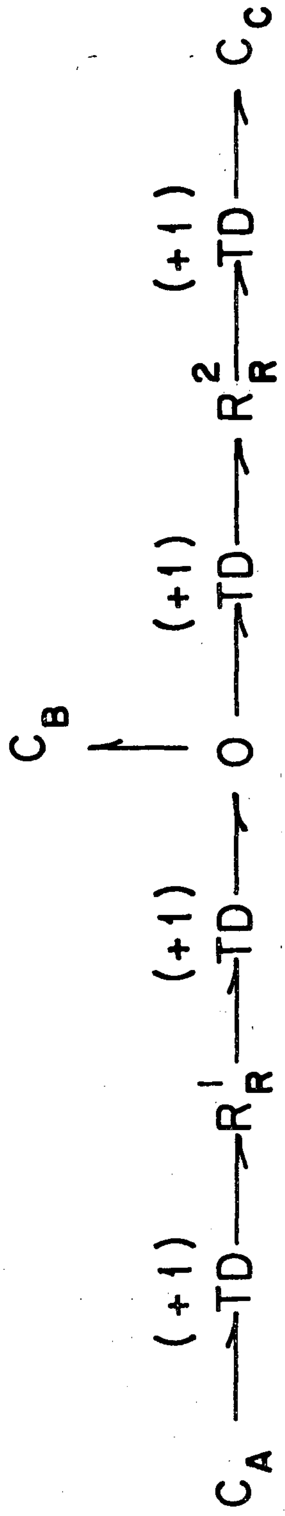

XBL722-2375

Fig. 5.7

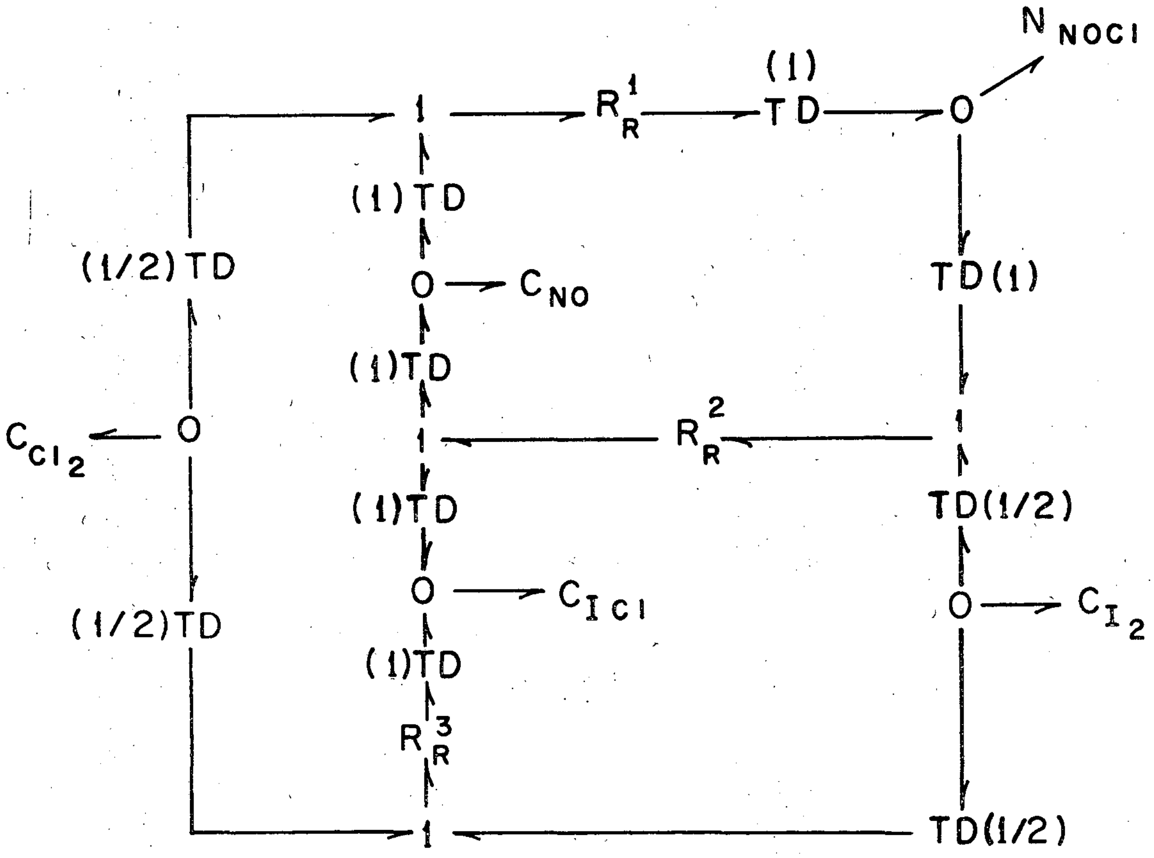

XBL722-2376

Fig. 5.8

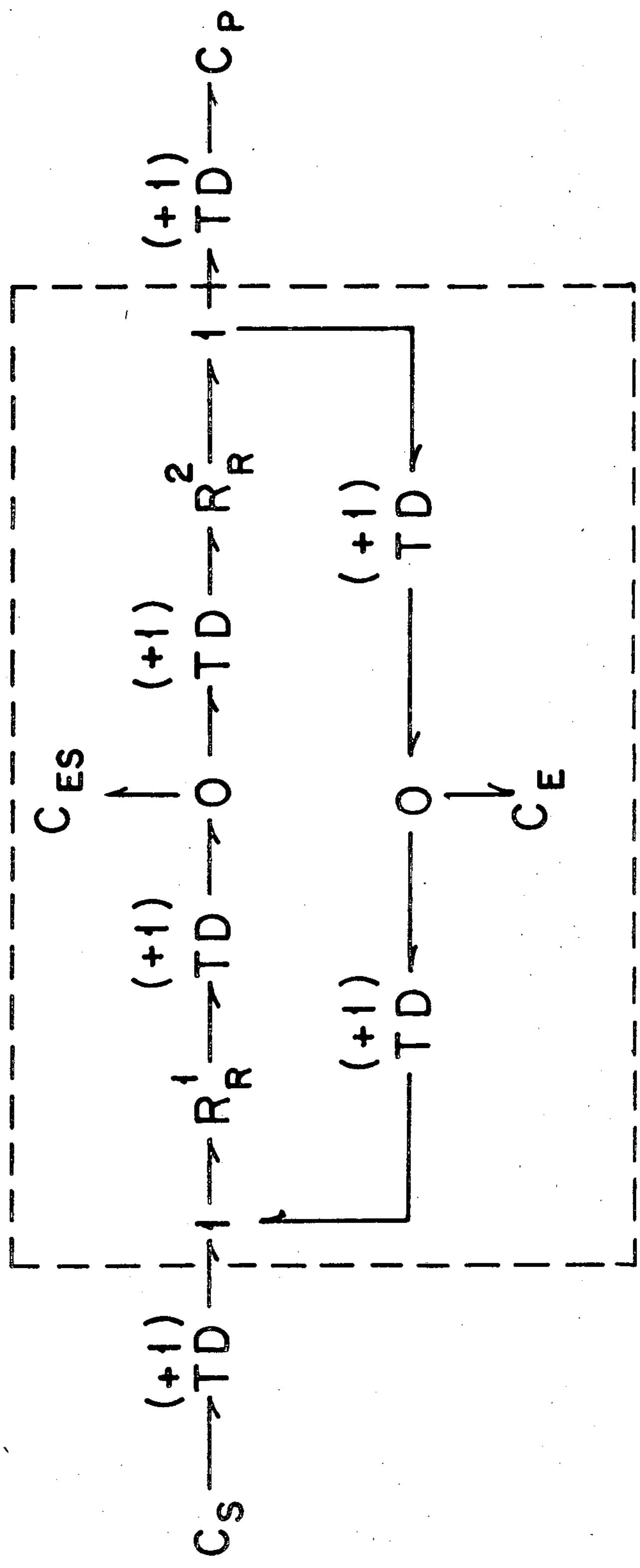

XBL722-2377

Fig. 5.9

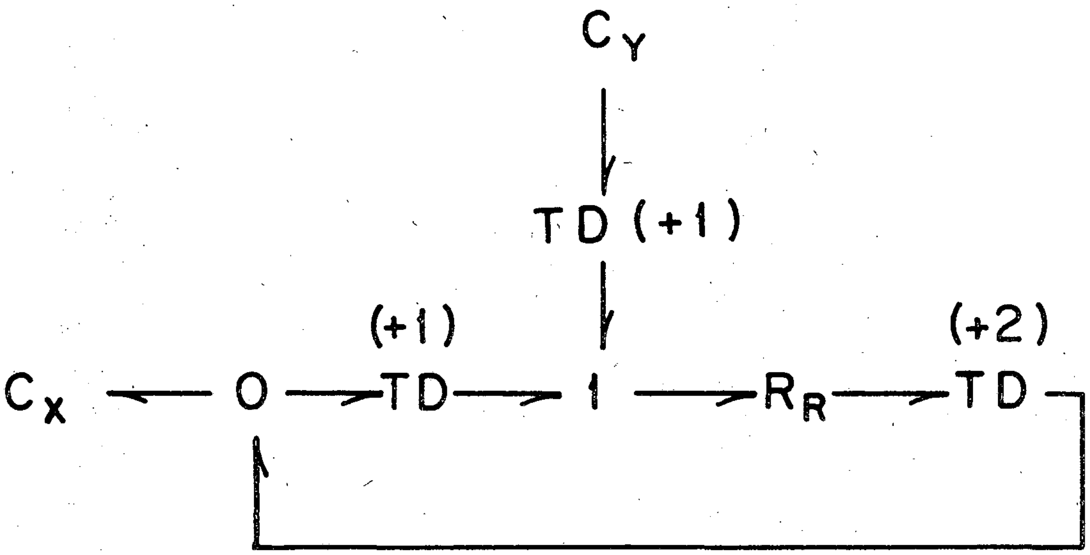

XBL722-2378

Fig. 5.10

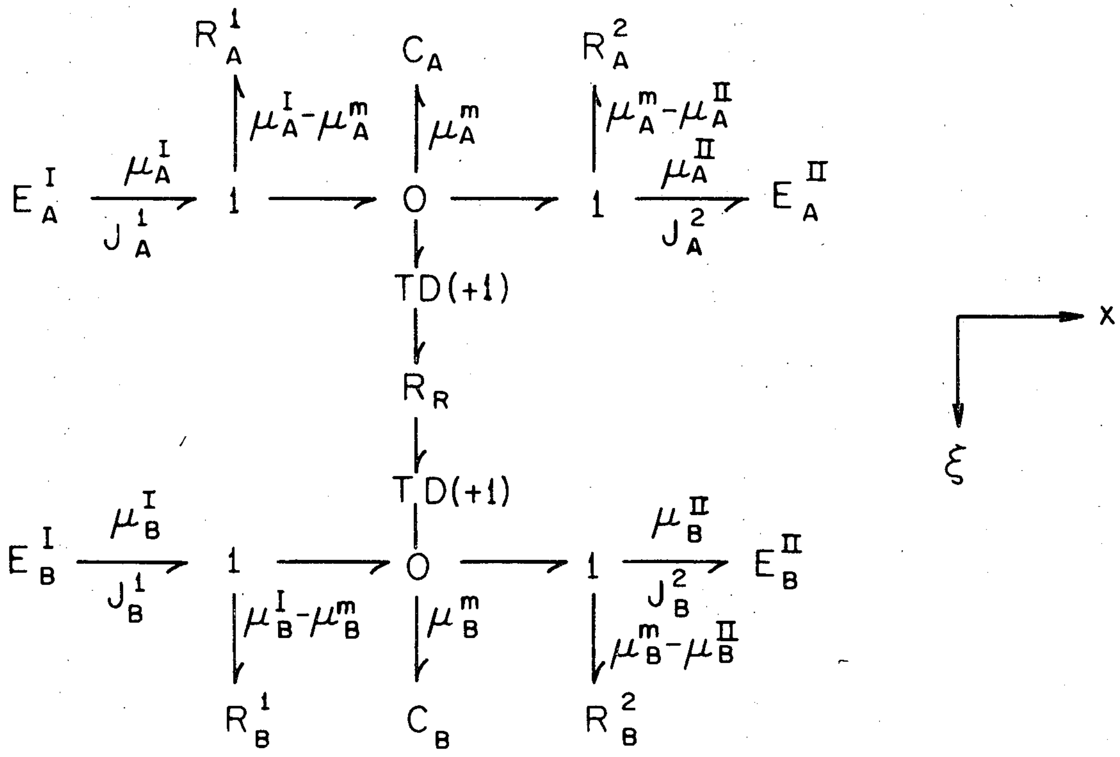

XBL722-2386

Fig. 6.1

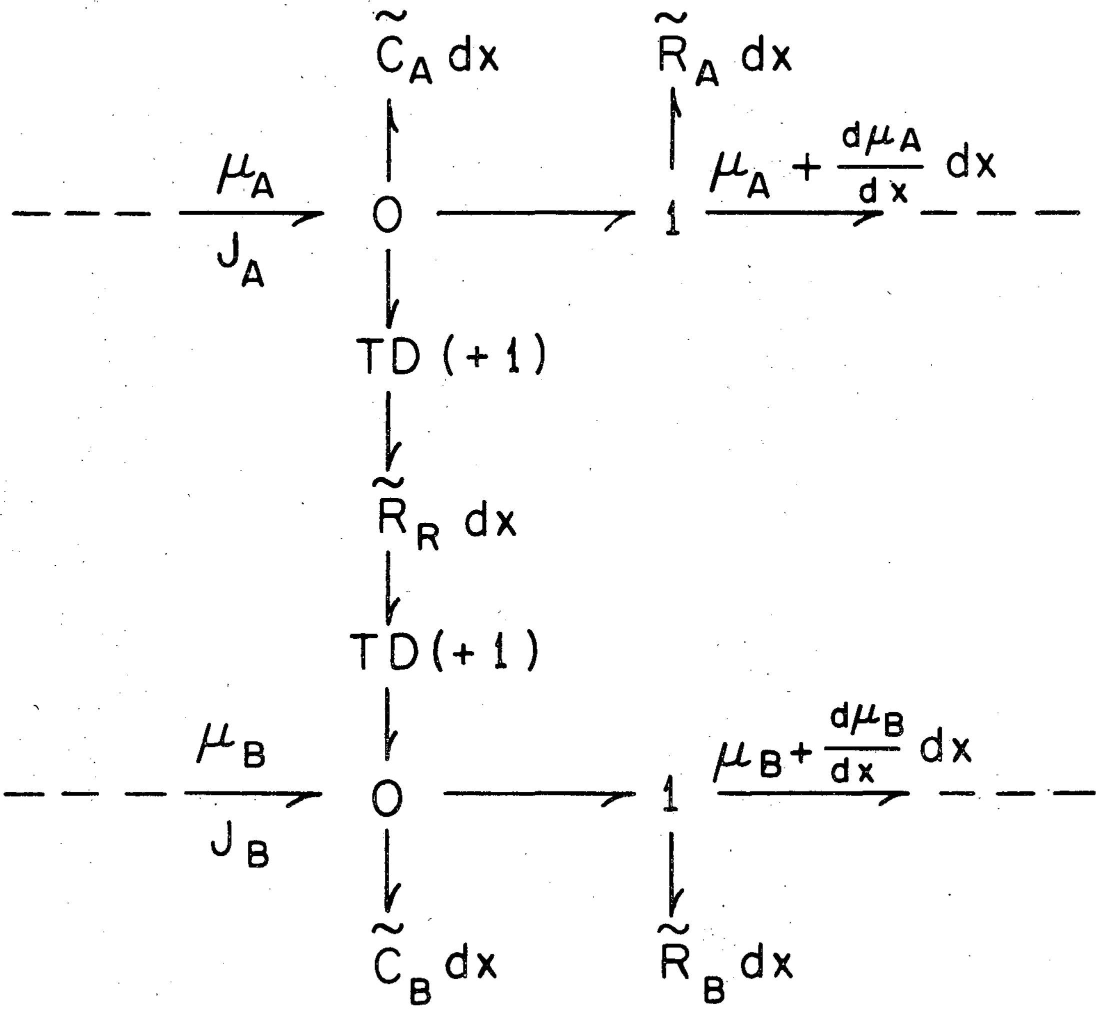

XBL722-2387

Fig. 6.2

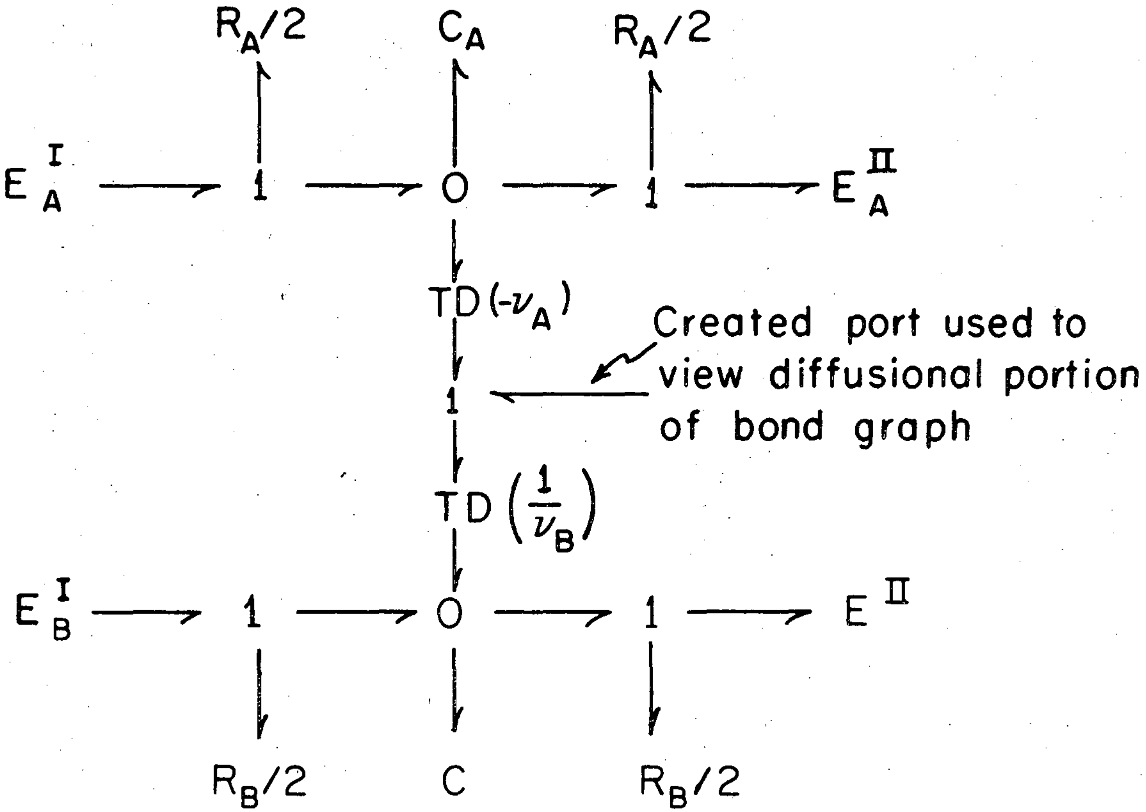

Created port used to view diffusional portion of bond graph

XBL722-2388

Fig. 6.3

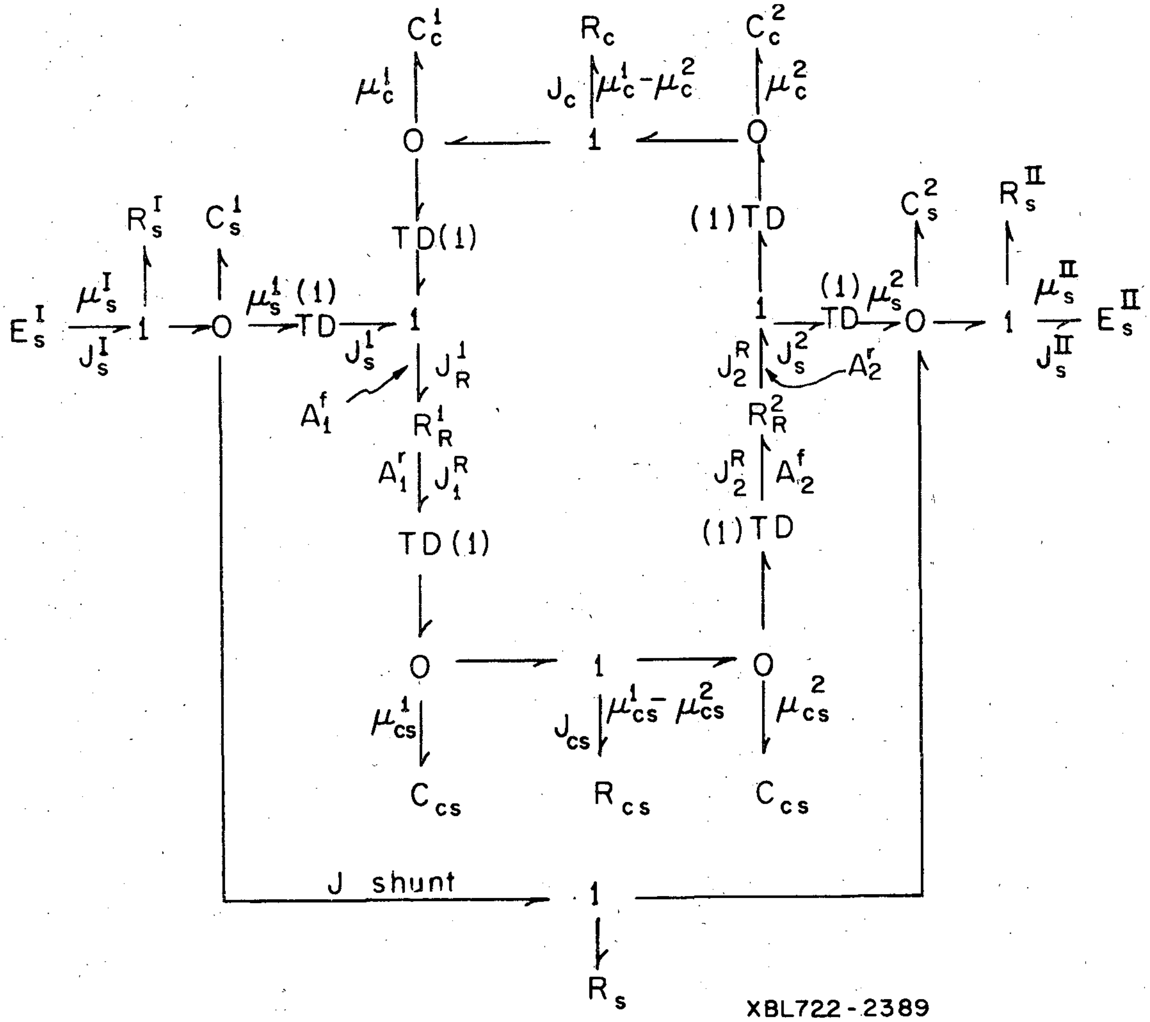
C_c^1
R_c
C_c^2
μ_c^1
J_c
$\mu_c^1-\mu_c^2$
μ_c^2
0
1
0
TD(1)
(1)TD
R_s^I
C_s^1
C_s^2
R_s^{II}
E_s^I
μ_s^I
J_s^I
1
0
μ_s^1 (1)
TD
1
J_s^1
J_R^1
A_1^f
R_R^1
A_1^r
J_1^R
TD (1)
1
(1) μ_s^2
TD
0
1
μ_s^{II}
J_s^{II}
E_s^{II}
J_2^R
J_s^2
A_2^r
R_R^2
J_2^R
A_2^f
(1)TD
0
1
0
μ_{cs}^1
J_{cs}
$\mu_{cs}^1-\mu_{cs}^2$
μ_{cs}^2
C_{cs}
R_{cs}
C_{cs}
J shunt
1
R_s
XBL722-2389

Fig. 6.4

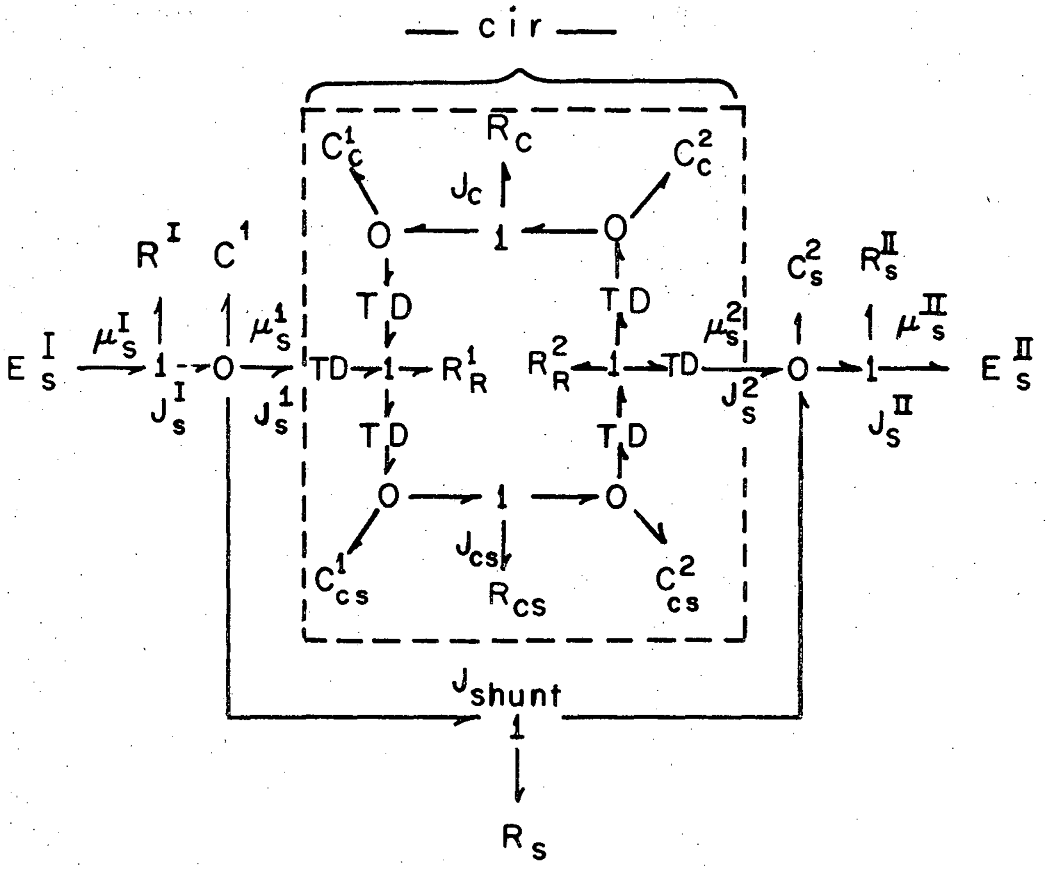

XBL722-2390

Fig. 6.5

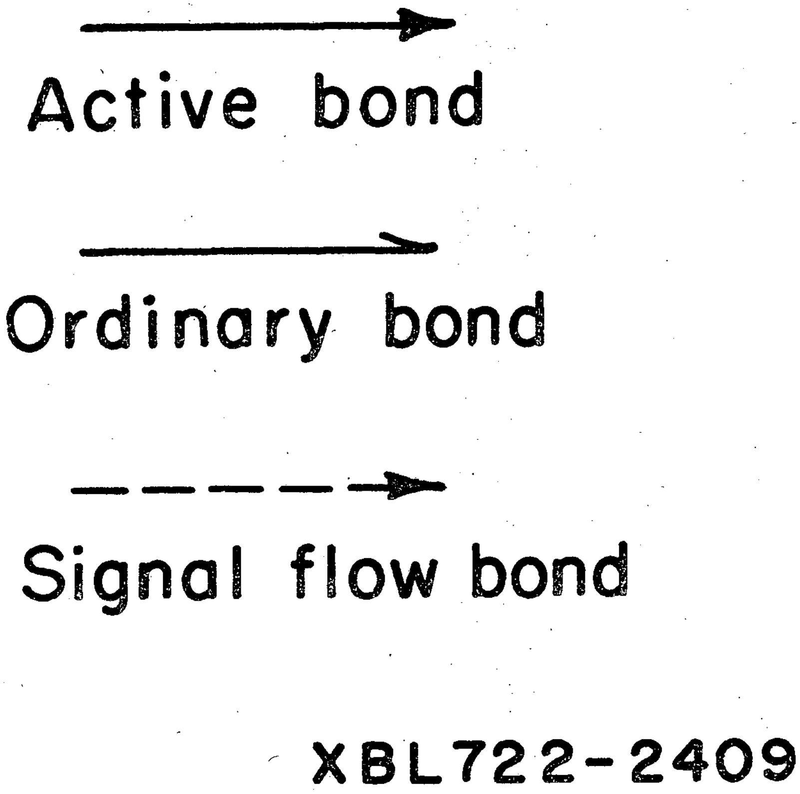

Fig. 7.1

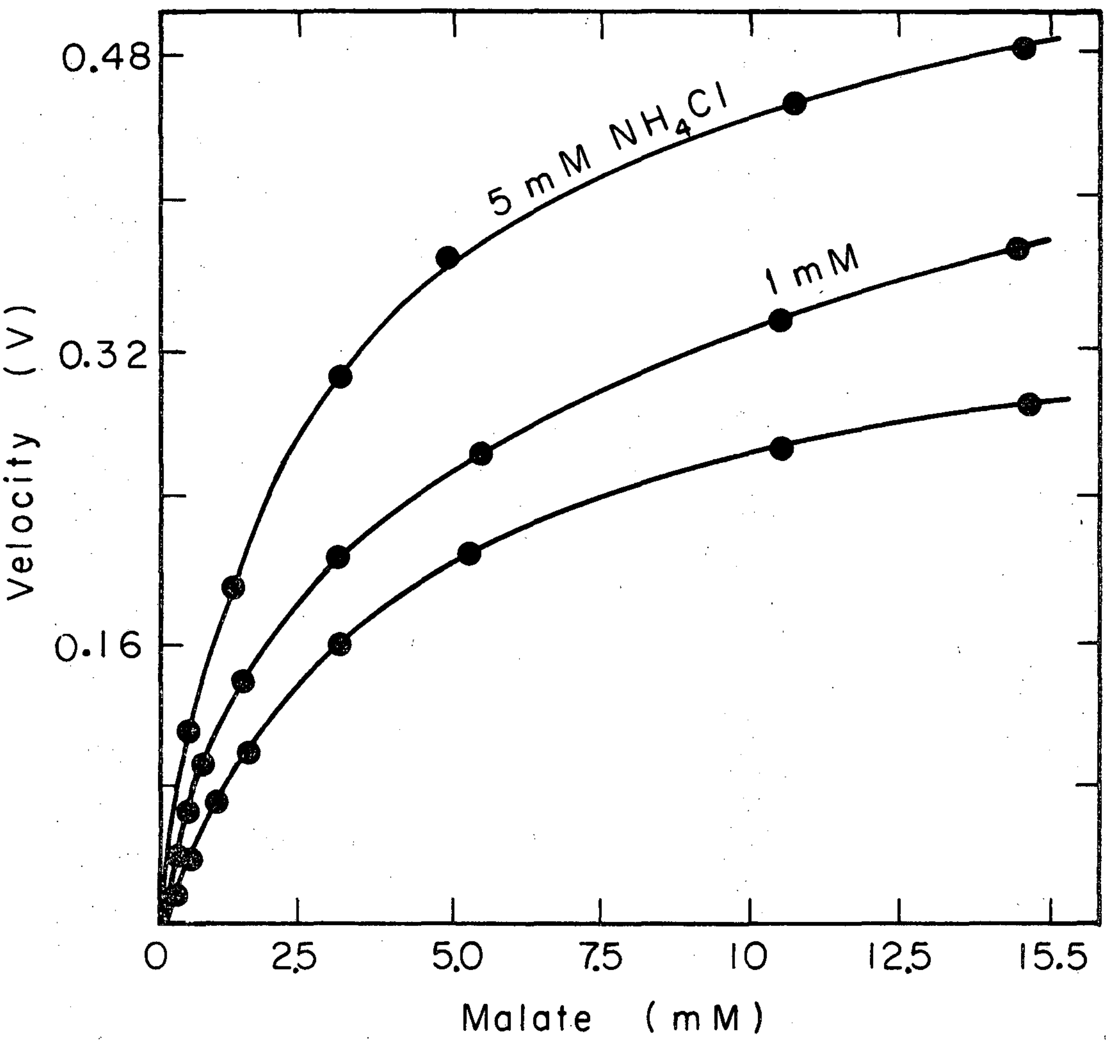

XBL 722-2410

Fig. 7.2

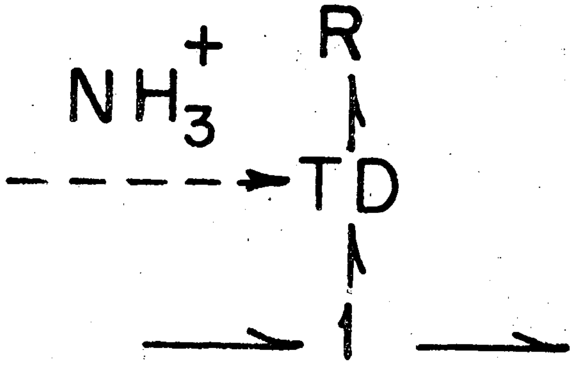

XBL722-2412

Fig. 7.3

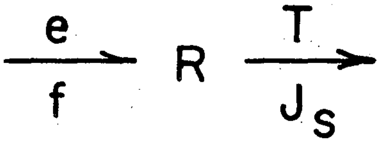

XBL723-2586

Fig. 7.4

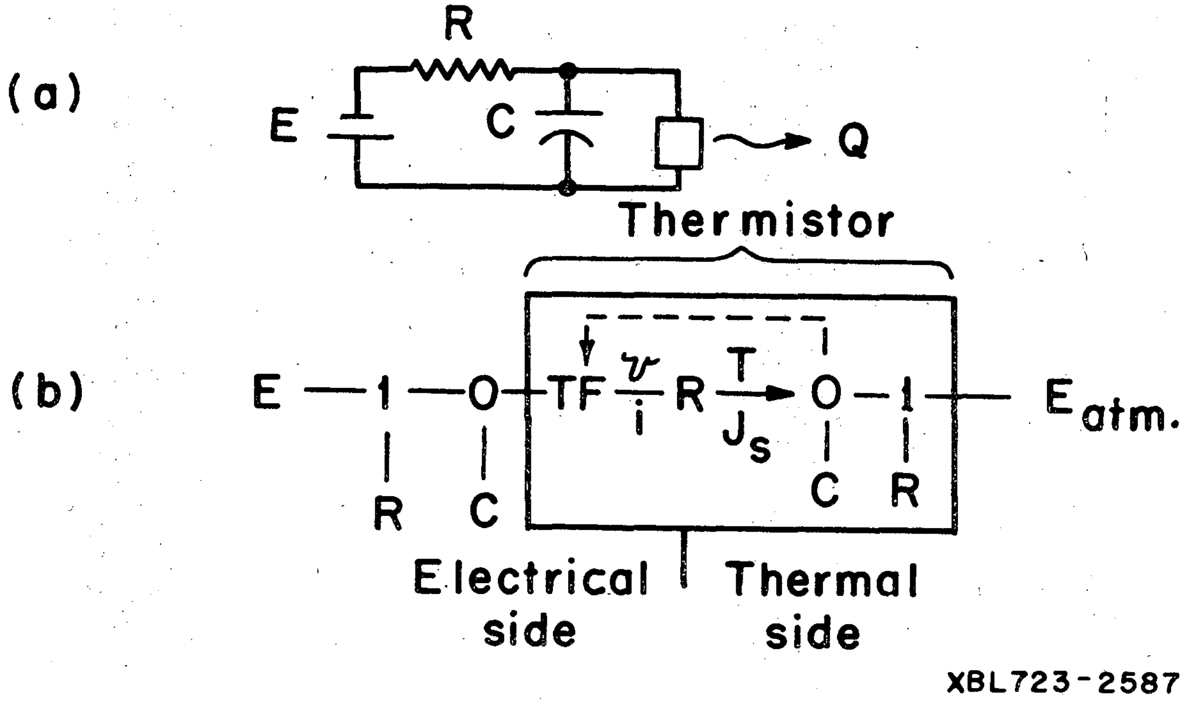
(a)
R
E
C
Q
Thermistor
(b)
E
1
0
R
C
TF
$\mathcal{v}$
i
R
T
J_s
0
1
C
R
$E_{atm.}$
Electrical side
Thermal side
XBL723-2587

Fig. 7.5

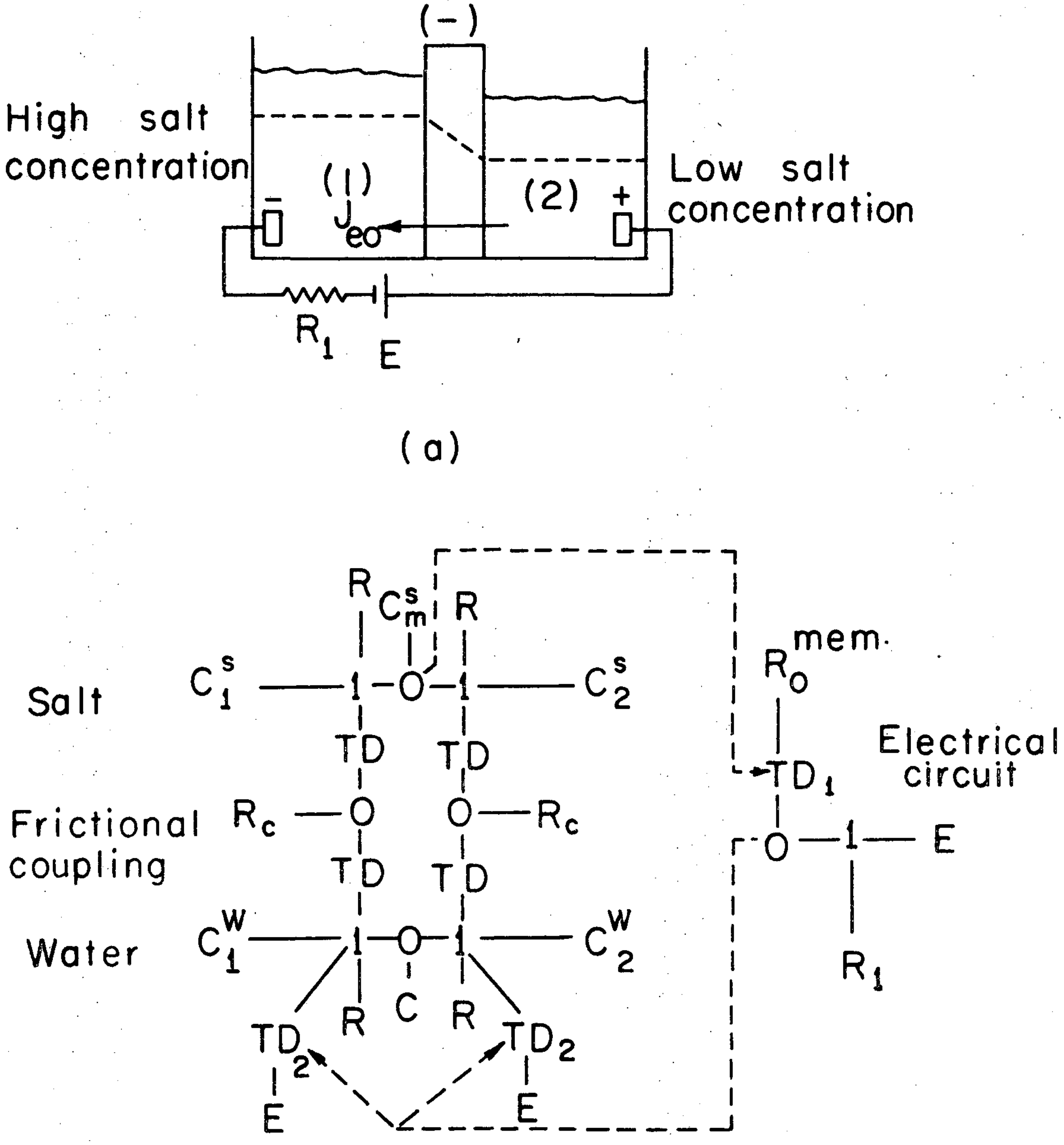

Fig. 7.6

XBL722-2413

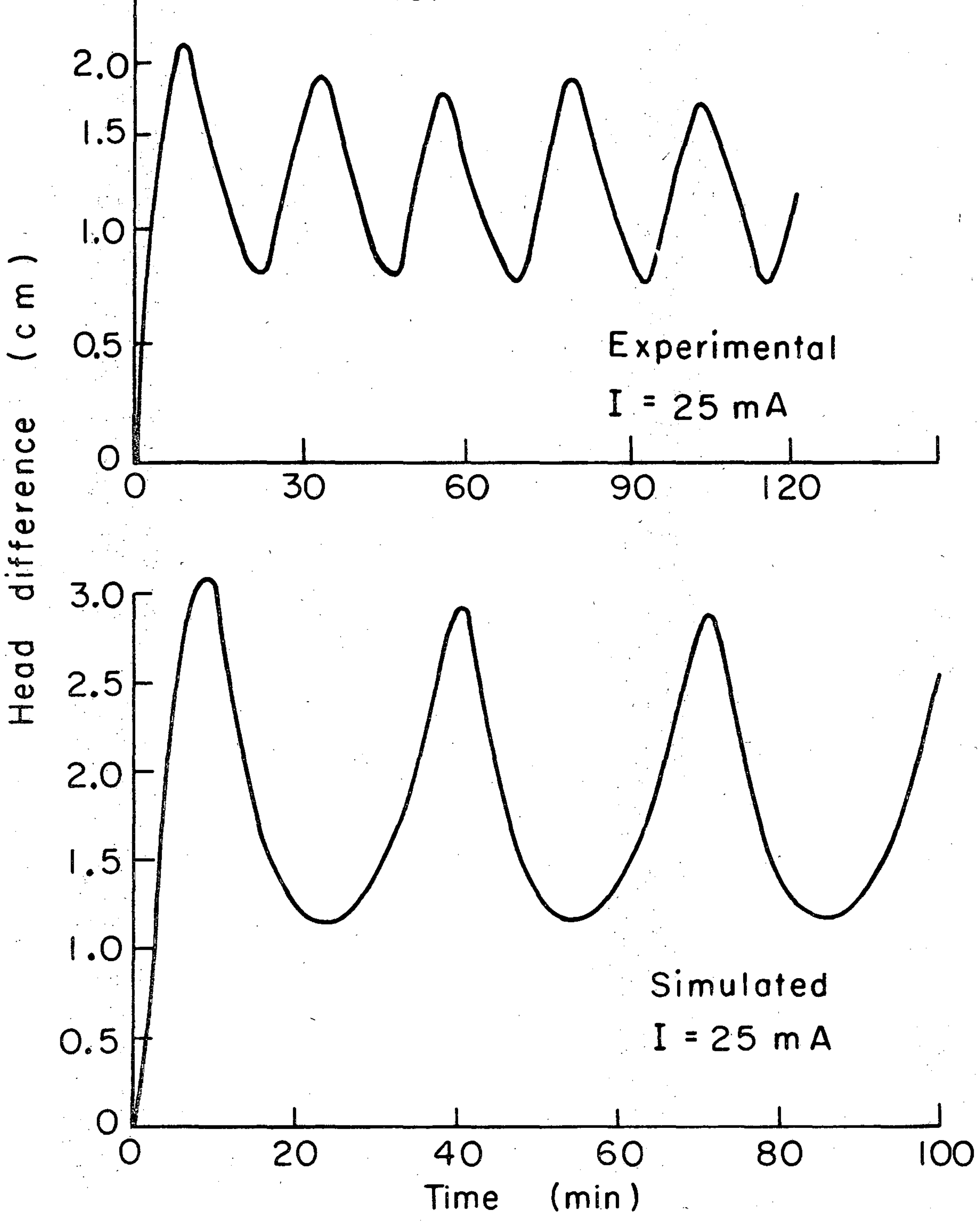

Fig. 7.7

XBL722-2414

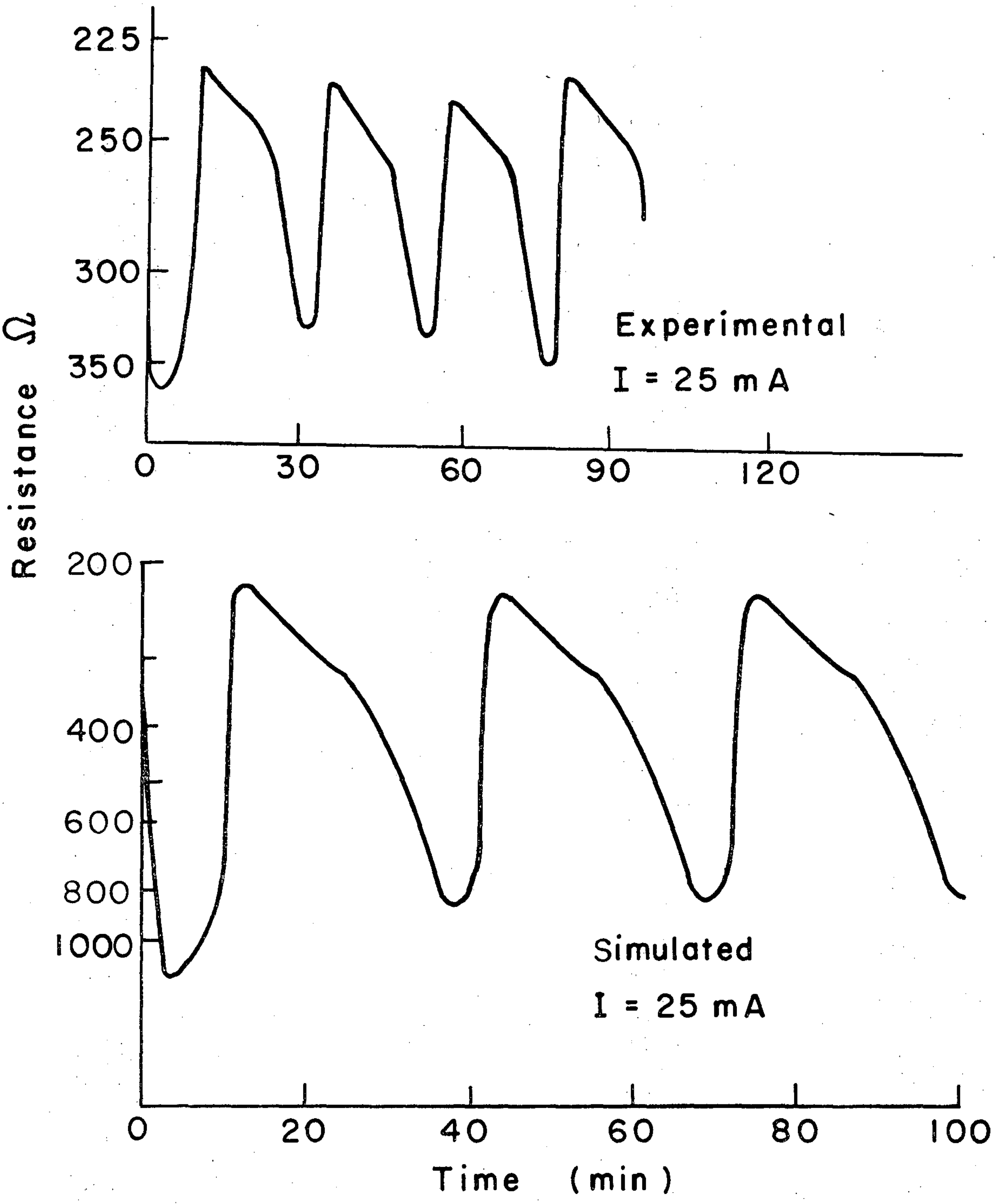

XBL722-2415

Fig. 7.8

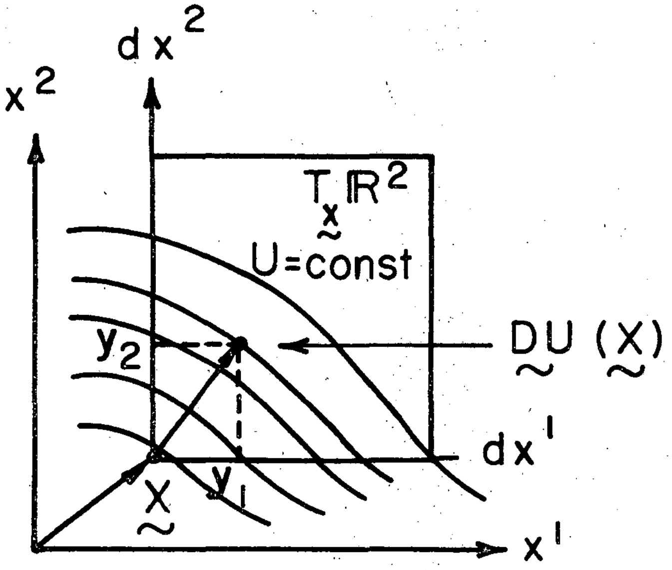

XBL722-2428

Fig. 8.1

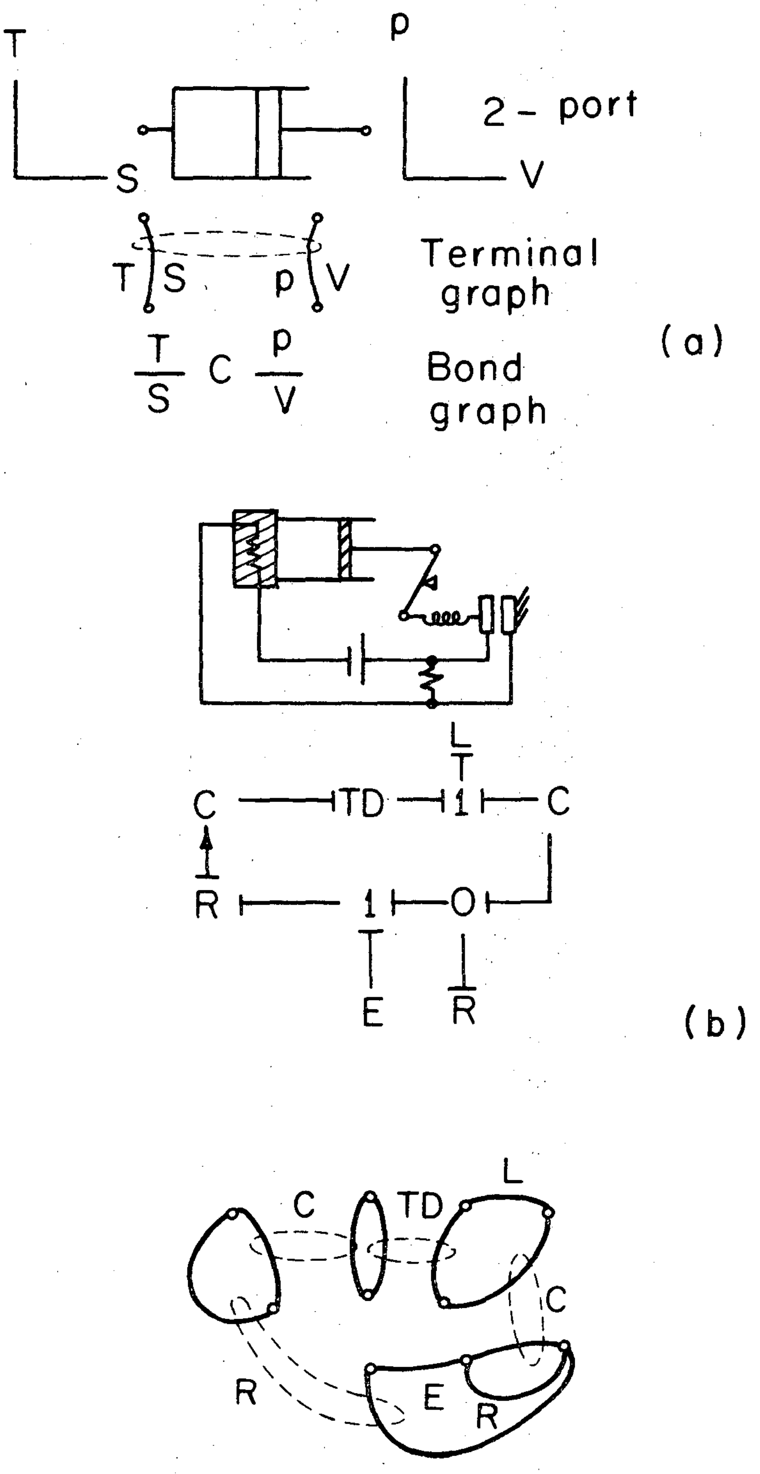

Fig. 8.2 XBL722-2494

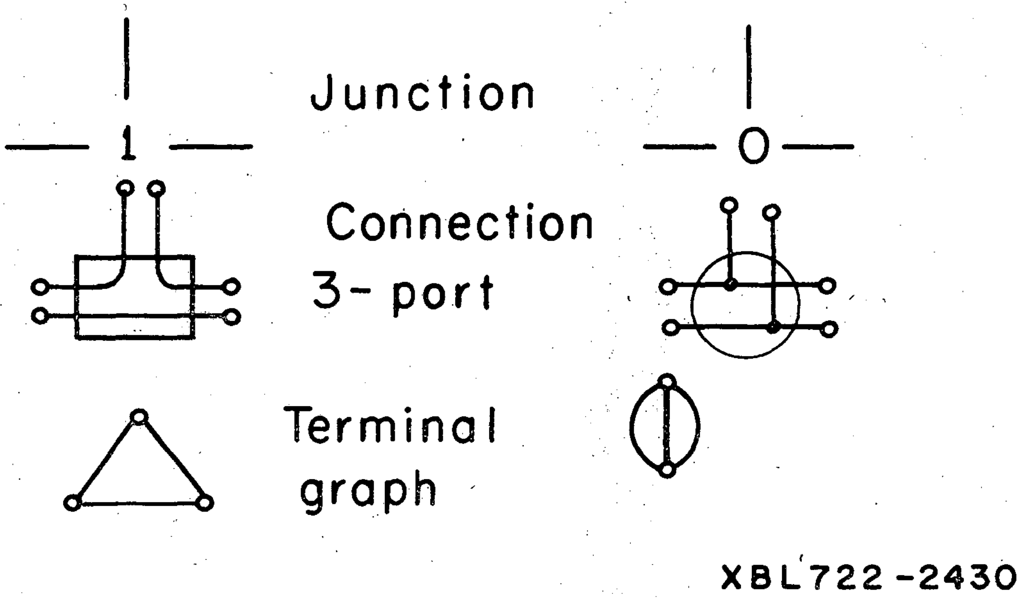

Fig. 8.3

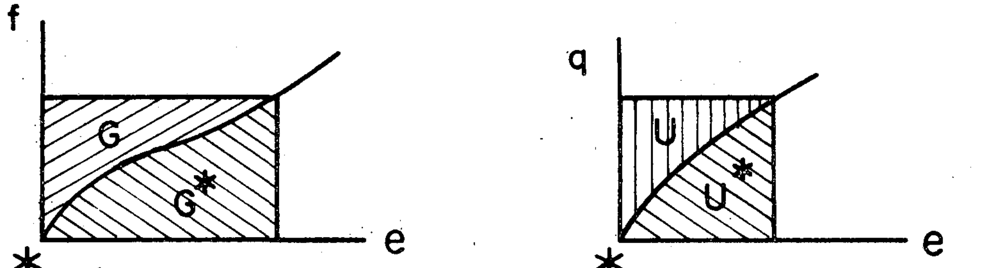

$G^*(e) = ef - G(f)$ $U^*(e) = eq - U(q)$

XBL722-2431

Fig. 8.4

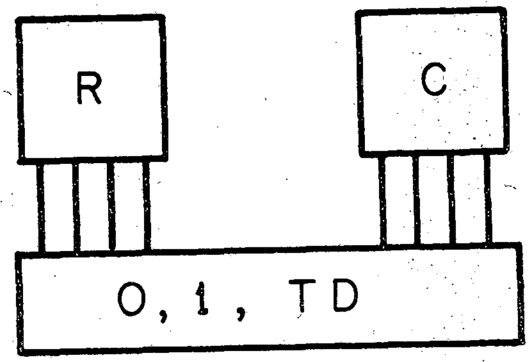

XBL722-2432

Fig. 8.5

APPENDIX A

A.1 In this appendix we briefly summarize some results from algebraic topology which underlie linear graph theory. The relation between the algebraic duality of the conjugate variables (effort, flow) and the topological duality of the conservation and continuity conditions (KCL, KVL) is indicated. The reader is referred to the literature for details and proofs.

A.2 A linear graph may be considered as a mathematical object whose properties are abstracted from the actual system whose topology it represents. The linear graph consists of a collection of nodes (0-cells, $\underset{\sim}{\sigma}_j^0$), branches (1-cells, $\underset{\sim}{\sigma}_j^1$), and, if the graph is planar, meshes (2-cells, $\underset{\sim}{\sigma}_j^2$) with appropriate orientations. It is easy to turn the collection of k-cells into a vector space, C_k, by defining linear combinations, called k-chains, $\underset{\sim}{c}_k$, with the k cells, $\underset{\sim}{\sigma}_j^k$, as a basis:

$$\underset{\sim}{c}_k = \sum_j a_j \underset{\sim}{\sigma}_j^k , \qquad \begin{matrix} a_j \in \mathbb{R} \\ \underset{\sim}{c}_k \in C_k \end{matrix} \tag{A.1}$$

The dimension of the 0 and 1 chain spaces C_0, C_1 are the number of nodes and branches, respectively, in the graph. The most important linear operator on the k-chain vector spaces is the boundary operator, $\partial_k : C_k \longrightarrow C_{k-1}$, defined by its action on the basis vectors $\underset{\sim}{\sigma}_j^k$:

for a node $\partial_0 \underset{\sim}{\sigma}^0 \equiv 1$,

for a branch $\partial_1 \underset{\sim}{\sigma}^1 = \partial(a_0, a_1) = a_1 - a_0$, $\overset{a_0}{\circ}\!\longrightarrow\!\overset{a_1}{\circ}$

for a mesh $\partial_2 \underset{\sim}{\sigma}^2 = \partial(a_0, a_1, a_2)$

$$= (a_1, a_2) - (a_0, a_2) + (a_0, a_1)$$
$$= (a_0, a_1) + (a_1, a_2) + (a_2, a_0);$$

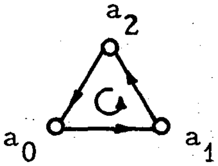

and since ∂_k is a linear operator,

$$\partial_k \underset{\sim}{c}_k = \partial \sum_j a_j \underset{\sim}{\sigma}_j^k = \sum_j a_j \partial \underset{\sim}{\sigma}_j^k . \qquad (A.2)$$

The fundamental property of the boundary operator is

$$\partial_{k-1} \cdot \partial_k(\cdot) = 0; \qquad (A.3)$$

i.e., the "boundary of the boundary" of any k-chain vanishes. Chains for which $\partial_k \underset{\sim}{c}_k = 0$ are called <u>k-cycles</u> and the collection of all k-cycles forms a subspace of C_k, denoted Z_k, where $Z_k = \text{kernel}(\partial_k)$. K-chains obtained from k + 1-chains by application of ∂_k are called <u>k-boundaries</u>; and we denote by B_k the space of all k-boundaries, i.e., $B_k = (\underset{\sim}{c}_k \in \underset{\sim}{C}_k \mid \underset{\sim}{c}_k = \partial_{k+1} \underset{\sim}{c}_{k+1}$ for some $\underset{\sim}{c}_{k+1} \in \underset{\sim}{C}_{k+1})$.

Since the C_k are linear vector spaces, one can define in a natural way the scalar product $\langle \cdot , \cdot \rangle : C_k^* \times C_k \longrightarrow \mathbb{R}$ by

$$\langle \underset{\sim}{c}_k, \underset{\sim}{c}_k^* \rangle = \sum a_j a_j^* , \qquad (A.4)$$

where C_k^* is the space dual to C_k(cochain)*.

Using this structure on C_k we can define the adjoint to ∂_k in the usual way.

$$\langle \partial_k \underset{\sim}{c}_k, \underset{\sim}{c}_{k-1}^* \rangle = \langle \underset{\sim}{c}_k , \partial_{k-1}^* \underset{\sim}{c}_{k-1}^* \rangle; \qquad (A.5)$$

$\partial_{k=1}^*$ is called the <u>coboundary operator</u> and is a linear map,

---

* Since C_k is finite dimensional there is a natural isomorphism between C_k and C_k^* (by the Euclidean inner product). However, as in paragraph 8.2, there are cogent reasons for maintaining the distinction between a vector space its dual.

$\partial^*_{k-1} : C^*_{k-1} \longrightarrow C^*_k$. It is easily verified that

$$\partial^*_k \cdot \partial^*_{k-1}(\cdot) = 0. \qquad \text{(A.6)}$$

(For $\langle \partial_k \underset{\sim}{c}_k, \partial^*_{k-2} \underset{\sim}{c}^*_{k-2} \rangle = \langle \underset{\sim}{c}_k, \partial^*_{k-1} \partial_{k-2} \underset{\sim}{c}^*_{k-2} \rangle$

$= \langle \partial_{k-1} \partial_k \underset{\sim}{c}_k, \underset{\sim}{c}^*_{k-2} \rangle = 0.$)

By analogy with the definition of k-cycles, k-cochains for which $\partial^*_k \underset{\sim}{c}^*_k = 0$ are called <u>k-cocycles</u>; and the collection of all k-cocycles forms a subspace of C^*_k, denoted by Z^*_k, where $Z^*_k = \text{kernel}\ (\partial^*_k)$. K-cochains which are obtained from k-1 chains via ∂^*_{k-1} are called <u>k-coboundaries</u>; and

$B^*_k = (\underset{\sim}{c}^*_k \in C^*_k \mid \underset{\sim}{c}^*_k = \partial^*_{k-1} \underset{\sim}{c}^*_{k-1}$ for some $\underset{\sim}{c}^*_{k-1} \in C^*_{k=1})$. If $\underset{\sim}{z}_k$ is a k-cycle, $\partial_n z_k = 0$, and $\underset{\sim}{b}^*_k$ a boundary, $\underset{\sim}{b}^*_k = \partial^*_{k-1} \underset{\sim}{c}^*_{k-1}$, then

$$\langle \underset{\sim}{z}_k, \underset{\sim}{b}^*_k \rangle = \langle \underset{\sim}{z}_k, \partial^*_{k-1} \underset{\sim}{c}^*_{k-1} \rangle = \langle \partial_k \underset{\sim}{z}_k, \underset{\sim}{c}^*_{k-1} \rangle = 0, \qquad \text{(A.7)}$$

i.e., k-cycles annihilate (are "orthogonal" to) k-coboundaries.

<u>A.3</u> We will summarize without proof the following key results:

<u>Theorem A.1.</u> Let $Z_1 = \ker (\partial_1)$, the cycle subspace of C_1;
$B^*_1 = \text{Im}\ (\partial^*_0)$, the coboundary subspace of C^*_1.

Then, for a linear graph with b branches and n nodes:

1) $\dim Z_1 = b - n + 1$; $\dim B^*_1 = n - 1$.

2) $\langle \underset{\sim}{z}_1, \underset{\sim}{b}^*_1 \rangle = 0 \ \forall \underset{\sim}{b}^*_1 \in B^*_1$, $\underset{\sim}{z}_1 \in Z_1$, i.e. $\langle$cycles, coboundaries$\rangle = 0$.

3) If $\langle \underset{\sim}{c}_1, \underset{\sim}{b}^*_1 \rangle = 0 \ \forall \underset{\sim}{b}^*_1 \in B^*_1$, then $\underset{\sim}{c}_1 \in Z_1$; i.e., a 1-chain orthogonal to every 1-coboundary is a cycle.

4) If $\langle \underset{\sim}{c}^*_1, \underset{\sim}{z} \rangle = 0 \ \forall \underset{\sim}{z}_1 \in \underset{\sim}{Z}_1$, then $\underset{\sim}{c}^*_1 \in B^*_1$ and $\exists\ \underset{\sim}{c}^*_0 \in C^*_0$ such that $\underset{\sim}{c}^*_1 = \partial^*_0 \underset{\sim}{c}^*$; i.e., a 1-cochain orthogonal to every 1-cycle is a 1-coboundary.

5) $\langle \underset{\sim}{c}_1, \partial_0^* \underset{\sim}{c}_0^* \rangle = \langle \partial_1 \underset{\sim}{c}_1, \underset{\sim}{c}_0^* \rangle$.

6) A chain has a unique decomposition as [cycle] + [boundary].

A.4 Kirchhoff's Laws are formulated as follows: Given a graph, G, with n nodes and b branches, we associate with each flow vector $\underset{\sim}{f} = (f_1, \cdots, f_b)$ a flow 1-chain

$$\underset{\sim}{f} = \sum_{j=1}^{b} f_j \underset{\sim}{\sigma}_j^1 \tag{A.9}$$

and to each effort vector $\underset{\sim}{e} = (e_1, \cdots, e_b)$ an effort 1-cochain.

$$\underset{\sim}{e}^* = \sum^{b} \underset{\sim}{e}_j \sigma_j^1 . \tag{A.10}$$

Then the following two theorems give alternate forms for KCL and KVL, respectively.

Theorem A.2 (KCL). The following statements are equivalent:

1) $\underset{\sim}{f}$ is orthogonal to all 1-coboundaries,

2) $\underset{\sim}{f}$ is a 1-cycle,

3) $\underset{\sim}{f} \in \ker(\partial_1)$.

The collection of all flows satisfying KCL forms a (b - n + 1) dimensional subspace of $\mathbb{R}^{2b} = \{f_1, e_i\}$.

Theorem A.3 (KVL). The following statements are equivalent:

1) $\underset{\sim}{e}^*$ is orthogonal to any 1-cycle,

2) $\underset{\sim}{e}^*$ is a 1-coboundary,

3) $\underset{\sim}{e}^* \in \mathrm{Im}(\partial_0^*)$.

The collection of all efforts satisfying KVL forms an n-1 dimensional subspace of $\mathbb{R}^{2b}$.

As a matter of fact, we may simply define the class of admissible flows and forces by the requirement (Smale, 1972)

$$\underset{\sim}{f} \in \ker(\partial_1), \ \underset{\sim}{e}^* \in \mathrm{Im}(\partial_0^*).$$

Since $\underset{\sim}{e}_1^* \in B_1^*$, by condition (2) of theorem A.3, it follows that there exists a 0-cochain $\underset{\sim}{e}_0^*$ such that $\underset{\sim}{e}_1^* = \partial_0^* \underset{\sim}{e}_0^*$, where $\underset{\sim}{e}_0^*$ represents the vector of node-to-datum potentials.

A.5 In paragraph 2.1 the incidence matrices $\underset{\sim}{A}$ and $\underset{\sim}{M}$ may be viewed as the matrix representations of the boundary and coboundary operators. Tellegen's Theorem is equivalent to (A.3) and/or (A.6), $\partial \cdot \partial = \partial^* \cdot \partial^* = 0$, which may be interpreted as an orthogonal partition of $\mathbb{R}^{2b}$ into invariant subspaces.

A.6. The duality between the topological structure described above and the algebraic structure accompanying the dynamical variables e and f is established via Stokes' Theorem. The integral of k-form $d\omega$ over a k-dimensional domain D in a manifold is related to the integral of the k-1 form ω over the k-1 dimensional boundary of D, ∂D, by (Spivak, 1965):

$$\int_D d\omega = \int_{\partial D} \omega . \tag{A.11}$$

If we regard the domain D as a linear functional on the space of k-forms, we may write

$$\langle \partial D, \omega \rangle = \langle D, d\omega \rangle .$$

In this fashion the space of k-forms has been put into duality with the "space of k-domains," which, in turn, may be constructed from the k-chains described above. This relationship is the so-called deRham cohomology. The identities $d \cdot d = 0$ (Poincaré Lemma) and $\partial \cdot \partial = 0$ are in a definite sense isomorphic, and generalize the familiar vector identities, div · curl = curl · grad = 0.

TECHNICAL INFORMATION DIVISION
LAWRENCE BERKELEY LABORATORY
UNIVERSITY OF CALIFORNIA
BERKELEY, CALIFORNIA 94720